



**UNIVERSITA' DEGLI STUDI DI VERONA  
FACOLTA' DI SCIENZE MM.FF.NN.**

**DIPARTIMENTO DI BIOTECNOLOGIE**

**DOTTORATO DI RICERCA IN  
BIOTECNOLOGIE MOLECOLARI, INDUSTRIALI ED AMBIENTALI**

**XXII CICLO**

**GRASPING THE PROTEOME:  
DETERGENTS SUB-FRACTIONATION OF HUMAN AND  
MICROBIAL CELLS LEADS TO IMPROVEMENTS IN  
DIFFERENTIAL PROTEOMICS**

**S.S.D. BIO/10**

**Coordinatore:  
Prof. ROBERTO BASSI**

**Tutor:  
Dott.ssa ALESSANDRA MARIA BOSSI**

**Dottorando:  
Dott.ssa RITA POLATI**



## RIASSUNTO

La mia tesi di dottorato approfondisce aspetti relativi all'analisi proteomica in gel bidimensionale: il lavoro svolto si è proposto di apportare da un lato un contributo al miglioramento dei metodi di pre-frazionamento del campione, finalizzato al raggiungimento di un alto livello di risoluzione, ad una selezione di popolazioni di proteine più omogenee per la separazione su gel, e ad una migliore riproducibilità delle mappe proteiche, e dall'altro l'impiego dei protocolli messi a punto nella prima fase della ricerca è stato immediatamente trasferito e messo alla prova su due problematiche specifiche e selezionate di ambito sia microbiologico, che biomedico. L'applicazione dei protocolli di pre-frazionamento unitamente ad un disegno sperimentale di proteomica differenziale ha permesso di ricavare importanti informazioni biochimico-cellulari e di operare correlazioni stimolo-effetto.

Gli obiettivi della tesi sono stati:

- 1) messa a punto di protocolli efficaci per la eliminazione di contaminanti (acidi nucleici e polisaccaridi) dal campione proteico per 2-DE;
- 2) indagine proteomica differenziale per delucidare i meccanismi molecolari dell'acido-resistenza di *Ga. hansenii* AAB0248;
- 3) messa a punto di protocolli di frazionamento del campione in: proteine di membrana, del citosol e proteine associate alle membrane;
- 4) indagine sull'omeostasi del ferro nei macrofagi con approccio di proteomica differenziale: effetti della stimolazione con ferro ionico;
- 5) indagine sull'omeostasi del ferro nei macrofagi con approccio di proteomica differenziale: effetti della stimolazione con eritrociti senescenti.

### *Proteomica microbiologica*

*In collaborazione con il Dott. Giacomo Zapparoli, laboratorio di microbiologia, Dipartimento di Biotecnologie, Università di Verona e con il Prof. Paolo Giudici, Dipartimento di Scienze Agrarie, Università degli Studi di Modena e Reggio Emilia.*

*Ga. hansenii* AAB0248 appartiene ai batteri acetici, è stato isolato dall'aceto ed è di sicuro interesse scientifico in quanto riesce a sopravvivere in un ambiente non solo acido, ma anche contenente acido acetico, molecola citotossica per la maggior parte delle specie microbiche. E' stata quindi pianificata un'analisi di proteomica differenziale per indagare i meccanismi molecolari coinvolti nell'acido-resistenza di questo peculiare batterio.

Tuttavia le prime mappe bidimensionali della popolazione delle proteine totali espresse da questi batteri, ottenute con i classici metodi di preparazione del campione (impiego di soluzione di solubilizzazione, trattamento con l'1% di anfoline 3-10, trattamento con fenolo:cloroformio:isoamilico), mostrano gravi problemi di focalizzazione, soprattutto nella

parte acida del gel, probabilmente dovuti alla presenza massiccia di DNA e polisaccaridi che complessandosi tra loro tendono a bloccare i pori delle IPGs e ad ostacolare l'entrata delle proteine. Per questi motivi è stato necessario, prima di procedere alla vera e propria analisi di proteomica differenziale, mettere a punto un metodo efficace per la preparazione del campione. Il protocollo che abbiamo concepito viene ampiamente descritto nel capitolo 1 della sessione 2 e si basa essenzialmente sull'utilizzo del CTAB. Il detergente anionico CTAB è comunemente usato dai genetisti per liberare gli acidi nucleici totali dai polisaccaridi. L'azione del CTAB si esplica nella sua capacità di formare complessi insolubili con acidi nucleici e/o polisaccaridi. Quando la concentrazione iniziale di NaCl è maggiore di 0.7 M, il CTAB resta in soluzione, se invece la concentrazione di NaCl si abbassa al di sotto di 0.7 M, il CTAB diventa insolubile e risulta nella formazione di una medusa costituita dal detergente stesso e da tutto ciò che ha legato. Gli altri componenti della cellula sono invece efficacemente allontanati nel supernatante, perché in tali condizioni essi non precipitano. Questo concetto è stato quindi sfruttato per mettere a punto un nuovo protocollo. I risultati ottenuti applicando al campione questo trattamento sono stati oltre modo incoraggianti: infatti sono stati eliminati tutti i problemi di strisciamento orizzontale nella zona acida dovuti a DNA e polisaccaridi e di focalizzazione e, contemporaneamente è stato recuperato un grande numero di proteine. Esperimenti di controllo hanno evidenziato l'effettiva rimozione di DNA e polisaccaridi da parte del detergente.

Il trattamento con CTAB è stato successivamente applicato a campioni di lisato batterico di *Ga. hansenii* AAB0248 sottoposti a condizioni di stress indotto dalla presenza di acido acetico e comparati con lisati controllo. Sono state trovate variate nella loro espressione a seguito dello stimolo 79 proteine (45 sotto-esprese e 34 sovra-esprese). Sono state identificate 94 singole catene polipeptidiche, appartenenti a proteine coinvolte nella totalità dei processi cellulari: infatti il 14% sono proteine della trascrizione, il 7.5% esplica la glicolisi ed il ciclo di Krebs, l'8.5% appartiene agli enzimi della traduzione ed il 7.5% è coinvolto nel ripiegamento delle proteine. Inoltre il 6.5% prende parte alla biosintesi degli acidi grassi, il 17% al metabolismo dei nucleotidi e degli amminoacidi, il 3% alla regolazione del ciclo cellulare, ed un altro 3% è adibito alla chemiotassi e al movimento cellulare. Il rimanente 33% è coinvolto nel trasporto di ioni attraverso le membrane, in reazioni di ossidazione e riduzione, nella fosforilazione, nella proteolisi, ed in molti altri processi cellulari.

I risultati suggeriscono come la presenza di acido acetico nel mezzo di crescita, porti ad un cambiamento globale a livello di espressione proteica nelle cellule batteriche: pressoché tutti i processi metabolici e non che si svolgono all'interno di questi batteri sembrano essere interessati dalla presenza di acido acetico, molecola citotossica per la maggior parte degli organismi viventi. E' interessante notare come tutti gli enzimi coinvolti nel processo glicolitico siano aumentati, mentre tutti quelli coinvolti nel ciclo di Krebs (siano diminuiti,

così come risulta sottoespresso anche la piruvate dehydrogenase, enzima che trasforma il piruvato in acetil-CoA.

E' interessante osservare il bilancio tra le variazioni di glicolisi e ciclo di Krebs risulta in una aumentata produzione di piruvato. Si può ipotizzare un ruolo chiave di questo aumento del piruvato nella sintesi di biomassa cellulosica. E' stato infatti ampiamente dimostrato che i batteri acetici, fatti crescere in opportuni terreni, sono in grado di produrre cellulosa partendo dal piruvato. É possibile perciò ipotizzare che questo ceppo in presenza di acido acetico, subisca una rinnovata spinta metabolica verso la produzione di cellulosa e che l'aumento nella biosintesi di cellulosa che probabilmente conferisce al batterio un certo vantaggio ecologico. Inoltre, sono trovate variate nelle cellule cresciute in presenza di acido acetico numerose proteine coinvolte nel macchinario di ripiegamento e turn-over, in grado cioè di permettere l'adattamento alle condizioni di stress.

Questi risultati possono avere applicazioni in futuro, specialmente nelle biotecnologie, per esempio per la produzione di una cellulosa estremamente pura per uso medico, oppure da utilizzare semplicemente come biocombustibile.

#### *Proteomica biomedica*

*In collaborazione con la Dott.ssa Annalisa Castagna e il Dott. Domenico Girelli, Dipartimento di Medicina Clinica e Sperimentale, Unità di Medicina Interna B, Università di Verona, con la Dott.ssa Ivana De Domenico, Division of Hematology, Department of Medicine, School of Medicine, University of Utah, ed il Prof. Jerry Kaplan, Department of Pathology, School of Medicine, University of Utah.*

Questa parte della tesi e' stata rivolta alla messa a punto di metodi di frazionamento delle proteine cellulari in popolazioni omogenee di proteine di membrana, del citosol e di proteine associate alle membrane, con il conseguente vantaggio di separare su un medesimo gel bidimensionale proteine con una comune localizzazione cellulare.

Nel caso presente si e' lavorato su colture di monociti/macrofagi ed e' stato messo a punto un metodo di frazionamento delle proteine che ponesse particolare attenzione al recupero delle proteine di membrana.

Le proteine di membrana e le proteine associate alle membrane sono state estratte sfruttando le peculiari caratteristiche di un detergente non ionico: il Triton X-114. Questo detergente cambia la sua solubilità in una soluzione acquosa, a seconda della temperatura: infatti a 0°C il Triton X-114 è completamente solubile, mentre a 23°C diventa insolubile e precipita. E' stata quindi utilizzata questa sua proprietà per l'estrazione e la precipitazione delle proteine di membrana. In particolare si formano due fasi, una fase acquosa superiore, contenente le proteine idrofiliche associate alle membrane, ed una fase inferiore, contenente le proteine idrofobiche. In questo caso quindi, quando si parla di proteine associate alle membrane, si intendono tutte quelle proteine presenti nella frazione intermedia che conterrà sia proteine solubili, sia proteine poco idrofobiche, sia proteine

associate a proteine di membrana o alle membrane stesse. Prove di western-blot hanno validato il metodo.

Il protocollo del Triton X-114 e' stato di seguito impiegato per l'analisi proteomica differenziale di un problema di alto interesse biomedico: lo studio dei meccanismi molecolari dell'omeostasi del ferro esplicita dai macrofagi.

I macrofagi sono cellule del sistema reticoloendoteliale deputate allo svolgimento di funzioni altamente specializzate, quali l'immunoregolazione, l'attività antimicrobica, la risposta all'infiammazione, attività antitumorale, la demolizione di cellule non più funzionali o danneggiate, il riciclo del ferro. Una caratteristica peculiare del metabolismo del ferro è la dinamica con cui questo metallo viene conservato e ri-distribuito all'interno dell'organismo (ogni giorno ben il 3-4% del ferro e' riciclato, a fronte di uno 0.4% assunto con la dieta e di uno 0.03% escreto). L'omeostasi del ferro si presenta dunque come un meccanismo finemente regolato. Nonostante il ruolo fondamentale che ricoprono i macrofagi nell'omeostasi del ferro, il riciclo del ferro da parte di queste cellule rimane a tutt'oggi uno dei processi metabolici meno compresi. Le problematiche aperte sul metabolismo del ferro sono relative a: i trasportatori a livello di membrana di ferro ionico e di ferro eme; il meccanismo e i relativi trasportatori coinvolti, nella traslocazione del ferro dal fagolisosoma al citosol del macrofago; la via di riciclo del gruppo eme, se esistano trasportatori intracellulari del gruppo eme, e come venga poi rilasciato il ferro; il sistema di coordinamento intracellulare del riciclo del ferro.

Il disegno sperimentale ha previsto la mappatura delle proteine espresse dalla linea cellulare C3H WT di macrofagi reticolo-endoteliali murini a seguito di trattamento, sia con 1) concentrazioni fisiologiche di ferro in forma ionica, per mimare la risposta del macrofago al ferro proveniente dalla dieta; mentre in un altro caso con 2) globuli rossi senescenti, per mimare l'attività di riciclo dei gruppi eme da parte del macrofago. In ciascun esperimento, il corredo proteomico dei macrofagi trattati e' stato confrontato con il corredo dei macrofagi controllo. In questo modo e' stato possibile identificare quelle proteine che variano la loro espressione in risposta al trattamento e di conseguenza correlarle con i meccanismi molecolari coinvolti nel metabolismo del ferro. La intensa relazione tra riciclo/internalizzazione del ferro e trasportatori di membrana rende evidente l'importanza del lavoro di messa a punto di un metodo di frazionamento per le proteine di membrane.

#### *Macrofagi stimolati con ferro ionico*

Nei macrofagi trattati con ferro in forma ionica, l'analisi statistica ha permesso individuare 19 proteine sovra espresse e 20 sotto espresse nella frazione citosolica. Nella frazione di membrana sono state individuate 24 proteine sovra espresse e 9 sotto espresse, mentre nelle proteine associate alle membrane sono state individuate 15 proteine sovra espresse e

3 proteine sotto espresse. Dopo l'identificazione tramite MS e MS/MS, le proteine differenzialmente espresse sono state suddivise in classi funzionali che rispecchiano il ruolo biologico da esse esplicato. In presenza dello stimolo del ferro è stato osservato un incremento del metabolismo basale e un incremento delle proteine coinvolte nella risposta allo stress ossidativo. Entrambi sono probabilmente classificabili come meccanismi di difesa messo in atto dai macrofagi, per contrastare l'ambiente ossidativo con la produzione di proteine coinvolte nella risposte redox. Sono attuati meccanismi di demolizione delle proteine danneggiate e di preservazione del loro corretto ripiegamento. Il trattamento con ferro, induce inoltre un rilevante incremento della proteina di accumulo del ferro, la ferritina. La ferritina è la principale proteina di deposito del ferro ed ha la capacità di accumularlo in una forma solubile, non tossica e facilmente utilizzabile. Per quanto concerne l'assorbimento del ferro è interessante notare che i nostri risultati indicano chiaramente la presenza della gliceraldeide 3 fosfato deidrogenasi (GADPH) sulle membrane dei macrofagi e oltretutto sovraespressa nelle cellule trattate con il ferro. In condizioni normali la GADPH è un enzima appartenente alla glicolisi e si trova di conseguenza nel citoplasma. Recentemente è stato però dimostrato che in presenza di ferro i macrofagi traslocano la GADPH sulle membrane e che essa ha la capacità di interagire con la transferrina, formando un complesso che viene internalizzato negli endosomi. Sembra quindi che la GADPH possa funzionare come recettore per la transferrina in alternativa al Tfr1 e Tfr2, probabilmente grazie ad un meccanismo ancestrale di ricezione. Il citoscheletro sembra essere fortemente coinvolto sia nell'assorbimento sia nel rilascio del ferro (risultano sottoespresse diverse forme dell'actina e proteine coinvolte nella sua polimerizzazione). Una possibile spiegazione a questo fenomeno è che le proteine del citoscheletro potrebbero essere coinvolte nel trasporto interno delle proteine tramite i microtubuli. Infine risulta di particolare interesse la nuova sintesi della proteina Mif (fattore di inibizione della migrazione dei macrofagi), che ha la capacità di indurre una risposta all'infiammazione. Il Mif è una citochina altamente conservata ed originariamente è stato descritto come un fattore espresso dai linfociti T che blocca la migrazione dei macrofagi. Il Mif potrebbe quindi essere l'anello di congiunzione tra il ferro e l'immunità per il controllo delle infezioni.

#### *Macrofagi trattati con globuli rossi senescenti*

I risultati ottenuti con macrofagi esposti a globuli rossi senescenti hanno mostrato 26 proteine sovra espresse e 27 sotto espresse nella frazione citosolica mentre nella frazione di membrana sono state individuate 33 proteine sovra espresse e 28 sotto espresse. Dopo l'identificazione tramite MS e MS/MS, le proteine differenzialmente espresse sono state suddivise in classi funzionali che rispecchiano il ruolo biologico da esse esplicato. In presenza dei globuli rossi senescenti, risultano regolate numerose proteine del

citoscheletro. In particolare risultano sovra espresse le proteine fondamentali per l'eritrofagocitosi, che comprende un rimodellamento veloce ed efficace della forma della cellula che si appresta a inglobare il globulo rosso. Non a caso sono state trovate sovra espresse quattro diverse isoforme di beta e gamma actina, sia nella frazione citosolica sia nella frazione di membrana. E' stato infatti stimato che durante la fagocitosi le cellule incrementano il loro contenuto di actina del 40%. Inoltre esistono una miriade di proteine che legano l'actina e che ne regolano spazialmente e temporalmente la crescita dei filamenti. Di tutte queste proteine noi abbiamo trovato regolate nell'espressione, in seguito ad eritrofagocitosi, la gelsolina, CapG, la coronina-1, ARP3, e una chaperonina (CCT). Le proteine appena elencate sono fondamentali nell'attività fagocitica e agiscono dalla polimerizzazione/depimerizzazione dell'actina sino alla formazione degli pseudopodi. Strettamente correlata alla fagocitosi è la richiesta di ATP. Si stima infatti che il 50% dell'ATP prodotta da una cellula venga utilizzata nella riorganizzazione del citoscheletro, è quindi plausibile che durante il processo di eritrofagocitosi aumenti la richiesta di ATP e a supporto di questa tesi noi abbiamo osservato la sovra espressione dell'ATP sintasi e della creatine-chinasi coinvolte rispettivamente nella sintesi e nella distribuzione dell'ATP nel citoscheletro. I dati indicano inoltre la presenza di uno stress a livello del reticolo endoplasmatico (RE) in seguito ad eritrofagocitosi. Risulta infatti sottoespressa la proteina BiP, la cui funzione è quella di bloccare i recettori dello stress su RE, questa regolazione e la contemporanea sovra espressione della valosin containing protein sono chiari segnali che stanno ad indicare un' inizio di stress a livello dell'RE. Inoltre, a supporto di questa ipotesi, abbiamo trovato sottoespressi una serie di enzimi metabolici e alcune proteine della traduzione: l'attenuazione del metabolismo e l'attenuazione del processo di traduzione sembrano essere la prima e immediata risposta della cellula all'attivazione dei sensori di stress RE. Lo stress del reticolo endoplasmatico appare inoltre essere correlato ad una risposta infiammatoria. Infatti numerose proteine coinvolte nell'infiammazione risultano essere regolate e di particolare importanza sono l' $\alpha$ -fetoproteina, la cui sottoespressione induce la sintesi delle citochine, l'E2N che è essenziale per la trasmissione dei segnali nella via di attivazione del fattore di trascrizione NF- $\kappa$ B ed infine l'endoplasmina (nuovamente indotta dopo l'eritrofagocitosi) che è considerata un chaperone fondamentale per i TLR e il principale induttore della sintesi delle citochine nei macrofagi. Questi dati sono di fondamentale importanza perché indicano che esiste un collegamento tra l'eritrofagocitosi e l'infiammazione e tale anello di congiunzione sembra essere lo stress a livello del reticolo endoplasmatico. Inoltre non vi è traccia dei gruppi eme legati alle emoglobine dei globuli rossi fagocitati. Né vi è regolazione delle eme-ossigenasi, che dovrebbero digerire i gruppi eme, né delle ferritine. Qual è dunque il destino dei gruppi eme? Saranno necessarie ulteriori analisi per aggiungere un altro pezzo al puzzle ancora incompleto dell'omeostasi del ferro.



*Siamo in attesa di dati di RT-PCR e microarrays sul ferro ionico e sull'internalizzazione dei globuli rossi dai nostri colleghi della University of Utah.*

Concludendo, tutti gli studi di analisi proteomica comparativa, effettuati durante questi tre anni di dottorato, confermano che l'elettroforesi bidimensionale, accoppiata all'analisi tramite spettrometria di massa, è una tecnica efficace per l'analisi globale della variazione dell'espressione proteica e per lo studio e la comprensione dei meccanismi molecolari che stanno alla base di importanti processi biologici.



## PREFACE

*Proteomics* is an emerging area of science that attempts to study proteins on a massively parallel scale. It is by essence a multidisciplinary science: physics, chemistry, bioinformatics and mathematics join biochemistry, biology and medicine to solve general life science questions. Scientists worldwide are applying proteomic technology to solve problems which cannot be resolved by traditional methods, particularly in the biochemical field. Methodologically, proteomics is based on highly efficient methods of separation and analysis of proteins in living systems, which need to be continuously improved in order to achieve and maintain high resolution standards. Proteomics is considered a key technology in many biomedical sectors such as molecular medicine, drug discovery, clinical diagnostics, as well as microorganisms and plant studies. Shared problem in proteomic analysis is the great complexity of the samples, thus the proteomic technology needs improvements and new contributes to overcome the actual limitations in the samples treatment and recovery, to shorten and ease the recovery protocols, to affirm reproducibility and to effectively remove contaminants, in order to reach the degree of automation and cross-laboratory reproducibility collectively expected by the scientific community.

The objectives of this thesis were both the development of protocols for protein recovery in order to achieve higher resolution and reproducibility in 2-DE, and at the direct applications of the set methods to the understanding of two selected and interesting proteomic cases. Concerning microbiological proteomics, we studied the molecular mechanism of acid-resistance in *Ga. hansenii*; and concerning the biomedical proteomics, the molecular basis of iron homeostasis in macrophages was studied.

*The thesis work was performed at the Biochemical Methodology and Proteomics laboratory of Department of Biotechnology of the University of Verona, in collaboration with other laboratories. Regarding the study on macrophages, we collaborated with Dr. Annalisa Castagna and Prof. Domenico Girelli, Unit of Internal Medicine B, Department of Clinical and Experimental Medicine of the University of Verona, with Dr. Ivana De Domenico, Division of Hematology, Department of Medicine, School of Medicine, University of Utah, and Prof. Jerry Kaplan, Department of Pathology, School of Medicine, University of Utah, and with Dr. Anna Maria Timperio and Prof. Lello Zolla, Department of Ambiental Science, University of "La Tuscia", Viterbo. Regarding the study on *Ga. hansenii* we collaborated with Dr. Giacomo Zapparoli, Department of Biotechnology of the University of Verona and with Prof. Paolo Giudici, Department of Agricultural and Food Science, University of Modena and Reggio Emilia.*



# CONTENTS

RIASSUNTO	I
PREFACE	IX
CONTENTS	XI
LIST OF ABBREVIATIONS	XIII
 <b>SESSION 1: PROTEOME AND PROTEOMICS</b>	 <b>1</b>
<b>CHAPTER 1: CLASSICAL PROTEOMICS</b>	<b>7</b>
1. Sample preparation and protein extraction	8
2. Methodologies and technologies in classical proteome study	13
<b>CHAPTER 2: GEL-FREE PROTEOMICS</b>	<b>23</b>
1. MS-based proteomics	23
2. SELDI	24
3. Protein microarray	25
4. Chemical proteomics	26
<b>BIBLIOGRAPHY of SESSION 1</b>	<b>29</b>
 <b>SESSION 2: PROTEOMICS MEETS MICROBIOLOGY</b>	 <b>33</b>
<b>CHAPTER 1: A METHOD FOR THE PREPARATION OF TOTAL PROTEIN EXTRACT OF MICROORGANISM FOR PROTEOMIC ANALYSIS</b>	<b>37</b>
1. Introduction	37
2. Materials and Methods	38
3. Results and Discussion	41
4. Conclusion	46
<b>CHAPTER 2: AN APPLICATION OF CTAB-METHOD: PROTEOMIC ANALYSIS OF MOLECULAR BASIS OF ACID-RESISTANCE IN <i>Ga. hansenii</i></b>	<b>47</b>
1. Introduction	47
2. Materials and Methods	48
3. Results and Discussion	51
4. Conclusion	58
<b>BIBLIOGRAPHY of SESSION 2</b>	<b>65</b>
 <b>SESSION 3: PROTEOMICS MEETS IRON</b>	 <b>69</b>
<b>CHAPTER 1: HIGH RESOLUTION PREPARATION OF MONOCYTE-DERIVED-MACROPHAGES (MDM) PROTEIN FRACTIONS FOR CLINICAL PROTEOMICS</b>	<b>75</b>
1. Introduction	75
2. Materials and Methods	76
3. Results and Discussion	80
4. Conclusion	87

<b>CHAPTER 2: PROTEOMIC RESPONSE TO IONIC IRON IN MURINE MACROPHAGES</b>	<b>91</b>
1. Introduction	91
2. Materials and Methods	93
3. Results	96
4. Discussion	101
5. Conclusion	105
<b>CHAPTER 3: PROTEOMIC RESPONSE TO HEME-IRON IN MURINE MACROPHAGES</b>	<b>113</b>
1. Introduction	113
2. Materials and Methods	115
3. Results	115
4. Discussion	119
5. Conclusion	123
<b>BIBLIOGRAPHY of SESSION 3</b>	<b>131</b>
<b>PUBLICATIONS</b>	<b>137</b>

## LIST of ABBREVIATIONS

**AA:** acrylamide

**AAB:** Acetic Acid Bacteria

**ABPs:** Activity Based Probes

**ARP 3:** Actin Related Protein 3

**BMDMs:** Bone Marrow Derived Macrophages

**BSA:** Bovine Serum Albumin

**CapG:** Macrophage Capping Protein

**CCT:** Chaperonin Containing TCP-1

**CHAPS:** 3-[(3-Cholamidopropyl) dimethylAmmonio]-1-PropaneSulfonate

**CK-B:** Brain Creatine Kinase

**CMC:** Critical Micellar Concentration

**CTAB:** CetylTrimethylAmmonium Bromide

**DDI:** Double Distilled Water

**2-DE:** Two Dimensional Electrophoresis

**DIGE:** two-dimensional Difference In-Gel Electrophoresis

**DMT 1:** Divalent Metal Transporter 1

**DTT:** DiThioThreitol

**EAM:** Energy Absorbing Matrix

**ECD:** Electron Capture Dissociation

**EF:** Elongation Factor

**EP:** ErythroPhagocytosis

**ER:** Endoplasmic Reticulum

**ERAD:** Endoplasmic Reticulum Associated Degradation

**ESI:** ElectroSpray Ionization

**ETD:** Electron Transfer Dissociation

**FAC:** Ferric Ammonium Citrate

**FTH:** Ferritin heavy chain

**FTL:** Ferritin light chain

**Ga:** Gluconoacetobacter

**GAPDH:** Glyceraldehyde 3 Phosphate Dehydrogenase

**GDI:** Rho GDP Dissociation Inhibitor

**Gln:** Glutamine

**GO:** Gene Ontology

**HGF:** Hepatocyte Growth Factor

**HH:** Hemochromatosis

**HO 1:** Heme Oxygenase 1

**HPLC:** High Performance Liquid Chromatography

**HSP:** Heat Shock Protein

**ICAT:** Isotope-Coded Affinity Tagging

**IEF:** IsoElectro Focusing

**Ig:** Immunoglobulin

**IPG:** Immobilized pH Gradient

**IRE:** Iron Responsive Elements

**IRPs:** Iron Regulatory Proteins

**IT:** Ion Trap

**LC:** Liquid Chromatography

**LPS:** LipoPolySaccharide

**MALDI:** Matrix Assisted Laser Desorption/Ionization

**MDMs:** Monocyte Derived Macrophages

**MIF:** Macrophage Migration Inhibitory Factor

**MMP 9:** Metalloproteinase 9

**Mr:** relative Molecular Mass

**MS:** Mass Spectrometry

**MudPit:** Multidimensional LC coupled to MS

**NO:** Nitrogen Oxide

**OD:** Optical Density

**PAGE:** PolyAcrylamide Gel Electrophoresis

**PAS:** Periodic Acid Schiff

**PFF:** Peptide Fragment Fingerprinting

**PGK I:** PhosphoGlycerate Kinase 1

**pI:** Isoelectric point

**PMF:** Peptide Mass Fingerprinting

**PVDF:** Polyvinylidene Fluoride

**Q:** Quadrupole

**RBC:** Red Blood Cell

**RES:** Reticulo Endothelial System

**SCX:** Strong Cation Exchange

**SDS:** Sodium Dodecyl Sulphate

**SELDI:** Surface Enhanced Laser Desorption Ionization

**SILAC:** Metabolic Stable-Isotope Labelling

**SPR:** Surface Plasmon Resonance

**SSP:** Standard Spot Number

**T:** Tween-20

**TBP:** TriButhylPhosphine

**TCA:** TrichloroAcetic Acid

**TLRs:** Tools Like Receptors

**TOF:** Time Of Flight

**VDAC:** Voltage Dependent Anion Channels





# SESSION 1



# PROTEOME AND PROTEOMICS

## PROTEOME AND PROTEOMICS

Proteomics is an emerging area of research in the postgenomic era that deals with the global analysis of gene expression via a combination of techniques for resolving, identifying, quantifying, and characterizing proteins (Banks *et al.*, 2000).

The terms proteomics and proteome were coined by Marc Wilkins and colleagues in the early 1990s, and have then been adopted by the research community at large. The proteome term refers to the full complement of proteins encoded by the genome of an organism (Wilkins *et al.*, 1996, Wilkins *et al.*, 1996 ). It can be seen as the end product of the genome: it is the set of expressed proteins at a given time under defined conditions.

Biochemical studies of protein activity have historically focused on the analysis of single molecular species. The rapid discovery of new gene products, via large-scale genomic initiatives, has necessitated the development of alternative strategies to evaluate protein function. The challenge in recent years has been to develop high-throughput approaches to facilitate systematic protein analysis of biological samples, to map functional interactions between proteins on a global scale, and to place them in a biological context.

To really understand biological processes, we need to understand how proteins work inside and around cells since they are the functioning units. Proteomic, the science that studies the proteome, includes not only the identification and quantification of proteins, but also the determination of their localization, modifications, interactions, activities, and, ultimately, their function. Cells express genes encoding proteins with unique, cell-specific functions in addition to proteins that carry out generic, yet essential functions. Many complex mechanisms involve deoxyribonucleic acid (DNA) conversion into protein. The central dogma describes the one-way mechanism by which protein is produced by DNA. This process begins by transcribing DNA into ribonucleic acid (RNA). The RNA molecule is complementary to the DNA template strand and, unlike DNA, has the ability to leave the nucleus. Once outside the nucleus, the process of translation converts RNA's nucleotide sequence into specific amino acid building blocks. The summation of these building blocks leads to the creation of a protein (Pierce *et al.*, 2007). Then the protein is subjected to post-translational modifications (PTMs). While it is often conceptualized that one gene produces one protein, it is known that the expressed products of a single gene in reality represent a protein population that can contain large amounts of micro-heterogeneities (Fig. 1-A). Consider the example of a protein that has three potential modification states: glycosylation,

phosphorylation and ubiquitination. There are eight potential protein forms that could be presented if each modification only occurs at a single site and is not mutually exclusive (Fig. 1-B). Each additional state (e.g. another phosphorylation, acetylation, protease cleavage, lipidation, acetylation, etc.) or modification site would add a large amount of additional diversity to the expression profile of that protein (64 potential forms for just six modifications).

Approximately 200 different post-translational modifications have been reported, encompassing a wide variety of reversible and irreversible chemical reactions, which influence the diversity, affinity, function, cellular abundance and transport of proteins (Peng and Gygi, 2001). The proteome comprises all of these forms, which make its analysis incredibly complex, as any protein may be present in a cell, in any form, at any given time.

As a consequence, every organism possesses one genome and multiple proteomes. Proteomes are constantly changing in response to environmental stimuli, chemicals and drug treatments, as well as growth and disease processes (Reynolds, 2002). Many of these changes hold considerable interest for researchers seeking to understand complicated pathologies, regulation of cell processes and response to stress. While proteomics initially encompassed just two-dimensional (2D) gel electrophoresis for protein separation and identification, now it refers to any procedure that characterizes large sets of proteins. The explosive growth of this field is driven by multiple forces: genomics and revelation of more and more new gene products; powerful protein technologies, (such as newly developed mass spectrometry approaches, global yeast two-hybrid techniques, and spin-offs from DNA arrays); and innovative computational tools and methods to process, analyze, and interpret prodigious amounts of data.

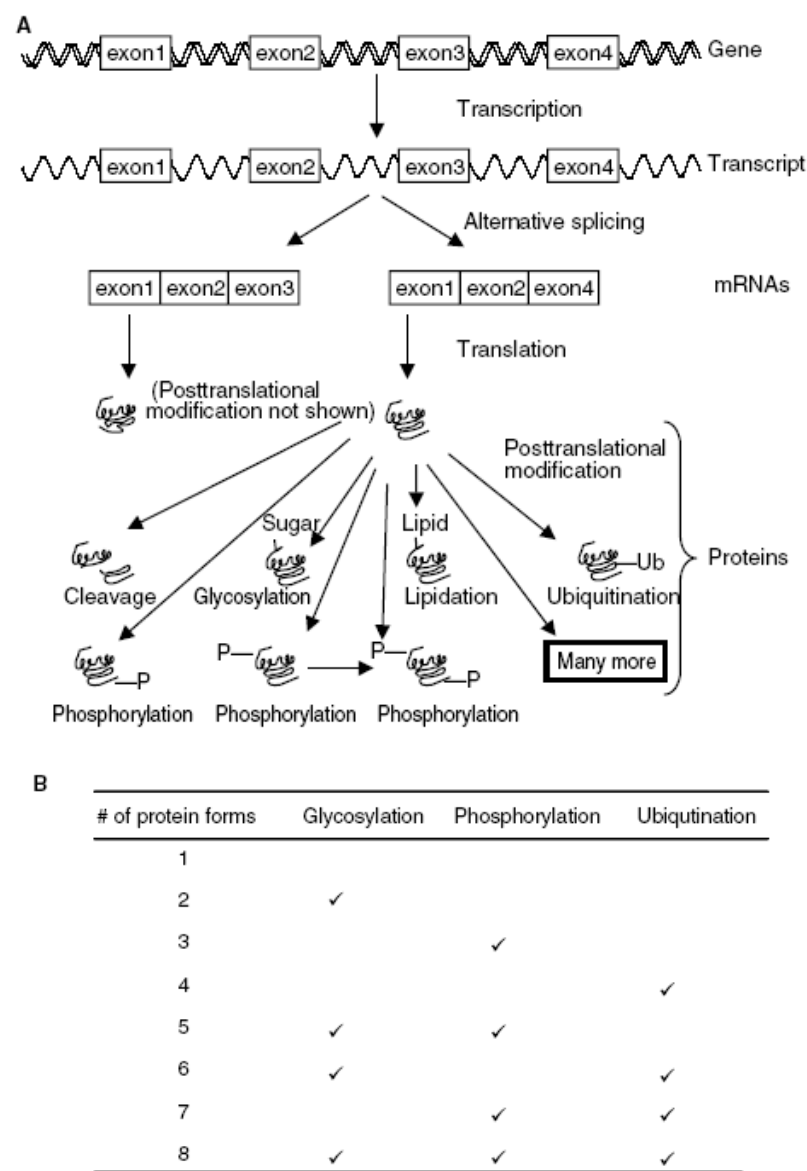


**Fig 1.** Complexity of the proteome. **A.** One gene can produce multiple mature mRNAs via alternative splicing of pre-mRNA transcripts. Following translation, a myriad of post-translational modifications can produce further variations in the number and types of protein forms. **B.** An example of a protein that exists with three potential post-translational modifications is shown: glycosylation, phosphorylation and ubiquitination. Eight potential protein types can be formed. The presence of each modification is noted by a tick. Adapted from Peng and Gygi, 2001.



# CHAPTER 1

## CLASSICAL PROTEOMICS

### 1. SAMPLE PREPARATION AND PROTEIN EXTRACTION

Extracting analytes from cells and biological tissues is often a serious challenge for analytical chemists. The challenge is even more difficult for proteins, due to their high degree of heterogeneity and to the difficulty of breaking their structural interactions and release them when they are bound in macromolecular assemblies. For this reason, cells and tissues should be treated as the sum of individual parts or fractions and cannot be considered as homogeneous substrates. Protein extracts can be used for a variety of purposes: identification and quantification, functional studies, proteomic analysis etc. (Canas *et al.*, 2007). The results of any experiment are dependent on the condition of the starting material. Therefore, choosing the proper experimental model and preparing the sample carefully is crucial for obtaining significant and trustworthy results.

Sample preparation is a matter of great importance, especially in comparative proteomics, where we are usually looking for minor differences between experimental and control samples. One of the main obstacles associated with analyzing such complex material as a biological sample is the dynamic range of protein abundance. In a single cell there could be only 10 copies of transcription factor at the bottom of this range, but at the other end we may expect up to 1,000,000 copies of a more abundant protein. To deal with this problem, it is advisable to remove the most abundant proteins, thus the complexity of the entire sample could be reduced. Several methods of samples fractionation and techniques of proteins enrichment could be used to achieve this goal (Bodzon-Kulakowska *et al.*, 2007).

Besides biological samples may contain contaminants that interfere with analysis by two dimensional electrophoresis (2-DE). Lysates or biological fluids are complex mixtures that contain a wide variety of non-protein substances in addition to the proteins to be analyzed. These substances often interfere with the resolution of the electrophoretic separation or the visualization of the result. Macromolecules (e.g., polysaccharides and DNA) can interfere with electrophoretic separation by clogging gel pores. Small ionic molecules can impair isoelectric focusing (IEF) separation by rendering the sample too conductive. Other substances (e.g., phenols and lipids) can bind to proteins, influencing their electrophoretic properties or solubility. In many cases, measures to remove interfering substances can result in significantly clearer 2D patterns with more visible spots and better resolution. It

should be borne in mind, however, that analysis of samples by 2-DE is usually most successful and informative when performed with minimally processed samples, so it is important that any steps taken to remove interfering substances is appropriate to the sample and performed only when necessary. Procedures for the removal of interfering substances therefore represent a compromise between removing non-protein contaminants, and minimizing interference with the integrity and relative abundances of the sample proteins (Berkelman, 2008). Depending on these remarks, demands on the extraction and preparation procedures are different.

## **1.1 SOURCE OF SAMPLES**

Tissues, cell lines, primary cell cultures and body fluids (such as plasma or cerebrospinal fluid (CSF)) can be used as protein source. Different branches of proteomics are also devoted to plant, bacteria and virus proteins. Anyway, independently from the experimental model, sample preparation is a matter of great importance, especially in comparative proteomics. Thus, not only an appropriate experimental model, but also an optimized protein extraction protocol, have to be carefully considered to obtain reliable results.

### **1.1.1 Eucaryotic source of sample: animal cells**

Recent advances in medical sciences would not be possible without animal research. Animal models for human diseases are indispensable in understanding the background and biology of a disease and in finding out the methods for its treatment. Mice and rats, for several reasons, are the models of choice. Well-characterized strains of animals are available. Physiological processes that occur in humans are often (but not always!) similar to those in rodents. Thus, studies on the physiopathology of various diseases at the proteome level are possible due to a relatively high similarity between the rats/mice and human proteins. Transgenic animals seem to be another great promise for obtaining appropriate and useful models. It has to be remembered that these models cannot be considered as a complete equivalent of human disorders, as they present only some of their aspects. We have to be aware that, apart from similarities, some systems could be different (for example, the rat steroid system is different from the human one). Aspects of gender, weight, feeding, etc., also need to be taken into consideration before establishing a model for a particular experiment. When a particular animal model has been established, usually the tissue connected with a particular disease is chosen for detailed analysis. It's obvious that every tissue has its own characteristics and has to be handled properly for protein extraction. During tissue preparation for proteomic analysis, it is important to diminish its heterogeneity, as much as it is possible. The sample should be pure and relevant. It seems to reflect the state of living organism, and sometimes, collected material could be cultured



for further experiments. On the contrary, simplification of the sample is one of the greatest advantages of cell culture serving as experimental model, especially in proteomics. This model allows for studying the behaviour of a single type of cell in the absence of the complexity of the entire tissue. This may help to reveal changes in low abundance proteins, which could be impossible in the whole tissue study. Body fluids are another important source providing vital information on the function of living organisms. Body fluids (such as blood, CSF, urine, and saliva) are relatively easily available; thus they are commonly used for clinical diagnosis (Hortin *et al.*, 2006, Sowell *et al.*, 2009).

### **1.1.2 Prokaryotic source of sample: bacteria**

Concerning bacterial samples preparation, problems can arise in disrupting cells, due to the presence of thick cell walls and polysaccharide capsule of certain bacterial groups (Cash, 1998). Some bacteria could simply be lysed by the constituents of the lysis buffer (reducing agents and detergents), but others must be disrupted mechanically (e.g. by sonication). Sometimes, removal of the cell wall by enzymatic digestion is necessary. It has to be remembered that 2-DE analysis or another technique, used to separate and analyze bacterial proteins, will reflect the proteome of the bacteria at the time when proteins were solubilized. It means that all manipulations, such as centrifugation, may stress the bacteria and thus, influence the protein pattern. Another promise of bacterial proteomics, arises from the fact that the genomes of some bacteria, e.g. *Escherichia coli*, are now determined; so the complementary proteome analysis may bring some new interesting facts concerning cellular metabolism. The relatively small size of bacterial genomes makes it likely that we obtain a complete description of the free living organism from its genes to its complementary proteins and their functions, in the next few years.

## **1.2 METHODS OF CELL DISRUPTION**

The first step in sample preparation for proteomic analysis is cell disruption. One of the simplest methods is homogenization that helps to break down the initial sample, to finer particles in the nano- to micro-meter scale, so that target molecules, such as proteins, can be released from the tissue for further processing. Ultrasonic homogenizers (also called disintegrators), are based on the piezoelectric effect. Alternatively, pressure homogenizers (such as French press) are an effective system for homogenization of eukaryotic, as well as microbial and plant cells in suspension. In addition, French press is often applied for the preparation of cell membranes for further experiments. Finally, osmotic lysis methods utilize osmotic pressure to destroy cell walls and membranes. Detergents are also efficient for cell disruption and extraction of nuclear and mitochondrial membranes. The most commonly applied detergents are Triton X-100, Tween 80, Nonidet P-40 (NP 40) and saponin.

### 1.3 PROTEIN SOLUBILIZATION

Protein solubilization strongly affects the quality of final results and thus determines the success of the entire experiment. Once isolated, proteins are often insoluble in their native state. To avoid protein modifications, aggregation or precipitation (resulting in the occurrence of artefacts and subsequent protein loss), sample solubilization implicates the use of chaotropes, detergents, reducing agents and protease inhibitors.

Usually, a neutral chaotropic agent, urea, is used at high concentrations ranging from 5 to 9 M to effectively disrupt secondary protein structure. As indicated by Rabilloud (1997), addition of thiourea to the denaturing solution containing urea, allows for substantial improvement of protein solubility. Addition of thiourea to the sample buffer decreases solubilization of urea. Therefore, when combined with 2 M thiourea, urea concentration should not exceed 5–7 M (Herbert, 1999).

Detergents and amphipathic molecules enable protein extraction and solubilization. It has already been reported the great solubilizing power of zwitterionic detergents (Chevallet *et al.*, 1998, Perdew *et al.*, 1983), in addition it has been proved that non-ionic detergents are also efficient (Luche *et al.*, 2003, Taylor *et al.*, 2003). Nowadays, sulfobetaine 3-[(3-cholamidopropyl)dimethylammonio]-1-propanesulfonate (CHAPS) is most commonly applied in proteomic studies due to its high solubility and a relative lack of detergent-induced artefacts. As regarding solubilization of the integral or membrane-associated proteins it has to be improved by using specific detergents (e.g. Triton X-114 (Polati *et al.*, 2009)).

Reducing agents disrupt disulfide bonds between cysteine residues, thus, promote protein unfolding and enable analysis of single protein subunits. Conventionally, phosphines, e.g. tributylphosphine (TBP) and triscarboxyethylphosphine (TCEP) are used as sulfhydryl reducing agents: they are apolar, therefore don't migrate out of the pH gradient while performing isoelectric focusing. Moreover phosphines do not interact with the alkylating substrates such as 4-vinylpyridine and acrylamide (Herbert *et al.*, 1998). Thus, reduction and alkylation may be performed in a single step.

Finally, if not inhibited during cell membrane disruption, endogenous proteases are responsible for uncontrolled enzymatic proteins degradation. Such proteolysis may produce artefacts and hence complicate further analysis (Olivieri *et al.*, 2001). In general, addition of specific protease inhibitors, or cocktails of them with a broader activity spectrum, is recommended (Rai *et al.*, 2005, Terry *et al.*, 2004).

## 1.4 REMOVAL OF CONTAMINANTS

Among most common contaminants, salts and lipids naturally occur in body fluids and tissues, and may interfere with electrophoretic separation of proteins (Yuana and Desiderio, 2005). Most often, salt removal is being accomplished via (spin, micro) dialysis (Manabe *et al.*, 1999, Lai *et al.*, 2000), ultrafiltration (Jiang *et al.*, 2004, Sickmann *et al.*, 2000), gel filtration, and precipitation (Simpson, 2004). In addition, the use of centrifugal filter devices and the sample buffer added of CHAPS allows for efficient lipid and salt removal. Alternatively, precipitation in acetone or in trichloroacetic acid (TCA)/acetone removes lipids efficiently. Polysaccharides and nucleic acids are negatively charged polymers which interact with proteins and clog the pores of the polyacrylamide gels causing streaking visible on 2D gels. In order to exclude polysaccharides and nucleic acids from the sample, precipitation may be beneficial (e.g. by complexing them with carrier ampholytes). This phenomenon is particularly serious in Gram negative bacteria. In fact, the cell wall is made of high molecular weight polysaccharides that tend to form complexes with nucleic acids that streak in the acidic part of the 2D map. Moreover in order to remove DNA and RNA, digestion with protease free DNase and RNase is often applied (Kikkawa *et al.*, 2006). Finally, buffers, salts and detergents (included in solubilizing solutions) often tend to interfere with further protein separation steps: they inhibit the in-gel digestion process and interfere with the mass spectrometry analysis. Thus they need to be removed at a proper time of analysis. Protein precipitation followed by resuspension in an adequate sample solution belongs to the most commonly applied procedures enabling removal of most of contaminants. Unfortunately, there is currently no method that would allow precipitating all proteins and, consequently, only precipitated proteins can be further resolubilized. Most commonly, precipitation with TCA, acetone, chloroform/methanol, ammonium sulphate or combinations of the above are being performed.

## 1.5 PROTEIN DEPLETION AND ENRICHMENT METHODS

The proteome and subproteomes of any living cell are highly dynamic and of unknown complexity, making the characterization of proteomes a formidable challenge. While the concentration range of proteins in a given sample may exceed 10 orders of magnitude (Anderson *et al.*, 2002), currently available proteomic approaches are estimated to focus on the 30% most abundant proteins in an extract. Proteomic analyses are, hence, complicated and detection of least abundant proteins is hampered by those molecules present at higher concentration. Plasma, serum and CSF, are protein sources of great importance to biomedicine, diagnostics and therapeutics, containing up to 90% of highly abundant proteins such as albumin, immunoglobulins (IgG and IgA), antitrypsin, transferrin, transthyretin,  $\alpha$ 1-antitrypsin, hemopexin and haptoglobin. Removal of these proteins may

increase detection of other molecules present at lower concentration. Various strategies have been presented for the removal of high-abundant proteins (Sitnikov *et al.*, 2006), most of which are based on affinity chromatography employing mimetic ligands (Kabir, 2002, Sato *et al.*, 2002), proteins A and G (Funtoulakis *et al.*, 2004), and antibodies.

On the other side, enrichment methods allow for increasing the concentration of proteins of interest. This statement is really important in the proteomics study, because usually low-abundance proteins carry valuable diagnostic information and are responsible for processes ongoing in cells. In order to increase the likelihood of detecting less abundant proteins, a variety of protein separation techniques are applied to reduce the complexity of a sample prior to proteome analysis (Funtoulakis *et al.*, 2003, Yates *et al.*, 2005). The fundamental idea of prefractionation is to isolate the sample into distinct fractions containing restricted numbers of molecules. Preparative liquid electrophoretic methods are common fractionation systems for proteome profiling. The latest technology platforms that have been developed for proteomics include the Rotofor, a multicompartiment instrument capable of fractionating proteins according to their pI (Righetti *et al.*, 2005).

Alternatively, common methods of protein enrichment and purification rely on selective precipitation and immunoprecipitation. A novel approach for mining the “unseen proteome” is ProteoMiner™ technology (Bio-Rad), which exploits solid phase combinatorial peptide ligand libraries (Guerrier *et al.*, 2008, Righetti *et al.*, 2008). ProteoMiner™ simultaneously reduces the concentration of high abundance proteins and enriches the concentration of trace proteins without depletion of any specific proteins, in a high throughput manner. Each bead binds a specific binding partner and a wide diversity of ligands is available (typically millions). The population of beads has such diversity that a binding partner should exist for most, if not all, proteins present in a sample. In this system the binding capacity for high abundance proteins is, in principle, equal to that for low abundance proteins. Thus, when a complex sample is incubated with the bead library, high abundance proteins saturate their binding partner and excess protein is washed away, whilst low abundance proteins are “concentrated” on their specific affinity ligand. In this way the abundance of trace proteins is increased relatively to the highly abundant proteins (see Fig. 2). Importantly, in this system, unlike the use of depletion methods, no fraction is discarded and proteins that may be complexed with high abundance species like albumin are not lost.

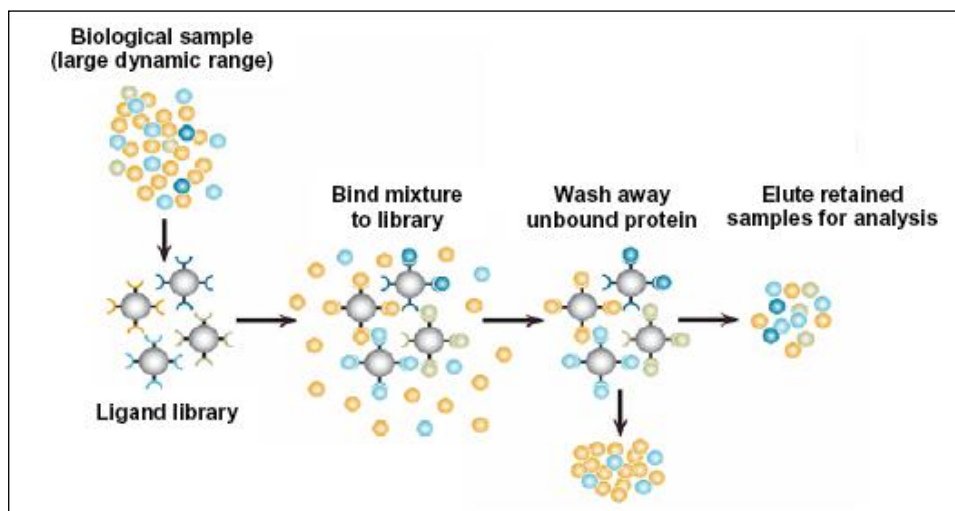


**Fig 2.** ProteoMiner™ technology: each bead has a different ligand, with affinity for specific proteins of the sample. Adapted from Guerrier *et al.*, 2008.

## 2. METHODOLOGIES AND TECHNOLOGIES IN CLASSICAL PROTEOME STUDY

Once proteins are purified and ready to be separated, there is a plethora of proteomic techniques to investigate the biological problem the scientist is dealing with. The choice of a given proteomic approach should depend on the type of biological question asked, since each proteomic technology is characterized by specific applications, technical advantages and limitations. In general, proteomic approaches can be used for a) proteome profiling, b) comparative expression analysis of two or more protein samples, c) localization and identification of posttranslational modifications, and d) studying protein–protein interactions. A classical widely used proteome approach relies on 2-DE coupled to mass spectrometry analysis.

### 2.1 TWO-DIMENSIONAL GEL ELECTROPHORESIS

The traditional two-dimensional gel electrophoresis (2-DE) method was introduced in 1975 by O’Farrell (O’Farrell, 1975) and represents now one of the most commonly applied techniques in proteomics. This method is based on orthogonal separation of proteins according to different physicochemical principles. Proteins in complex mixtures are electrophoretically separated, first according to their isoelectric point (pI) by isoelectric focusing (IEF) and, subsequently, according to their relative molecular mass (Mr) by sodium-dodecyl sulphate polyacrylamide gel electrophoresis (SDS-PAGE). Depending on the gel size and pH gradient, it is possible to resolve simultaneously more than 5000 protein spots (Goerg *et al.*, 2000). 2-DE is used for large-scale protein separation since its invention for purification, identification as well as quantification of proteins (Fig. 3). Moreover, 2-DE provides information on changes in protein expression, as well as on different protein isoforms and post-translational modifications (Mukherji, 2005).

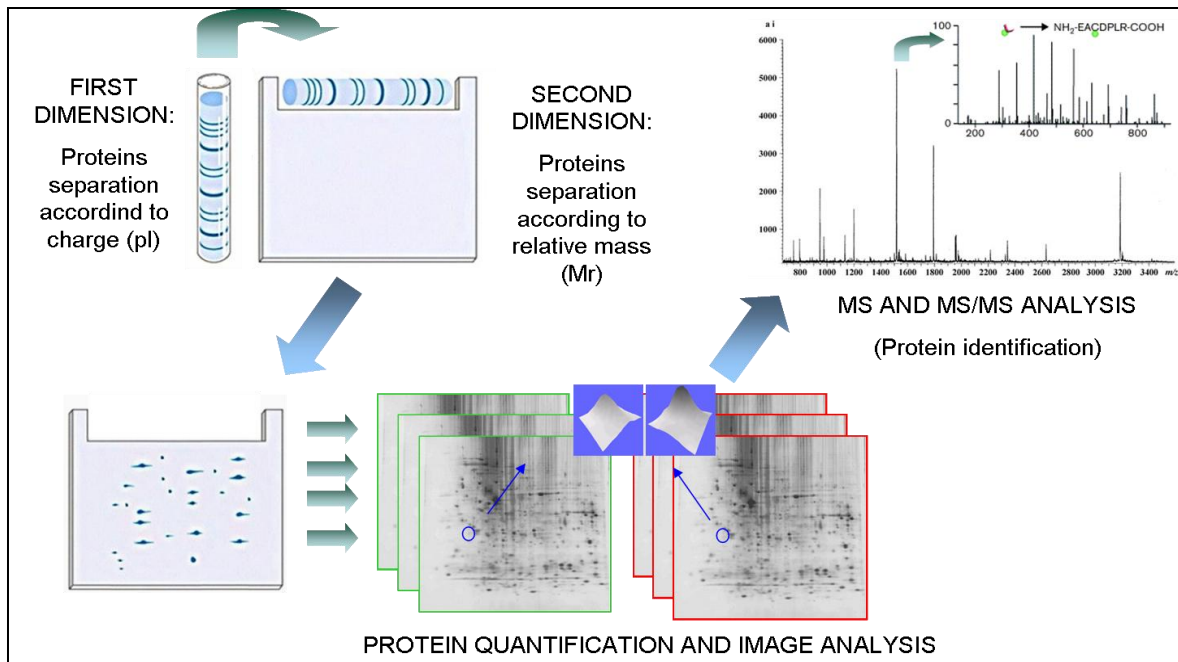


**Fig 3.** Overview of two-dimensional gel electrophoresis (2-DE) based strategy.

### 2.1.1 2-DE Methodologies

As mentioned in previously, the success of any protein separation and purification techniques depends on the protein solubilization method. A traditional sample preparation for 2-DE involves cell or tissue disruption and protein solubilization in presence of high concentrations of urea, reducing agents and detergents. A common 2-DE sample buffer contains 7 M urea, 2 M thiourea, 20 mM Tris, 3% CHAPS. The immobilized pH gradient strip (IPG strip) is then rehydrated with sample, and proteins are separated by IEF.

During IEF, under the influence of an electric field, each protein migrates through the pH gradient until it reaches its pI. Until recently, a mixture of carrier ampholytes was commonly used to create the pH gradient for IEF. However, problems were occurring with these carrier ampholytes-created pH gradients, such as so-called “cathode drifting” and pH flattening near the anode (Righetti *et al.*, 1973). In order to circumvent the ampholyte-linked technical difficulties, commercially available immobilized pH gradients (Bjellqvist *et al.*, 1982) are now generally used. The pH gradient in IPG strips is created by acrylamido-buffers (containing weakly acidic or basic buffering groups) admixed to neutral acrylamide monomers and poured gradient-wise via a two-vessel gradient mixer. Covalent immobilization of the buffering groups inside the polyacrylamide gel prevents drifting of the pH gradient under the influence of an electric current, thus increasing the resolution as well as the reproducibility of 2-DE patterns. Moreover, by using IPG strips with a reduced slope of the pH gradient it is possible to significantly increase the resolution of protein separation. Another application of IPG strips is the creation of the so-called zoom-gels, where narrow pH gradients are used allowing for high-resolution separation of spots containing proteins with the same molecular mass but slightly different pI.

After IEF, the IPG strips (with focused proteins) is equilibrated in a SDS-containing solution in order to proceed with the second dimension, where proteins are separated according to their molecular mass by means of SDS-PAGE. Also the resolution of second dimension may be improved by changing the percentage of polyacrylamide and by using pore gradient gels (Fountoulakis *et al.*, 1998). However, SDS-PAGE separation of high molecular mass proteins as well as very low molecular mass ones is still rather challenging. The applicability of 2-DE analysis generally remains limited to proteins with molecular size between approximately 10 and 150-200 kDa.

### 2.1.2 Protein Detection And Quantification

Protein spots on 2-DE gels can be visualized by a variety of protein staining techniques, each characterized by specific technical aspects, sensitivity, linear range for quantitation, reproducibility and compatibility with mass spectrometric analysis (Table 1). In fact, the major challenge for protein visualization in 2-DE is the compatibility of sensitive protein staining methods with mass spectrometric analysis. Among the most commonly used protein staining methods, Coomassie Blue staining has a sensitivity of up to 30 ng/spot and compatibility with mass spectrometry, while silver staining has an higher sensitivity (1 ng/spot), but was originally incompatible with mass spectrometric analysis, due to the aldehyde fixation steps. Several fluorescent staining methods have been also developed, including Sypro staining and Cy-dyes.

**Table 1.** Commonly used protein staining methods for 2-DE analysis.

Staining Method	Sensitivity	Reversible	MS compatibility	Straightforward protocol	Highly reproducible	Linearity: order of magnitude
Silver	1 ng	-	-	-	±	1
Coomassie	100 ng	+	+	+	+	2
Coomassie R250	50 ng	+	+	+	+	2
Colloidal coomassie	10 ng	+	+	+	+	2
Sypro Ruby	1 ng	+	+	+	+	> 3
Cy-dyes	125 pg	+	+	+	+	4

Sypro Ruby staining (Berggren *et al.*, 2000) allows for a much higher sensitivity, a significantly wider dynamic range, less false-positive staining, and is compatible with mass spectrometric analysis. In addition, Sypro Ruby allows for the detection of lipoproteins, glycoproteins, metalloproteins, calcium-binding proteins, fibrillar proteins and low molecular mass proteins that are very difficult to stain by using other methods. The recently developed

Flamingo stain (Bio-Rad) proved to be even more sensitive than Sypro Ruby. Based on Cy-dyes, two-dimensional difference in-gel electrophoresis (DIGE) technology has been developed. It permits the simultaneous separation of two samples on the same gel by the differential labelling with different cyanine dyes prior to the first dimension (Unlu *et al.*, 1997). Cyanine dyes carrying an N-hydroxysuccinimidyl ester reactive group covalently bind the  $\epsilon$ -amino group of lysine residues in proteins. Staining with these dyes is more sensitive than silver staining, giving a linear response to protein concentrations of up to four orders of magnitude. In addition, no fixation or destaining steps are required during DIGE analysis, reducing protein loss from the gels. Hence, a major advantage of this technique is a significant reduction in inter-gel variability, facilitating spot identification and matching during image analysis, thus increasing the number of analyzable spots.

### 2.1.3 Two-Dimensional Gel Image Analysis

The possibility of detecting protein expression changes (associated with diseases and treatments or finding therapeutic molecular targets) has been, among many other applications, a major incentive to the development of dedicated software systems for 2-DE gel image analysis. In the early 1980s, the first packages started to be delivered to the public and some of them have survived the computational evolution of the last two decades. Among these were PDQuest and ImageMaster 2D Platinum (based on Melanie). Table 2 gives a list of the major available packages. In general, besides basic visualisation properties, the major functions of software systems for 2-DE gel image analysis are (i) detection and quantification of protein spots on the gels, (ii) matching of

**Table 2.** Major commercialised 2-DE image analysis software.

Software	Company	Source website
DeCyder	GE Healthcare	<a href="http://www.gehealthcare.com">www.gehealthcare.com</a>
Delta2D	Decodon	<a href="http://www.decodon.com">www.decodon.com</a>
ImageMaster 2D Platinum	GE Healthcare	<a href="http://www.gehealthcare.com">www.gehealthcare.com</a>
PDQuest	Bio-Rad	<a href="http://www.bio-rad.com">www.bio-rad.com</a>
Progenesis (formerly Phoretix)	Nonlinear Dynamics	<a href="http://www.nonlinear.com">www.nonlinear.com</a>
Proteomeweaver	Definiens/Bio-Rad	<a href="http://www.definiens.com/www.bio-rad.com">www.definiens.com/www.bio-rad.com</a>

corresponding spots across the gels, and (iii) detection of significant protein expression changes. Any other additional feature, such as data management and database integration, may or may not be included. Moreover, detection algorithms included in the packages generally comprise filtering steps to automatically remove streak artefacts and noise spikes. Spot detection algorithms also produce quantitative information of the protein spots, such as the spot area and OD (maximum intensity value in the area). Matching of gel images is a critical process: it depends on the similarity of the spatial distribution of spots across all the gels, which may vary according to experimental gel running conditions and gel scanning.



Some tools propose the initialisation of a few corresponding spots representing the same proteins in different gels: a landmarking step. These landmarks will then be used to warp the gel images and correct possible distortions, and consequently improve the matching quality. Anyway, each tool has its own strengths and weaknesses that vary depending on the gel type and experimental conditions. In the software that deals with DIGE gels, only the spot detection function is adapted. Since the same proteins will be localised in the same x and y coordinates on the gels, the spot detection procedure is the same for the co-detected gels. The matching step is thus straightforward and subject to much less errors. Finally, it should be noted that, despite continuous optimization of algorithms used by these software, a time-consuming visual verification remains necessary for all steps of software analyses of 2-DE patterns.

#### **2.1.4 Advantages And Limitations Of 2-DE Based Proteomics**

2-DE has the enormous advantage to display simultaneously thousand of proteins on a single 2D map, obtaining a picture of any complete proteome being studied. Furthermore, it permits to analyze polypeptides in their full-length form, thus allowing for characterization of single PTMs by detection with specific antibodies, as well as with specific staining (e.g. Pro-Q® Diamond phosphoprotein stain). However, while the scientific community is digging more deeply in proteomes, also thanks to fractionation methodology, there are still 2-DE based studies which are “re-discovering similar proteomes in different samples”. This observation creates the impression of scratching the surface: it seems that many studies still reveal similar “housekeeping proteomes” as found in many cell and tissue types, or that the candidate biomarkers for a specific disease are often markers for a generic phenomenon underlying several diseases, such as inflammation (Petrak *et al.*, 2008). Indeed many proteins are expressed at such low levels that they will escape detection, and other technical problems linked with 2-DE proteomic approach remain, such as co-migration of proteins and loss of insoluble ones (Bronstrup, 2004). Nevertheless, 2-DE remains a very useful method for displaying and quantification of a majority of proteins in almost any kind of biological samples, and its technologies are robust and increasingly reproducible. Moreover, the sensitivity and applicability of presently available technologies are improving continuously, and for many types of biological questions, specific proteomic approaches are currently available.

## 2.2 MASS SPECTROMETRY TECHNOLOGIES

The invention of mass spectrometers made possible the analysis of proteins and peptides – molecules that have classically been studied individually or in small numbers – in a large-scale and in a high-throughput mode (Wilkins *et al.*, 1996). Remarkable progress has been achieved in the meantime: current mass spectrometric platforms can cover a dynamic range of up to  $10^4$  (Lescuyer *et al.*, 2007), and extensive protein and peptide pre-fractionation and sophisticated data acquisition and processing are in place. Today's shotgun proteomic approaches reveal up to some 2000 protein identities and the number of true positive protein identifications within those long lists has enormously increased over the years. This important achievement can be attributed to (a) improved mass spectrometric instrumentation with better sensitivity and specificity, the latter based on superior mass accuracy and resolution (e.g. Orbitrap (Makarov, 2000)); and (b) more sophisticated software for peptide sequencing and protein identification.

### 2.2.1 Protein Identification By Mass Spectrometry

In a typical proteomic experiment, proteins of interest are digested with enzymes for identification by mass spectrometric analysis. Trypsin is the most commonly used protease in proteomic analysis and displays good activity with in-gel digestion, as well as with in-solution digestion.

Mass spectrometers consist of an ion source that converts analyte molecules into gas-phase ions, a mass analyzer that separates ionized analytes on the basis of their mass-to-charge ( $m/z$ ) ratio, and a detector that records the number of ions at each  $m/z$  value. Regarding ion sources, matrix-assisted laser desorption/ionization (MALDI) (Karas *et al.*, 1988) and electrospray ionization (ESI) (Fenn *et al.*, 1989) are central in proteomics.

MALDI is generally more salt-tolerant than ESI and it is typically coupled to time-of-flight (TOF) analyzers. For successful MALDI analysis, the key point is the proper choice of matrix and sample deposition method, to achieve the highest possible sensitivity and accuracy. The most popular matrices for proteomic applications include  $\alpha$ -cyano-4-hydroxycinnamic acid (CHCA), sinapinic acid (SA) and 2,5-dihydrobenzoic acid (DHB). Particularly, MALDI mass spectrometry, thanks to its speed, sensitivity, accuracy, satisfactory tolerance to impurities and ease of automation, allows for protein identification by the set of measured proteolytic peptide masses. This process is known as peptide mass fingerprinting (PMF) and Mascot is among the most used algorithms in this identification approach (Perkins *et al.*, 1999). Briefly, the experimental mass profile is matched against those generated *in silico* from the protein sequences in the database using the same enzyme cleavage sites. Unfortunately, the lack of sequence data makes identification by PMF ambiguous. The recent introduction of LC-MALDI technology offered a sophisticated and efficient mean of sample purification

and separation combining the advantages of capillary liquid chromatography (LC) with the sensitivity and accuracy of MALDI-MS; in fact in the newest instruments, peptides eluted from the column are directly spotted onto target plate by robot machines (Ro *et al.*, 2006). ESI, instead, is often coupled to ion trap (IT) or quadrupole (Q) analyzers as this combination enables efficient peptide sequencing by induced fragmentation (MS/MS). In an ESI ion source the ionization process occurs under atmospheric pressure and the sample is introduced as liquid, therefore electrospray may be coupled directly to liquid chromatography systems. In particular, reversed-phase liquid chromatography coupled to tandem mass spectrometry (RP-LC-MS/MS) is a well established and commonly used procedure for identification of the in-gel digested proteins. Furthermore, newly introduced nano HPLC combined with ESI-MS/MS has emerged among the most widely used and the most powerful tools for proteomic research. Indeed, miniaturizing the HPLC separation column inner diameter improves electrospray sensitivity, because the concentration of equally abundant analytes in the LC mobile phase is proportional to the square of the column internal diameter. Moreover, because the sample must be loaded at flow rates of 200 nL/min, the sample volume to be injected onto a conventional nano HPLC system is usually only 1-2  $\mu$ L. This approach usually requires an additional salt removal step during peptides preparation. In fact, a disposable C18 RP extraction tip, to remove insoluble particles and salts, and to pre-concentrate peptides has been introduced (Rappsilber *et al.*, 2003). For similar reasons, commercially available capillary chromatography systems include trapping pre-columns, where the sample is purified, desalted and pre-concentrated prior to injection onto the capillary column. In proteomic applications, the positive ion mode is mostly used, in which ionization is based on protonation of the analyte molecules, therefore the sample is often acidified, e.g. with formic or trifluoroacetic (TFA) acids, to facilitate ion formation.

Very recently, a new ionization technique was devised termed desorption electrospray ionization (DESI). Here the charged droplets of solvent are sprayed onto the analyzed object, so that molecules present on its surface are ionized (Takats *et al.*, 2004). DESI can be applied to solids, liquids (including complex biological samples) and adsorbed gases. Importantly, DESI apparently does not require sophisticated sample pre-treatment and tissue sections could be directly analyzed.

The mass analyzer is central to mass spectrometric technology, and in the proteomics context, its key parameters are: sensitivity, resolution, mass accuracy and ability to produce information-rich fragment mass spectra from peptide ions (tandem mass or MS/MS spectra). There are five basic types of mass analyzers currently used in proteomics (Aebersold *et al.*, 2003): ion trap (IT), time-of-flight (TOF), quadrupole (Q), Fourier transform ion cyclotron resonance (FT-ICR), and the newly developed Orbitrap system (Makarov,

2000). Often, they work as stand-alone mass analyzer, but the current trend points towards hyphenated systems in order to combine the advantages of different analyzers in one mass spectrometer (Fig. 5). In reflector TOF instruments (Fig. 5a), the ions are

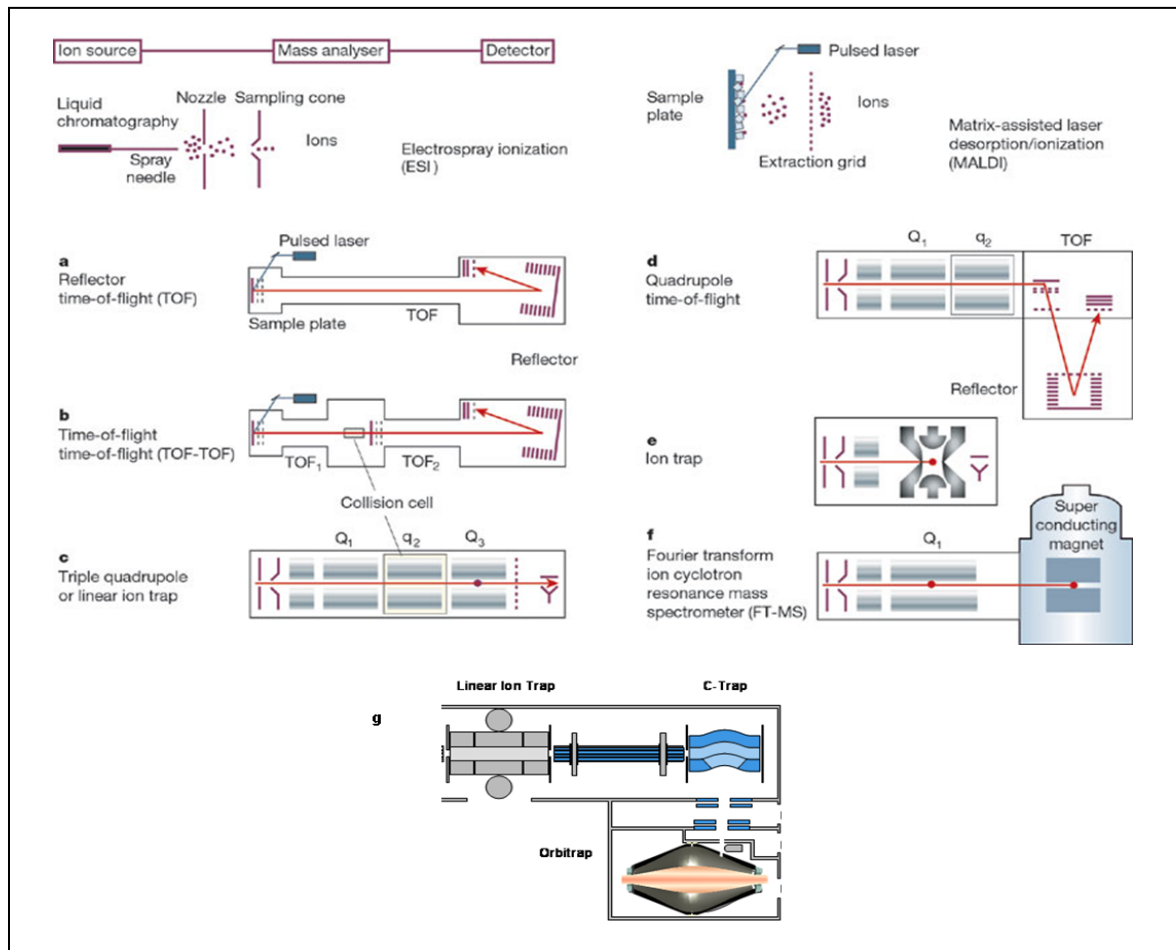


**Fig 5.** Mass spectrometers used in proteomic research. The left and right upper panels depict the two ionization technologies, electrospray ionization (ESI) and matrix-assisted laser desorption/ionization (MALDI). The different instrumental configurations (a–f) are shown with their typical ion source. Adapted from Aebersold and Mann, 2003.

accelerated to high kinetic energy and are separated along a flight tube as a result of their different velocities. The ions are turned around in a reflector, which compensates for slight differences in kinetic energy. The TOF-TOF instrument (Fig. 5b) incorporates a collision cell between two TOF sections. Ions of one  $m/z$  ratio are selected in the first TOF section, fragmented in the collision cell, and the masses of the fragments are separated in the second TOF section. Quadrupole mass spectrometers select ions by time-varying electric fields between four rods, which permit a stable trajectory only for ions of a particular desired  $m/z$ . In the triple quadrupole analyzer or linear ion trap (LTQ) (Fig. 5c), ions of a particular  $m/z$  are selected in a first section ( $Q_1$ ), fragmented in a collision cell ( $q_2$ ), and the fragments separated and scanned out in  $Q_3$ . The Q-TOF instrument (Fig. 5d) combines the front part of a triple quadrupole instrument with a reflector TOF section for measuring the

mass of the ions. The (three-dimensional) ion trap (IT) (Fig. 5e) captures the ions as in the case of the linear ion trap, fragments ions of a particular  $m/z$ , and then scans out the fragments to generate the tandem mass spectrum. The FT-ICR instrument (Fig. 5f) also traps the ions, but does so with the help of strong magnetic fields. In the Orbitrap technology (Fig. 5g) ions orbit around a central spindle-like electrode and oscillate harmonically along its axis with a frequency characteristic of their  $m/z$  values.

On the basis of this development, a new hybrid mass spectrometer became commercially available very recently: it consists of a LTQ coupled to an IT and the Orbitrap. It combines the robustness, sensitivity, and MS/MS capability of the LTQ with very high mass accuracy and high resolution capabilities of the Orbitrap. The IT-FT-ICR and IT-Orbitrap instruments are especially efficient when combined with fragmentation techniques such as electron capture dissociation (ECD) (Zubarev *et al.*, 2000) or electron-transfer dissociation (ETD) (Syka *et al.*, 2004).

Irrespective to the type of ion source and mass analyzer, MS/MS provides access to sequence data, which allows to more confidently identify peptides. In an MS/MS experiment, daughter ions obtained from fragmentation of a precursor ion produce a unique signature which can be used for database searching. This process is described as peptide fragment fingerprinting (PFF) as opposed to PMF. Identification of proteins using MS/MS data is nowadays performed using three different approaches: (i) peptide sequence tag (Mann *et al.*, 1994), (ii) cross-correlation method and (Eng *et al.*, 1994), (iii) probability based matching (typical example is Mascot (Perkins *et al.*, 1999)). All previously described approaches are based on the assumption that a proteomic or translated genomic databases is available to perform the search. *De novo* sequencing approach, instead, uses the MS/MS spectra as the only reference to directly deduce the peptide sequence using specifically developed string similarity search algorithms. They require spectra of higher quality with smaller fragment errors (such as those obtained with FT-ICR or Orbitrap instruments). Currently, PFF is the most common strategy for identifying proteins because of the greater robustness than PMF or *de novo*.



## CHAPTER 2

# GEL-FREE PROTEOMICS

### 1. MS-BASED PROTEOMICS

MS-based proteomics gives the possibility to identify and quantify as many proteins as possible in a single experiment. Nowadays, LC-MS/MS systems have become one of the preferred methods to conduct large-scale characterization of proteomes. High-performance liquid chromatography (HPLC) is an important separation technique in proteomics. It can easily be coupled to mass spectrometry, which makes it a perfect tool for separation of proteins and peptides directly prior to mass analysis. Liquid chromatography may be used both in top-down and bottom-up proteomics approaches. In the first case, the protein sample is separated and then individual proteins (or simple mixtures) are identified directly by means of tandem mass spectrometry. In the bottom-up approach, the protein, or protein mixture is digested. Single- or multidimensional LC coupled to MS (MudPit) is then used for separation of peptide mixtures and identification of their compounds (Fig. 6). In particular, strong cation exchange (SCX) chromatography is usually adopted as a part of 2D systems, where sample components are first separated on an SCX column and then transferred to the RP column. Chromatographic separation also lowers sample complexity, which makes the analysis more sensitive for low-level components (Kislinger *et al.*, 2005, Yates *et al.*, 2009).

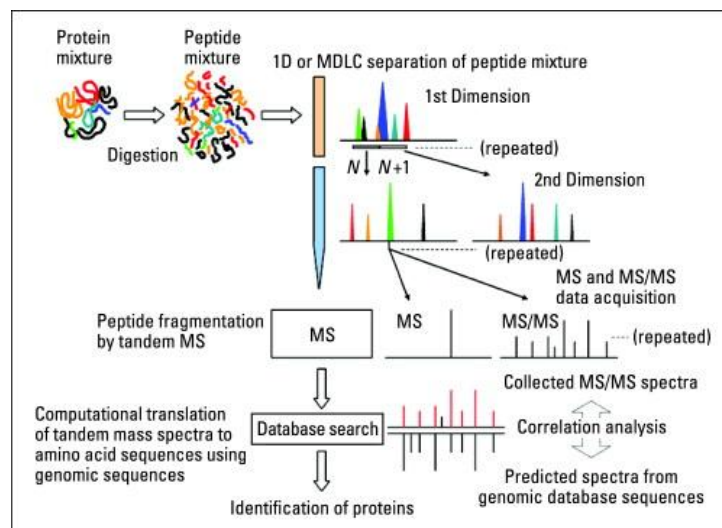


**Fig 6.** Overview of MudPit based strategy. Adapted from Motoyama and Yates, 2008.

While still producing excellent results, “gel-based” quantitative proteomics is going to be superseded by “gel-free” MS-based quantitative proteomics approaches, where

quantification is performed using the mass spectrometric data. In both MALDI- and ESI-MS the relationship between the amount of protein present and the measured signal intensity is measured via different approaches. A first solution came with the technique of stable-isotope dilution. This method is based on the fact that pairs of chemically identical molecules (in this case peptide pairs), but with different stable-isotope composition ( $^2\text{H}$  instead of  $^1\text{H}$ , for example) can be differentiated in a mass spectrometer owing to their mass difference only. Thus the ratio of signal intensities for such peptide pairs should be a direct and accurate measure of the abundance ratio between the two peptides, or proteins, derived from two different biological conditions. To accomplish this purpose, three main approaches exist today which are: (i) metabolic stable-isotope labelling (for example by amino acids in cell culture, SILAC (Ong *et al.*, 2002)), (ii) isotope tagging by chemical reaction and (iii) stable-isotope incorporation via enzyme reaction (Mirgorodskaya *et al.*, 2000). Regarding the second method, a wide variety of isotopically labelled chemicals has been reported (Panchaud *et al.*, 2008). Isotope-coded affinity tagging (ICAT was the first approach described in 1999 by Gygi and co-workers ) (Gygi *et al.*, 1999). Recently, Gygi and colleagues have described a new method called catch-and-release (CAR) (Gartner *et al.*, 2007). Several strategies have been reported that target amines isobaric tag for relative and absolute quantification (iTRAQ) (Ross *et al.*, 2004). A clear advantage of all these chemical approaches is the multitude of available functional groups in proteins allowing designing almost any kind of quantitative tag. However, reactions have to be specific, proceed to completion and involve minimal sample handling. Side reactions are problematic, too, as they considerably increase the sample complexity. It has to be noted that, if such experiment is undertaken, one needs to be able to quantify thousands of labelled peptides using automatic tools capable of extracting the intensity for both peptides of a pair and report a protein ratio based on all identified and quantified peptides. Even more important, such tools should be able to process data from different instrument manufacturers and should also be able to accept result input from different search engines (Mascot, SEQUEST, etc.). Several open-source softwares have been developed by scientific laboratories performing large-scale quantitative proteomic experiments and in general each of them has been developed according to supported instruments or database search algorithms.

## 2. SELDI

As a conceptual modification of MALDI-TOF measurements, surface-enhanced laser desorption/ionization (SELDI) technique, that combines chromatographic separation and mass spectral measurement for proteomic profiling and biomarker discovery is marketed by Bio-Rad. The SELDI chips contain chromatographic coating of selected type (i.e.



hydrophobic, ion-exchange, metal-binding, etc.), on which sample components of a given type are captured. Unbound compounds are washed off, thus contaminants are removed and sample complexity is markedly reduced. After application of a proper energy-absorbing matrix, such as CHCA or SA, the proteins bound to the stationary phase are analyzed for MS profiling. The great advantage of SELDI lies in its ability to remove salts and other impurities prior to MS analysis, thanks to which crude samples can be analyzed, such as urine (Nguyen *et al.*, 2005), cerebrospinal fluid (Ranganathan *et al.*, 2005), serum (Fig. 6) (Ho *et al.*, 2006), etc.

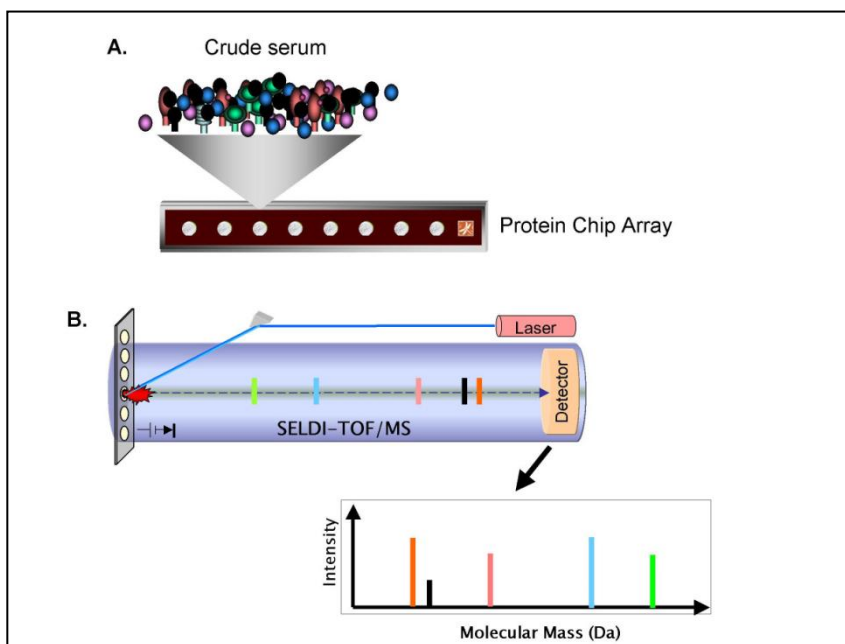


**Fig 6.** Analysis of serum proteins using ProteinChip arrays and SELDI-TOF/MS. **A.** Crude serum sample is placed (and processed) on a ProteinChip array which contains chemically (cationic, anionic, hydrophobic, hydrophilic, etc.) or biologically treated surfaces for specific interaction with proteins of interest. Proteins, thus, bind to chemical or biological "docking sites" on the ProteinChip surface. Non-binding proteins, salts, and other contaminants are washed away, eliminating sample "noise". **B.** Retained proteins are "eluted" from the ProteinChip array by Surface-Enhanced Laser Desorption/Ionization (SELDI). Ionized proteins are detected and their mass accurately determined by Time-of-Flight Mass Spectrometry (TOF/MS). Adapted from Abramovitz and Leyland-Jones, 2006.

### 3. PROTEIN MICROARRAY

Protein microarrays are valuable platforms for both classical and functional proteome analysis and can provide valuable information at the systems-level which is not possible using other techniques. In protein microarrays, antibodies or purified proteins are immobilized on glass slides, which are then used for screening cellular responses to a stimulus (e.g. challenge with plant pathogens) directed against the immobilized proteins and for screening protein-protein interactions (Duburcq *et al.*, 2004, LaBaer *et al.*, 2005) (Fig. 7). The application of protein microarray technologies in proteomics is now becoming more widespread and many approaches involving antibody and other protein have been used for

generating these microarrays. Protein microarrays can be integrated with new techniques such as surface plasmon resonance (SPR) and MS.

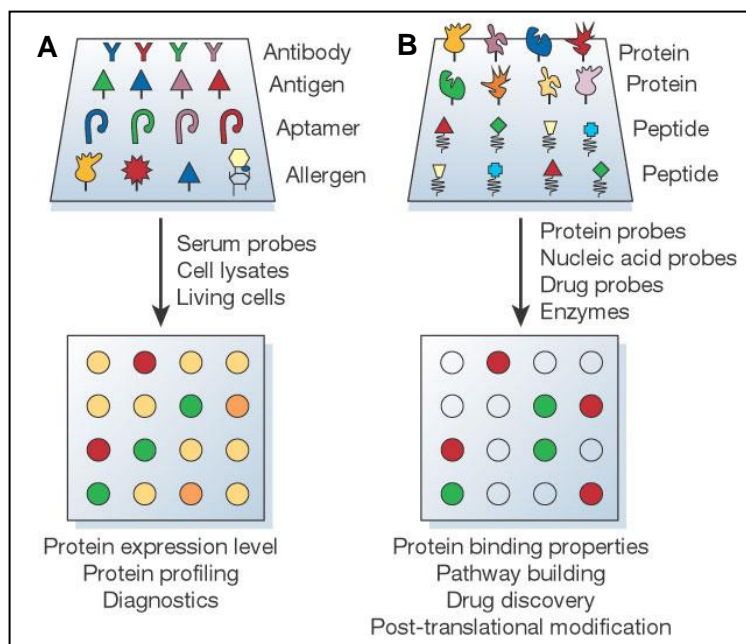


**Fig 7. A.** Analytical protein microarray. Different types of ligands, including antibodies, antigens, DNA or RNA aptamers, carbohydrates or small molecules, with high affinity and specificity, are spotted down onto a derivatized surface. These chips can be used for monitoring protein expression level, protein profiling and clinical diagnostics. Similar to the procedure in DNA microarray experiments, protein samples from two biological states to be compared are separately labelled with red or green fluorescent dyes, mixed, and incubated with the chips. Spots in red or green colour identify an excess of proteins from one state over the other. **B.** Functional protein microarray. Native proteins or peptides are individually purified or synthesized using high-throughput approaches and arrayed onto a suitable surface to form the functional protein microarrays. These chips are used to analyse protein activities, binding properties and post-translational modifications. With the proper detection method, functional protein microarrays can be used to identify the substrates of enzymes of interest. Consequently, this class of chips is particularly useful in drug and drug-target identification and in building biological networks. Adapted from Phizicky *et al.*, 2003.

#### 4. CHEMICAL PROTEOMICS

Most classical proteomic techniques do not allow direct assessment of post-translational regulation by factors such as protein–protein and/or protein–inhibitor interactions so they often fail to provide an understanding of global protein function (Gygi *et al.*, 1999). In particular, many enzymatic proteins such as proteases are synthesized as precursor (zymogen) forms that must be post-translationally activated resulting in activity profiles that are often poorly correlated with overall abundance. In order to address this limitation in classical proteomic methods, the field of chemical proteomics has recently been established as a means to profile global patterns of enzyme activity through the use of synthetic small molecules known as activity-based probes (ABPs) (Cravatt and Sorensen, 2000, Greenbaum *et al.*, 2002). These chemical reagents can be designed to target a distinct subset of enzymatic targets and facilitate identification as well as activity-based protein profiling (ABPP) of enzymes in complex proteomes. These methods have proven to be a powerful addition to the proteomics toolbox, however, as with the use of any kind of small molecule

tool there exists the possibility of off-target effects that are difficult to resolve. Generally, these issues can be addressed with detailed follow-up studies using classical genetics and biochemistry and by using multiple classes of probes that modify the same enzyme target. The central component of this method is the ABP which consists of three basic structural elements: a reactive group (or 'warhead'), a linker/specificity region and a tag region (Jeffery and Bogoy, 2003). The warhead group serves as the key functional element that directs covalent, activity-dependant modification of a target enzyme or enzyme family. The linker region serves as a scaffold for attachment of functional groups that direct the selectivity of the probe and the tag is used to visualize the resulting modified target enzymes. A number of different warheads, linkers and tags have been used and are the focus of several other extensive reviews (Adam *et al.*, 2002; Jeffery and Bogoy, 2003, Berger *et al.*, 2004, Speers and Cravatt, 2004). Two basic approaches have been taken in the design of ABPs: a directed approach aimed at designing probes to target a specific enzyme or class of enzymes and a non-directed approach aimed at characterizing enzyme families for which selective active-site reagents have not yet been identified. In both cases, the ABP provides a facile means to simplify a complex proteome into a 'functional' proteome thus allowing a focused look at regulation of a small set of enzymatic targets (Phillips and Bogoy, 2005).



## BIBLIOGRAPHY

- Abramovitz M.** and B. Leyland-Jones, *Proteome. Sci.* 4 (2006) 4.
- Adam G.C.**, E.J. Sorensen, B.F. Cravatt, *Mol. Cell. Proteomics.* 1 (2002) 781.
- Aebersold R.** and M. Mann, *Nature.* 422 (2003) 198.
- Anderson N.L.** and N.G. Anderson, *Mol. Cell. Proteomics.* 1 (2002) 845.
- Banks R.E.**, M.J. Dunn, D.F. Hochstrasser, J.C. Sanchez, W. Blackstock, D.J. Pappin, P.J. Selby, *Lancet.* 356 (2000) 1749.
- Berger A.B.**, P.M. Vitorino, M. Bogyo, *Am. J. Pharmacogenomics.* 4 (2004) 371.
- Berggren K.**, E. Chernokalskaya, T.H. Steinberg, C. Kemper, M.F. Lopez, Z. Diwu, R.P. Haugland, W.F. Patton, *Electrophoresis.* 21 (2000) 2509.
- Berkelman T.**, *Methods. Mol. Biol.* 424 (2008) 51.
- Bjellqvist B.**, K. Ek, P.G. Righetti, E. Gianazza, A. Görg, R. Westermeier, W. Postel, *J. Biochem. Biophys. Methods.* 6 (1982) 317.
- Bodzon-Kulakowska A.**, A. Bierczynska-Krzysik, T. Dylag, A. Drabik, P. Suder, M. Noga, J. Jarzebinska, J. Silberring, *J. Chromatogr. B Analyt. Technol. Biomed. Life. Sci.* 849 (2007) 1.
- Brønstrup M.**, *Expert Rev. Proteomics.* 1 (2004) 503.
- Cañas B.**, C. Piñeiro, E. Calvo, D. López-Ferrer, J.M. Gallardo, *J. Chromatogr. A* 1153 (2007) 235.
- Cash P.**, *Anal. Chim. Acta.* 372 (1998) 121.
- Chevallet M.**, V. Santoni, A. Poinas, D. Rouquie, A. Fuchs, S. Kieffer, M. Rossignol, J. Lunardi, J. Garin, T. Rabilloud, *Electrophoresis.* 19 (1998) 1901.
- Cravatt B.F.** and E.J. Sorensen, *Curr. Opin. Chem. Biol.* 4 (2000) 663.
- Duburcq X.**, C. Olivier, F. Malingue, R. Desmet, A. Bouzid, F. Zhou, C. Auriault, H. Gras-Masse, O. Melnyk, *Bioconjug. Chem.* 15 (2004) 307.
- Eng J.K.**, A.L. McCormack, J.R. Yates, *J. Am. Soc. Mass. Spectrom.* 5 (1994) 976.
- Fenn J.B.**, M. Mann, C.K. Meng, S.F. Wong, C.M. Whitehouse, *Science.* 246 (1989) 64.
- Fountoulakis M.** and J.F. Juranville, *Anal. Biochem.* 313 (2003) 267.
- Fountoulakis M.**, J.F. Juranville, L. Jiang, D. Avila, D. Roder, P. Jakob, P. Berndt, S. Evers, H. Langen, *Amino. Acids.* 27 (2004) 249.
- Fountoulakis M.**, J.F. Juranville, D. Roder, S. Evers, P. Berndt, H. Langen, *Electrophoresis.* 19 (1998) 1819.
- Gartner C.A.**, J.E. Elias, C.E. Bakalarski, S.P. Gygi, *J. Proteome. Res.* 6 (2007) 1482.
- Goerg A.**, C. Obermaier, G. Bought, A. Harder, B. Scheibe, R. Wildgruber, W. Wiess, *Electrophoresis.* 21 (2000) 1037.
- Greenbaum D.**, A. Baruch, L. Hayrapetian, Z. Darula, A. Burlingame, K.F. Medzihradsky, M. Bogyo, *Mol. Cell. Proteomics.* 1 (2002) 60.
- Guerrier L.**, P.G. Righetti, E. Boschetti, *Nature. Protocols.* 3 (2008) 883.
- Gygi S.P.**, B. Rist, S.A. Gerber, F. Turecek, M.H. Gelb, R. Aebersold, *Nat. Biotechnol.* 17 (1999) 994.
- Herbert B.**, *Electrophoresis.* 20 (1999) 660.
- Herbert B.**, M.P. Molloy, A.A. Gooley, B.J. Walsh, W.G. Bryson, K.L. Williams, *Electrophoresis.* 5 (1998) 845.
- Ho D.W.**, Z.F. Yang, B.Y. Wong, D.L. Kwong, J.S. Sham, W.I. Wei, A.P. Yuen, *Cancer.* 107 (2006) 99.
- Hortin G.L.**, S.A. Jortani, J.C. Ritchie, R. Valdes, D.W. Chan, *Clin. Chem.* 52 (2006) 1218.
- Jeffery D.A.** and M. Bogyo, *Curr. Opin. Biotechnol.* 14 (2003) 87.
- Jiang L.** and L. Hea, M. Fountoulakis, *J. Chromatogr. A* 1023 (2004) 317.
- Kabir S.**, *Immunol. Invest.* 31 (2002) 263.
- Karas M.** and F. Hillenkamp, *Anal. Chem.* 60 (1988) 2299.
- Kikkawa R.**, M. Fujikawa, T. Yamamoto, Y. Hamada, H. Yamada, I. Horii, *J. Toxicol. Sci.* 31 (2006) 23.
- Kislinger T.**, A.O. Gramolini, D.H. MacLennan, A. Emili, *J. Am. Soc. Mass. Spectrom.* 16 (2005) 1207.
- LaBaer J.** and N. Ramachandran, *Curr. Opin. Chem. Biol.* 9 (2005) 14.
- Lai C.C.** and G.R. Her, *Rapid. Commun. Mass. Spectrom.* 14 (2000) 2012.
- Lescuyer P.**, D. Hochstrasser, T. Rabilloud, *J. Proteome. Res.* 6 (2007) 3371.

- Luche S.**, V. Santoni, T. Rabilloud, *Proteomics*. 3 (2003) 249.
- Makarov A.**, *Anal. Chem.* 72 (2000) 1156-1162.
- Manabe T.**, H. Miyamoto, K. Inoue, M. Nakatsu, M. Arai, *Electrophoresis*. 20 (1999) 3677.
- Mann M.** and M. Wilm, *Anal. Chem.* 66 (1994) 4390-4399.
- Mirgorodskaya O.A.**, Y.P. Kozmin, M.I. Titov, R. Korner, C.P. Sonksen, P. Roepstorff, *Rapid. Commun. Mass. Spectrom.* 14 (2000) 1226.
- Motoyama A.** and J.R.3rd. Yates, *Anal. Chem.* 80 (2008) 7187.
- Mukherji M.**, *Expert. Rev. Proteomics*. 2 (2005) 117.
- Nguyen M.T.**, G.F. Ross, C.L. Dent, P. Devarajan, *Am. J. Nephrol.* 25 (2005) 318.
- O'Farrell P.H.**, *J. Biol. Chem.* 250 (1975) 4007.
- Olivieri E.**, B. Herbert, P.G. Righetti, *Electrophoresis*. 22 (2001) 560.
- Ong S.E.**, B. Blagoev, I. Kratchmarova, D.B. Kristensen, H. Steen, A. Pandey, M. Mann, *Mol. Cell Proteomics* 1 (2002) 376-386.
- Panchaud A.**, M. Affolter, P. Moreillon, M. Kussmann, *J. Proteomics*. 71 (2008) 19.
- Peng J.** and S.P. Gygi, *J. Mass. Spectrom.* 36 (2001) 1083.
- Perdew G.H.**, S.W. Schaup, D.P. Selivonchick, *Anal. Biochem.* 135 (1983) 453-455.
- Perkins D.N.**, D.J. Pappin, D.M. Creasy, J.S. Cottrell, *Electrophoresis*. 20 (1999) 3551.
- Petrak J.**, R. Ivanek, O. Toman, R. Cmejla, J. Cmejlova, D. Vyoral, J. Zivny, C.D. Vulpe, *Proteomics*. 8 (2008) 1744.
- Phillips C.I.** and M. Bogyo, *Cell. Microbiol.* 7 (2005) 1061.
- Phizicky E.**, I. Philippe, H. Bastiaens, H. Zhu, M. Snyder, S. Fields, *Nature*. 422 (2003) 208.
- Pierce J.D.**, M. Fakhari, K.V. Works, J.T. Pierce, R.L. Clancy, *Nurs. Health. Sci.* 9 (2007) 54.
- Polati R.**, A. Castagna, A. Bossi, N. Campostrini, F. Zaninotto, A.M. Timperio, L. Zolla, O. Olivieri, R. Corrocher, D. Girelli, *Proteome. Sci.* 19 (2009) 7.
- Rabilloud T.**, C. Adessi, A. Giraudel, J. Lunardi, *Electrophoresis*. 18 (1997) 307.
- Rai A.J.**, C.A. Gelfand, B.C. Haywood, D.J. Warunek, J. Yi, M.D. Schuchard, R.J. Mehig, S.L. Cockrill, G.B. Scott, H. Tammen, P. Schulz-Knappe, D.W. Speicher, F. Vitzthum, B.B. Haab, G. Siest, D.W. Chan, *Proteomics*. 13 (2005) 3262.
- Ranganathan S.**, E. Williams, P. Ganchev, V. Gopalakrishnan, D. Lacomis, L. Urbinelli, K. Newhall, M.E. Cudkowicz, R.H.J. Brown, J.R. Bowser, *J. Neurochem.* 95 (2005) 1461.
- Rappsilber J.**, Y. Ishihama, M. Mann, *Anal. Chem.* 75 (2003) 663.
- Reynolds T.**, *J. Natl. Cancer. Inst.* 94 (2002) 1664.
- Righetti P.G.**, A. Castagna, P. Antonoli, E. Boschetti, *Electrophoresis* 26 (2005) 297-319.
- Righetti P.G.** and E. Boschetti, *Mass. Spectrom. Rev.* 27 (2008) 596.
- Righetti P.G.** and J.W. Drysdale, *Ann. N.Y. Acad. Sci.* 209 (1973) 163.
- Ro K.W.**, J. Liu, D.R. Knapp, *J. Chromatogr. A* 1111 (2006) 40.
- Ross P.L.**, Y.N. Huang, J.N. Marchese, B. Williamson, K. Parker, S. Hattan, N. Khainovski, S. Pillai, S. Dey, S. Daniels, S. Purkayastha, P. Juhasz, S. Martin, M. Bartlet-Jones, F. He, A. Jacobson, D.J. Pappin, *Mol. Cell. Proteomics*. 3 (2004) 1154.
- Sanchez J.C.**, P. Wirth, S. Jaccoud, R.D. Appel, C. Sarto, M.R. Wilkins, D.F. Hochstrasser, *Electrophoresis*. 18 (1997) 638.
- Sato A.**, D.J. Sexton, L.A. Morganelli, E.H. Cohen, Q.L. Wu, G.P. Conley, Z. Streltsova, S.W. Lee, M. Devlin, D.B. DeOliveira, J. Enright, R.B. Kent, C.R. Wescott, T.C. Ransohoff, A.C. Ley, R.C. Ladner, *Biotechnol. Prog.* 18 (2002) 182.
- Sickmann A.**, W. Dormeyer, S. Wortelkamp, D. Woitalla, W. Kuhn, H.E. Meyer, *Electrophoresis*. 13 (2000) 2721.
- Simpson R.J.**, *Purifying Proteins for Proteomics: A Laboratory Manual*, CSHL Press, New York, (2004) 393.
- Sitnikov D.**, D. Chan, E. Thibaudeau, M. Pinard, J.M. Hunter, *J. Chromatogr. B* 832 (2006) 41.
- Sowell R.A.**, J.B. Owen, D.A. Butterfield, *Ageing. Res. Rev.* 8 (2009) 1.
- Speers A.E.** and B.F. Cravatt, *Chem. Biol.* 11 (2004) 535-546.
- Syka J.E.**, J.J. Coon, M.J. Schroeder, J. Shabanowitz, D.F. Hunt, *Proc. Natl. Acad. Sci. U.S.A.* 101 (2004) 9528.
- Takats Z.**, J.M. Wiseman, B. Gologan, R.G. Cooks, *Science*. 306 (2004) 471.
- Taylor C.M.** and S.E. Pfeiffer, *Proteomics*. 3 (2003) 1303.

**Terry D.E.**, E. Umstot, D.M. Desiderio, *J. Am. Soc. Mass. Spectrom.* 6 (2004) 784.

**Unlu M.**, M.E. Morgan, J.S. Minden, *Electrophoresis.* 18 (1997) 2071.

**Wang W.**, M. Scali, R. Vignani, A. Spadafora, E. Sensi, S. Mazzuca, M. Cresti, *Electrophoresis.* 24 (2003) 2369.

**Wilkins M.R.**, J.C. Sanchez, A.A. Gooley, R.D. Appel, I. Humphery-Smith, D.F. Hochstrasser, K.L. Williams, *Biotechnol. Genet. Eng. Rev.* 13 (1996) 19.

**Wilkins M.R.**, J.C. Sanchez, K.L. Williams, D.F. Hochstrasser, *Electrophoresis.* 17 (1996) 830.

**Yates J.R.**, A. Gilchrist, K.E. Howell, J.J. Bergeron, *Nat. Rev. Mol. Cell Biol.* 6 (2005) 702.

**Yates J.R.**, C.I. Ruse, A. Nakorchevsky, *Annu. Rev. Biomed. Eng.* 11 (2009) 49.

**Yuana X.** and D.M. Desiderio, *J. Chromatogr. B* 815 (2005) 179.

**Zubarev R.A.**, D.M. Horn, E.K. Fridriksson, N.L. Kelleher, N.A. Kruger, M.A. Lewis, B.K. Carpenter, F.W. McLafferty, *Anal. Chem.* 72 (2000) 563.





## SESSION 2



# PROTEOMICS MEETS MICROBIOLOGY

## MICROBIAL PROTEOMICS

With the completion of over 1000 prokaryotic and eukaryotic genome sequences and with hundreds of sequencing projects currently underway (Celestino *et al.*, 2004), researchers are now facing the daunting task of assigning functions to the thousands of predicted gene products. While microarray technologies (Shalon *et al.*, 1996) provide invaluable information concerning the levels of global mRNA expression, it is clear that in many cases mRNA transcripts do not directly correlate with protein expression (Anderson and Seilhamer, 1997; Gygi *et al.*, 1999a). Therefore, the field of proteomics is challenged with the task of providing both quantitative and functional data to further complement genomics efforts.

In particular the sequencing of the genomes of most economically important microbial cells, allow the application of proteomic technologies during various steps of process development, starting with the selection and optimization of the functions of the industrial strains, application of the knowledge of cell function in response to the changes of production parameters, validation of the downstream processing, and thorough characterization of the final product.

Proteomic methods in food technology and biotechnology, as well as in quality control were at the beginning rather limited. However, this has changed rapidly and proteomics technology is now becoming more practical, and the terms “industrial process proteomics” (Incamps *et al.*, 2005) and “industrial proteomics” (Josic *et al.*, 2007) have been introduced. Nowadays proteomic technologies can be used in “classical” fermentation industry, for identification of targets for bioprocess improvement (Wang *et al.*, 2003). In addition, proteomics is also used for quality control in industrial processes of other food products of animal origin (Pineiro *et al.*, 2003). While classical proteomic techniques provide methods to determine the identity and abundance of proteins within a given proteome, an understanding of protein function can only be inferred from changes in expression. In the case of enzymes, activity is often tightly regulated by a series of post-translational controls and therefore may not be directly correlated with protein abundance. To address the need to profile global patterns of enzyme activity, a new set of proteomic techniques has been developed that make use of small molecule chemical probes that provide an indirect readout of enzyme activity (Phillips and Bogoy, 2005).

Yeast fermentation in food processing has been a tradition for thousands of years, and optimization of the fermentation process, purification, productivity, yield and purity, and characterization of the final process are crucial steps in integral process development. For these reasons, baker's yeast (*Saccharomyces cerevisiae*) was the first eukaryote to have its complete genome sequenced, and it is also the eukaryote with the deepest level investigations of its proteome.

On the other hand, bacteria are widely used in biotechnology, for production of proteins and chemicals (Lee *et al.*, 2003), and also for unusual applications like the recovery of ancient frescos (Antonioli *et al.*, 2005). In both the above-mentioned cases, proteomic techniques are used to follow the production process, such as biosynthesis of recombinant proteins and digestion of hardened glue. Among the most important bacterial organisms, *Escherichia coli* was one of the first sequenced genomes due to its small genome size and prevalent use in laboratory. As a host organism for production of therapeutic proteins, *E. coli* has been for a long time a topic for intensive proteomic analyses (Lee *et al.*, 2003, Zhang *et al.*, 2007). *Acetobacter* and *Lactobacillus* strains are also important industrial microorganisms in wine and other food fermentations, for production of acetic and lactic acid and other bioconversions, and as a source of bactericidal agents. The physical and molecular responses to environmental stress of different species, important for processing of food and beverages, have already been described extensively (De Angelis *et al.*, 2004). An increasingly important topic in microbial research is that concerning "biofilms". Biofilms are medically important, accounting for over 80% of microbial infections in the body (Davies, 2003). Proteomic analyses of biofilm forming microorganisms give important information about their behaviour during industrial processes, infection of the host organism, symbiosis, and their defence against antimicrobial agents. Furthermore, several recent large-scale screening efforts have been addressed to search for novel pharmacological tools to assess global protein function in pathogenic organisms such as *Toxoplasma gondii* (Carey *et al.*, 2004).

Because of incomplete genome sequencing of some microbes of major industrial importance, analysis of their proteome during the production process is still not possible. Nevertheless, in the near future, proteomics will play, together with genomics and metabolomics, an important role in process development. Possibly, these technologies will be used to enhance productivity of microbial cells or to influence targeted properties of the final product.

# CHAPTER 1

## A METHOD FOR THE PREPARATION OF TOTAL PROTEIN EXTRACT OF MICROORGANISM FOR PROTEOMIC ANALYSIS

### 1. INTRODUCTION

Two-dimensional electrophoresis (2-DE) has proven to be extremely effective to map most of the proteins expressed by a microorganism in a defined moment of its life. However often streaks and smears on the first or on the second dimension of the gel hamper the resolution of the maps. In particular, the proteome analysis of microorganisms that are equipped with inner and outer membranes and a cell wall compartment can be tricky. The cell wall is made of high molecular weight polysaccharides, that tend to form complexes with nucleic acids and to obstruct the pores of the IEF in immobilised pH gradients (IPG) gel, precluding the access of proteins to the gel matrix (Herbert *et al.*, 2006). Moreover, during the IEF step, proteins could bind to polysaccharides and nucleic acids, forming complexes with poor focalization properties, that streak in the acidic part of the 2D map, or that shift the protein apparent isoelectric point (pI) towards the acidic part of the gradient (Berkelman, 2008, Rabilloud, 1996).

We developed a protocol based on the use of the cationic detergent CTAB for the preparation of clean total protein extracts for 2-DE. CTAB, cetyltrimethylammonium bromide, is a strong ionic denaturing detergent. This surfactant has been used to facilitate the separation of proteins from nucleic acids in extractions of biological materials. The CTAB method capitalizes on the previous observations that nucleic acids can be selectively precipitated with CTAB (Ralph and Bellam, 1964). RNA and DNA are soluble in CTAB and 0.7 M NaCl but precipitate when the salt is reduced below 0.4 M. However, many polysaccharides are insoluble over this salt range and are thus not solubilized (Murray and Thompson, 1984). The technique was first developed to isolate DNA from barley seedlings by Doyle and Doyle (1987) using the buffer system reported by Saghai-Marooof *et al.* (1984) and has been widely used to obtain high-quality nucleic acids from plants for various applications (Allen *et al.*, 2006, Bekesiova *et al.*, 1999, Chang *et al.*, 1993, Flagel *et al.*, 2005, Jaakola *et al.*, 2001, Kim and Hamada, 2005, Puchooa, 2004, Wang *et al.*, 2005). CTAB-based methods have also been used to prepare samples from infected plants for PCR-based detection of DNA viruses, bacteria and phytoplasmas (Francis *et al.*, 2006, Hren *et al.*, 2007, Hu *et al.*, 1996, Li *et al.*, 2006, Wyatt and Brown, 1996), but its application for

PCR-based detection of plant RNA viruses and viroids is less reported (Chang *et al.*, 2007, Harjua *et al.*, 2005, López *et al.*, 2006, Mumford *et al.*, 2000, Parmessur *et al.*, 2002). CTAB-based methods have been previously reported for extraction of high-quality nucleic acids from plants, especially from plants with high levels of polyphenols and polysaccharides (Li *et al.*, 2008). Thus we exploited the properties of CTAB to clean our 2-DE protein sample. In particular the method that we developed was applied for the preparation of total protein extracts of wine spoilage microorganisms (acetic acid bacteria and an acid adapted yeast). Such microorganisms are interesting for their particular physiology and for their relevance in industrial processes (Gullo *et al.*, 2006, Gupta *et al.*, 2001, Park *et al.*, 2003); they are also often associated with detrimental organoleptic effects in wines (Silva *et al.*, 2004). Their main characteristic is the ability to survive to acidic environments as wines. AABs endure high level of acetic acid, which has been reported acting as cytotoxic for the majority of the microbial species known (Steiner and Sauer, 2001). To date, studies on the proteome of AAB had to overcome the presence of cell wall polysaccharides, and of celluloses in cellulose producing strains (Bossi *et al.*, 2007). Here, the treatment with CTAB proved to be effective in the removal of such interferents: the 2D gels obtained were very clean and highly resolved. *Gluconoacetobacter hansenii* AAB0248, a cellulose productive strain (Gullo *et al.*, 2006), was used to set up the protocol. Further, the CTAB protocol was tested with success on the following microorganisms: *Acetobacter malorum* AAB01, *Gluconoacetobacter europaeus* AAB017, *Acetobacter pasteurianus* AAB0246 and the yeast *Brettanomyces bruxellensis* DSM70001.

## 2. MATERIALS AND METHODS

### 2.1 Cell culture

AAB strains of *Acetobacter malorum* AAB01, *Acetobacter pasteurianus* AAB0246, *Gluconoacetobacter europaeus* AAB017, *Gluconoacetobacter hansenii* AAB0248 and the yeast *Brettanomyces bruxellensis* DSM70001 were cultivated respectively in GYP for AAB and in YM for the yeast and incubated at 28 °C without agitation. The growth was estimated as CFU ml<sup>-1</sup> by plate count on GYP or YM agar, after the incubation of the plates aerobically for seven days at 28 °C.

### 2.2 Lysis protocol

Cells were precipitated by centrifugation at 3900 × g for 20 min, and washed one time with physiological solution (0.9% NaCl). Cell lysis was in 6 ml of 0.9% NaCl and sonicated for 10 cycles (15 s sonication and 30 s standing each time). Protein were precipitated in acetone : methanol (8:1 v/v) for 2 h at -20 °C, followed by centrifugation at 18,300 × g for

10 min. The protein content was measured with Bradford assay (Sigma, MA, USA), calibration curve  $y$  (Abs 595 nm) =  $0.0879 \times (\text{protein\_g})$ .

### 2.3 CTAB protein protocol

Pellet obtained from cell lysates has been treated with CTAB as follows (Table 1 for a visual summary): the pellet of acetone : methanol (8:1 v/v) re-suspended in 100  $\mu$ l of 1 M Tris, 4 M NaCl, 2% (w/v) CTAB, double distilled (DDI) water, protease inhibitors MiniComplete (Roche) and incubated for 1 h at 37 °C. Then, upon addition of 900  $\mu$ l of DDI water, CTAB was let precipitated by centrifuging 5 min at  $1000 \times g$ . The supernatant was then precipitated 2 h on ice in acetone : methanol 8:1 (v/v) and centrifuged for 10 min at  $18,300 \times g$ , washed twice with 70% ethanol to get rid of CTAB residues. Proteins were then re-suspended in 7 M urea, 2 M thiourea, 3% CHAPS, 40 mM Tris, centrifuged 30 min at  $21,200 \times g$ , the pellet discharged and the supernatant collected, quantified and run onto 2D gels, in quadruplicate.

**Table 1.** The CTAB protocol.

Step #	Description	Practical details and recipes	Time and conditions
Step 1.	Pellet re-suspension and incubation	Add 100 $\mu$ l of 1 M Tris, 4 M NaCl, 2% (w/v) CTAB, DDI water, protease inhibitors MiniComplete (Roche) to pellets and vortex Let incubate	1 h at 37 °C
Step 2.	Precipitation of CTAB, collection of supernatant	Add 900 $\mu$ l of DDI water and centrifugation ( $1000 \times g$ )	5 min
Step 3.	Protein recovery	Supernatant of Step 2. is precipitated with acetone:methanol 8:1 (v/v) Pellet recovery by centrifugation $18,300 \times g$	2 h on ice 10 min
Step 4.	Washing steps to eliminate traces of CTAB from pellet	Wash twice with 70% ethanol	–

### 2.4 Other re-solubilisation protocol

Pellet obtained from cell lysates has been treated according to the following methods: (1) re-suspended in the usual buffer used for the 2D electrophoresis (Bossi *et al.*, 2007); (2) treated with 1% ampholines pH 3–10 (Galante *et al.*, 1976, Righetti *et al.*, 1978); (3) treated with phenol : chloroform : isoamyl alcohol (25:24:1 v/v) as described for the removal of nucleic acid (Yolles and Freeman, 1967); (4) treated with acidic extraction, as described in (Herbert *et al.*, 2006). The proteins collected are re-suspended in the usual buffer used for the 2D electrophoresis (7 M urea, 2 M thiourea, 3% CHAPS, 40 mM Tris) and run as explained below.

## 2.5 2-DE electrophoresis

Gels were run in quadruplicate. Conditions are as indicated in (Bossi *et al.*, 2007). Proteins were mixed with solubilisation buffer (2 M thiourea, 7 M urea, 3% CHAPS, 40 mM Tris) to obtain a final volume of 450 µl and a final quantity of 66 µg of proteins. Each sample was reduced and alkylated with 5 mM tributylphosphine and 10 mM acrylamide. The mixture was then applied to the dry gel strip (IPG 70mm, pH 3–10 linear gradient, and pH 4–7) for reswelling. Focusing was performed at 300 V for 2 h, 400 V for 1 h, 1000 V for 6 h, 2000 V for 2 h, 3500 V for 5 h, 10,000 V until the complete focalization (25,000 Vh). The current was limited to 50 µA *per strip*, and the temperature was kept at 20 °C for all IEF steps. For SDS-PAGE, the IPG strips were incubated in equilibration buffer (6 M urea, 2% SDS, 20% glycerol, 0.375 M Tris–HCl pH 8.8) for 26 min and then transferred for the second dimension onto 10–20% gradient acrylamide gels. The gels were run (10 mA *per gel*) until the bromophenol blue front had reached the bottom of the gel (20 mA *per gel*). The 2-DE gels were stained in Sypro Ruby: the proteins were first fixed in a solution of 7% acetic acid and 10% methanol for 1 h, then incubated in Sypro Ruby overnight and finally destained in 7% acetic acid and 10% methanol for 2 h. Sypro Ruby stained 2-DE gels were digitized using VersaDoc (BioRad) and bioinformatic analysis was performed with PDQuest 7.3.0 (BioRad).

## 2.6 Control of the quality of proteins trapped within CTAB fraction

CTAB fractions were re-suspended in 100 µl of 1 M Tris, 4 M NaCl, proteins content recovered by precipitation for 2 h on ice in acetone : methanol 8:1 (v/v) and centrifuged for 10 min at 18,300 × g, washed twice with 70% ethanol to get rid of CTAB residues. Quantity of proteins was determined with Bradford assay, then 50 µg of proteins run onto 2-DE.

## 2.7 Detection of nucleic acids

Nucleic acid detection on the various fractions (control, CTAB treated, CTAB trapped) was performed with gel electrophoresis on 2% agarose. Sample A (control) was 15 µl of bacterial lysate added of 3 µl loading buffer 6× (0.25% bromophenol blue, 0.25% xylene cyan, 40% w/v saccharose). Sample B was CTAB trapped components, resolubilised in 200 µl 4 M NaCl. An aliquot added of loading buffer. Sample C: protein fraction recovered after CTAB treatment, precipitated with acetone : methanol 8:1, resolubilised in MilliQ water. An aliquot added of 15 µl added of loading buffer. Samples have been loaded onto a 2% agarose gel in TAE (40 mM Tris–acetate, 1 mM EDTA) added of 0.5 µg/ml ethidium bromide and run at 95 V constant for 30 min. Fluorescence has been used to detect bands.



## 2.8 Detection of polysaccharides

It has been performed with gel electrophoresis of the fractions obtained at the end of the CTAB treatment and coupled to a polysaccharides specific staining method based on periodic acid Schiff (PAS) (Konat *et al.*, 1984). Glycols treated with periodic acid are oxidised to aldehydes, Schiff reagent forms an adduct with such groups and pararosaniline stains of bright red the glycols. Control sample, 20 µl of bacterial lysate was added to 5 µl loading buffer 4× (0.5% bromophenol blue, 40% glycerol). Protein fraction recovered after CTAB treatment, precipitated with acetone : methanol 8:1, resolubilised in MilliQ water. An aliquot added of 5 µl loading buffer 4×. Aliquots of 25 µl of samples have been loaded and run onto 12% T polyacrylamide gels in three steps: 5 mA 1 h, 10 mA 1 h and 20 mA to the completion. At the end of the run, gel have been fixed with 50% methanol 30 min, washed twice with 3% acetic acid 20 min and kept in 1% periodic acid, 3% acetic acid 20 min. Washed twice with 3% acetic acid and incubated 15 min in the dark with Schiff reagent. Staining developed in a 5 min washing in 0.5% (w/v) sodium bisulphite and destained in 3% acetic acid.

## 3. RESULTS AND DISCUSSION

CTAB, has a cationic nature that has been described to interact strongly with nucleic acids, for such a reason it has been used since many years in genetic and molecular biology, for the recovery of nucleic acids (Murray and Thompson, 1980). In solution, CTAB forms complexes with nucleic acids also below its critical micellar concentration (CMC) and with polysaccharides (Mel'nikov *et al.*, 1995). CTAB stays in solution when the concentration of NaCl is higher than 0.7 M, while when the concentration of NaCl drops below 0.7 M, it forms insoluble aggregates, which trap all the molecules bound earlier in the soluble form (Murray and Thompson, 1980, Mel'nikov *et al.*, 1995, Möller *et al.*, 1992). Here the treatment with CTAB was tested to eliminate nucleic acids and polysaccharide contaminants in the sample preparation prior to 2-DE. Treated and control samples were run onto 2-DE. Fig. 1 shows the 2D map of the total protein population of *G. hansenii* AAB248 obtained upon CTAB treatment and compared with the map of the protein extract precipitated just with acetone : methanol (8:1, v/v).

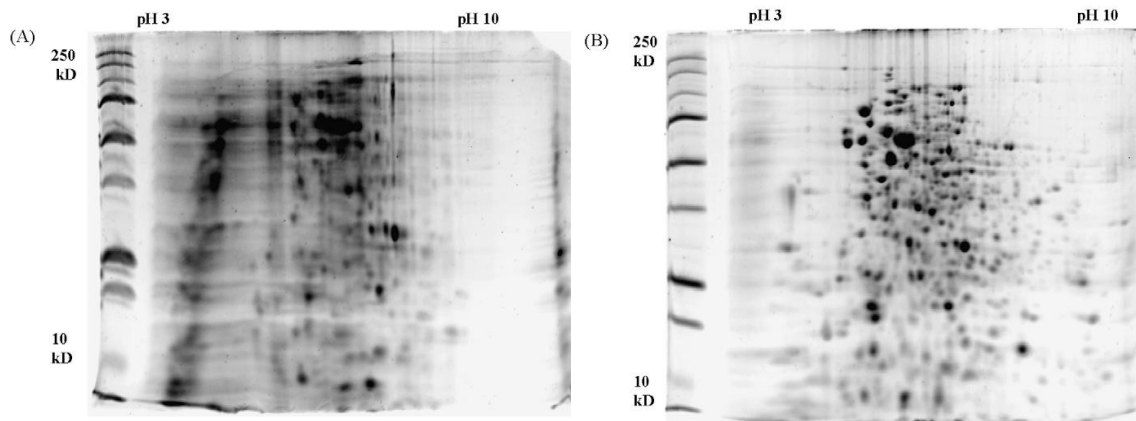


**Fig 1.** Comparison between the proteomic map of *G. hansenii* AAB0248 control (A) and after CTAB treatment (B).

The maps resulted more sharply resolved upon CTAB treatment. To proof the nature of the components removed by CTAB, the CTAB trapped fraction was resolubilised, added of ethidium bromide and run on agarose (2%) gel electrophoresis together with control (non-treated) and with CTAB treated samples (Table 1, step 4): as shown in Figure 2, no nucleic acids were detected in CTAB treated samples, while the CTAB trapped fraction was rich in nucleic acids.

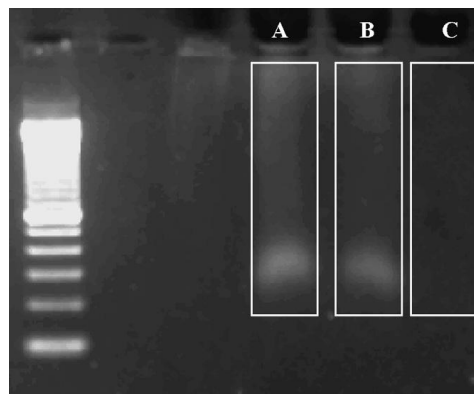


**Fig 2.** Assay on agarose gel of the nucleic acids content in non treated samples, CTAB treated sample and CTAB trapped fraction. (A) Control sample that shows the presence of nucleic acid. (B) CTAB trapped fraction: the nucleic acid content is clear. (C) CTAB treated sample shows no residual presence of nucleic acids.

In another experiment, the CTAB trapped fraction was resolubilised, increasing again the ionic strength and run on gel electrophoresis (12% acrylamide gels). Parallel lanes were used to run the CTAB treated fraction (Table 1, step 4) and a control (non treated) sample. The staining with Schiff reagent (Konat et al., 1984), specific for polysaccharides, evidenced that control, non treated sample, resulted in a smear and material deposited at the top of the lane was visible (Fig. 3, lane A), while the CTAB treated sample resulted in the separation in bands, possibly of glycoforms (Fig. 3, lane B).

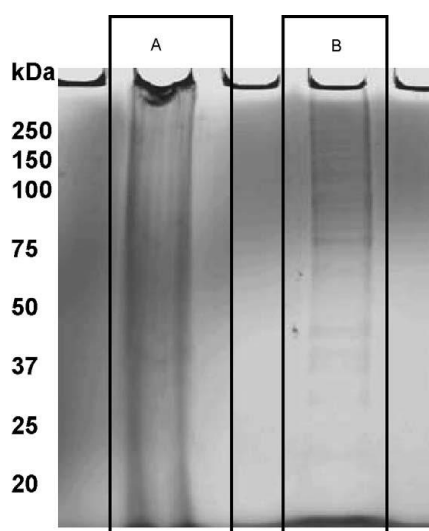


**Fig 3.** Electrophoresis followed by detection of polysaccharides with PAS staining. (A) Control sample and (B) CTAB treated sample.

These experiments accounted for the role of CTAB in removing nucleic acid and polysaccharides. Digitalised images of 2D maps of CTAB treated samples were qualitatively compared with maps obtained with four other protocols described in the literature (use of usual buffer used for the 2D electrophoresis (Bossi *et al.*, 2007); ampholines (Galante *et al.*, 1976, Righetti *et al.*, 1978); phenol : chloroform : isoamyl alcohol (25:24:1 v/v) (Yolles and Freeman, 1964) and treated with acidic extraction). Table 2 compares the results by indicating the number of protein spots counted with the PDQuest Software (BioRad) on each set of maps. The highest number of spots resulted from the CTAB protocol: 507 were counted on Minigels (7 cm length), thus allowing to detect a hundred protein more, respect the other protocols tested. The treatment with CTAB proved to be superior also in terms of resolution: the spots on the 2D map (e.g. Fig. 1B) appeared highly focused with no streaks and smears.

**Table 2.** Comparison of the 2D maps upon different treatments for the removal of nucleic acid and polysaccharides. Sample was total protein extract of *G. hansenii* AAB0248. Gels for a single treatment were run in quadruplicate, a same quantity of protein extract was loaded on each gel to allow comparison.

Treatment	Spot counted
CTAB	507 ± 12
No treatment	357 ± 8
Ampholines 1%	392 ± 11
Phenol:chloroform:isoamyl acid	188 ± 13
Acidic extraction	381 ± 4

The number of spots counted after CTAB treatment and the resolution of CTAB treated maps, accounted for an efficient removal of contaminants by CTAB. The loss in proteins,

possibly segregated into the CTAB fraction, was evaluated by mapping the proteins trapped in the CTAB (Fig. 4). The quantity of proteins recovered after CTAB treatment was 1 mg, while the quantity of proteins trapped into CTAB was 50 µg, thus the loss in proteins was considered negligible.

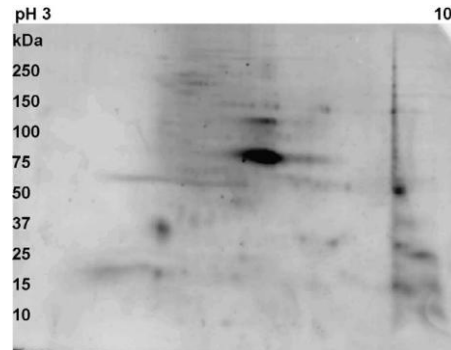


**Fig 4.** CTAB trapped proteins were re-solubilised and analysed in 2-DE. The map shows the relevant presence of a sole central spot.

Fig. 4 indicates the evident presence of a single central spot, surrounded by the faint presences of other proteins. According to literature evidences, it could be hypothesised that nucleic acid and polysaccharides have higher affinity for the detergent and compete effectively with the acidic proteins in the binding of CTAB (Husale *et al.*, 2008), thus corroborating the results that only a minimal part of proteins are sequestered with this treatment. CTAB was also applied to treat the total protein extracts of some acetic acid bacteria. The 2D maps are reported in Figure 5.

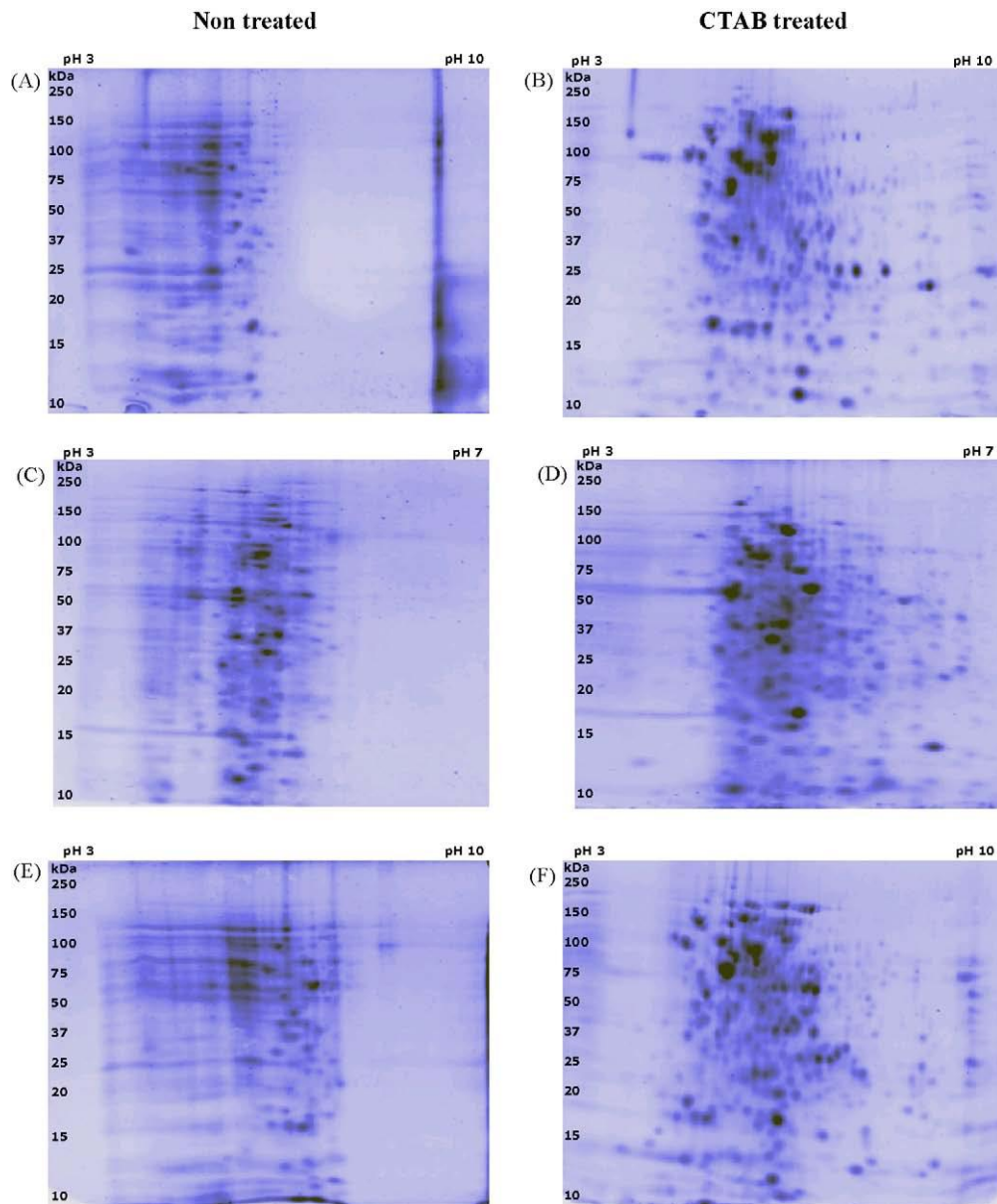


**Fig 5.** 2D maps of *A. malorum* control (A) and CTAB treated (B); *G. europaeus* control (C) and CTAB treated (D); *A. pasteurianus* control (E) and CTAB treated (F).

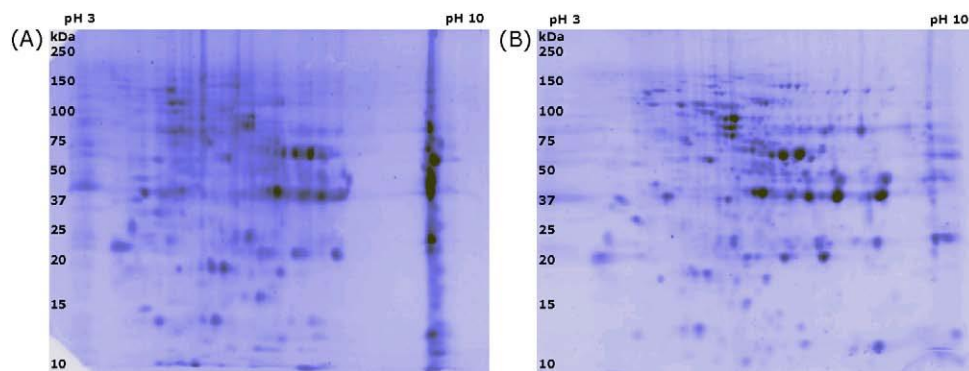


**Fig 6.** 2D maps of the yeast *B. bruxellensis* control (A) and CTAB treated (B).

The CTAB treatment resulted always in highly resolved maps. Eventually, a yeast adapted to acidic environment (Silva *et al.*, 2004), *B. bruxellensis*, was treated with CTAB and mapped (Fig. 6), showing again the advantage of CTAB in terms of sharpness of resolution. According to Yamaguchi *et al.* (2008), CTAB was the most effective agent for the solubilisation of highly hydrophobic proteins (e.g. myelin proteins) and integral membrane proteins, thus a possible limitation of our method could lie in the loss, by entrapment in the CTAB fraction, of the more hydrophobic proteins. Nevertheless, we propose the CTAB protocol for the analysis of cytosol and total protein extracts, where the vast majority of proteins are hydrophilic, thus it could be expected that in the present case the loss in hydrophobic proteins will be limited or negligible. It should be noted that the identification of hydrophobic proteins is rare in 2-DE proteomics maps because of low abundance, poor solubility, and inherent hydrophobicity (Pedersen *et al.*, 2003). Membrane proteins still remain elusive in proteomic studies and specific protocols of extraction are necessary to investigate cell surface proteins of bacteria and yeasts by 2-DE (Zoubi-Hasona *et al.*, 2004). It could be evaluated the opportunity to employ the CTAB both for the removal of contaminants and for the selective entrapment of the hydrophobic proteins, to promote the 2D mapping of membranes.

#### 4. CONCLUSIONS

In conclusions, the cationic detergent CTAB was here used to complex and remove polysaccharides and nucleic acids from a total protein extract, playing on its salt solubility, prior to proteome analysis. The proteome analysis showed a significant improvement in the 2D map upon CTAB treatment. The comparison with other methods showed CTAB treatment gave superior results. Despite we were primarily interested in mapping the proteome of the acidic adapted bacteria *G. hansenii* AAB0248, the CTAB protocol was of benefit in general of wine spoilage bacterial and yeast 2D maps. This protocol could provide a general solution for microbial proteomic analysis where it could significantly alleviate the problems of contamination by nucleic acid and polysaccharides.

## CHAPTER 2

# AN APPLICATION OF CTAB-METHOD: PROTEOMIC ANALYSIS OF MOLECULAR BASIS OF ACID-RESISTANCE IN *Ga. hansenii*

### 1. INTRODUCTION

The microorganisms oxidizing ethanol to acetic acid are commonly called acetic acid bacteria (AAB). Even though AAB have been extensively studied, researchers are still unravelling the mechanisms of their unique metabolism. In recent years, there have been major advances in understanding AAB taxonomy, molecular biology, and physiology, and in methods for their isolation and identification, but the knowledge obtained remains somewhat scattered (Rapsor and Goranovic, 2008)..

AAB are polymorphous, cells are gram negative, ellipsoidal to rod shaped, straight or slightly curved, 0.6 to 0.8  $\mu\text{m}$  long, and occurring singly, in pairs, or in chains. There are non-motile and motile forms with polar or peritrichous flagella. They are mesophilic obligate aerobes and some produce pigments, some valuable cellulose. Cellulose produced by *Ga. xylinus*, for example, has excellent properties such as transparency, tensile strength, fiber-binding ability, adaptability to the living body, biodegradability and high purity (Takai and Erata, 1998) so that it has a number of potential uses, including the manufacture of wound dressings for patients with burns, chronic skin ulcers, or other extensive loss of tissue (Alvarez *et al.*, 2004; Czaja *et al.*, 2006; Fontana *et al.*, 1990).

Physiologically, AAB oxidize a broad range of substrates such as sugars, sugar alcohols, and ethanol, with the production of acetic acid as the major end product. During acetic acid production, ethanol is almost quantitatively oxidized to acetic acid. The ability of AAB to oxidize several substrates has long been known and is still attracting attention. Based on this characteristic, several useful oxidation products are produced industrially, and such processes are called oxidative conversions. The principal biotransformation involving AAB is the production of L-sorbose from D-sorbitol, a fundamental intermediate for the synthesis of L-ascobic acid (vitamin C) (Gonzales, 2006, Hancock and Viola, 2002, Kim *et al.*, 1999, Kubicek and Karaffa, 2006, Stefanova *et al.*, 1987).

This special primary metabolism at low pH differentiates them from all other bacteria. In fact AAB exhibit resistance to low pH (as low as 2.0 to 2.2 (Du Toit and Pretorius, 2002)) and high acetic acid concentrations (Rapsor and Goranovic, 2008). For instance in industrial settings, *Acetobacter aceti* can grow at acetate concentrations of up to about 60 g/liter (Park *et al.*, 1991) and accumulate final concentrations exceeding 140 g/liter in semicontinuous

processes (Ebner *et al.*, 1996). As one of the most prominent low-molecular-weight products of microbial metabolism, acetate is well known for its cytotoxicity that includes retardation of growth and product formation at concentrations below 5 g/liter. These toxic effects are related to the weak lipophilic nature of the undissociated acid that enables the molecule to cross the cytoplasmic membrane. This diffusion is generally thought to dissipate ion gradients, increase the internal acetate concentration, and/or disrupt membrane processes, thereby poisoning the cell. While most microorganisms are sensitive to higher concentrations of acetate, a few are known to be relatively resistant. The molecular mechanism of resistance in AAB, however, remains essentially unknown (Steiner and Sauer, 2001).

Here we investigate the changes in global protein expression levels during long-term adaptation of *Ga. hansenii* to low pH, as a first step to the characterization of the molecular mechanisms underlying acetate resistance. For this purpose, *Ga. hansenii* AAB0248 wild-type was exposed to mild acetate concentrations (50 mM) in serial batch and subsequently analyzed by two-dimensional protein electrophoresis (2-DE). Detection and sequences of proteins that are induced exclusively in response to acetate adaptation are described.

## 2. MATERIALS AND METHODS

### 2.1 Strain

In this study the strain AAB0248 belonging to *Ga. hansenii* was used. This strain was isolated from balsamic vinegar (De Vero and Giudici, 2008).

### 2.2 Culture conditions

Cells of *Ga. hansenii* were grown in two different mediums: for control cultures, the bacteria were cultivated in batch culture in 1 liter flasks at a working volume of 200 ml at 28 °C in GYP medium for AAB at pH 5.8 (2.0 g yeast extract, 3.0 g peptone, 5.0 g glucose). For acetate adaptation experiments, the cultures were grown in GYP medium added with 50 mM acetic acid to reach pH 4 and 3% ethanol. The growth was estimated as CFU ml<sup>-1</sup> by plate count on GYP agar, after the incubation of the plates aerobically for seven days at 28 °C.

### 2.3 Growth kinetics

The growth kinetic of the *Ga. hansenii* AAB0248 strain was estimated through OD measurements that were used to follow cell growth at a wavelength of 595 nm. The OD measurements were performed with Microplate Reader model 680 (BIORAD).



## 2.4 Protein sample preparation for 2-DE electrophoresis

Cells were harvested by centrifugation for 20 min at  $6,000 \times g$  and  $4^\circ\text{C}$ . The pellets were resuspended in 0.9% NaCl aliquoted in microcentrifuge tubes, and centrifuged again for 10 min at  $10,000 \times g$  and  $4^\circ\text{C}$ , the washing was repeated three times. Protein samples for 2-DE were prepared according to the protocol of Polati *et al.* (2009). Briefly cells were lysed in 1 ml of 1 M Tris, 4 M NaCl, 2% (w/v) CTAB, double distilled (DDI) water, protease inhibitors MiniComplete (Roche), sonicated for 10 cycles (15 s sonication and 30 s standing each time) and incubated for 1 h at  $37^\circ\text{C}$ . Then, upon addition of DDI water, CTAB was let precipitated by centrifuging 5 min at  $1000 \times g$ . The supernatant was then precipitated 2 h on ice in acetone : methanol 8:1 (v/v) and centrifuged for 10 min at  $18,300 \times g$ , washed twice with 70% ethanol to get rid of CTAB residues. Proteins were then re-suspended in 7 M urea, 2 M thiourea, 3% CHAPS, 40 mM Tris, centrifuged 30 min at  $21,200 \times g$ , the pellet discharged and the supernatant collected and quantified with Bradford assay (Sigma, MA, USA), calibration curve  $y(\text{Abs } 595 \text{ nm}) = 0.0879 \times (\text{protein mg})$ .

## 2.5 2-DE electrophoresis

Proteins samples (800  $\mu\text{g}$ ) were mixed with solubilization buffer (2 M thiourea, 7 M urea, 3% CHAPS, 20 mM Tris) to obtain a final volume of 450  $\mu\text{l}$ . Each sample was reduced and alkylated with 5 mM tributylphosphine and 10 mM acrylamide. The mixture was then applied in gel for reswelling with a dry IPG 170 mm, pH 3-10 linear gradient. Focusing was performed at 300 V for 2 h, 400 V for 1 h, 1000 V for 6 h, 2000 V for 2 h, 3500 V for 5 h, 10000 V until the complete focalization (65000 Vh). The current was limited to 50  $\mu\text{A}$  *per* strip, and the temperature was kept at  $20^\circ\text{C}$  for all IEF steps. For SDS-PAGE, the IPG strips were incubated in equilibration buffer (6 M urea, 2% SDS, 20% glycerol, 0.375 M Tris-HCl pH 8.8) for 26 minutes and then transferred for the second dimension onto 10%-20% gradient acrylamide gels. The gels were run overnight (10 mA *per* gel) until the bromophenol blue front had reached the bottom of the gel (20 mA *per* gel). The 2-DE gels were stained in Sypro Ruby: the proteins were first fixed in a solution of 7% acetic acid and 10% methanol for 1 h, then incubated in Sypro Ruby overnight and finally destained in 7% acetic acid and 10% methanol for 2 h. Sypro Ruby stained 2-DE gels were digitized using Versadoc (BIORAD) and bioinformatic analysis was performed with PDQuest 7.3.0 (BIORAD).

## 2.6 Protein Pattern Differential Analysis

Gels were scanned using a Bio-Rad VersaDoc 1000 imaging system. 2D gel analysis was performed by PDQuest software (Bio-Rad), version 7.3. Each gel was analysed for spot detection, background subtraction and protein spot OD intensity quantification (spot quantity definition). The gel image showing the higher number of spots and the best protein

pattern was chosen as a reference template, and spots in a standard gel were then matched across all gels. Spot quantity values were normalised in each gel dividing the raw quantity of each spot by the total quantity of all the spots included in the standard gel. Gels were divided into two separated groups (acetic acid and glucose-grown cells) and, for each protein spot, the average spot quantity value and its variance coefficient in each group were determined. Data were log transformed and quantitative and a Student's t-test were performed in order to compare the two groups and identify sets of proteins that showed a statistically significant difference with a confidence level of 0.05 and a minimum two fold of variation.

## 2.6 In-Gel Digestion

Spots showing a statistically significant differential expression were carefully manually cut out from 2D Sypro Ruby stained gels and subjected to in-gel trypsin digestion according to Shevchenko *et al.* (2001) with minor modifications. The gel pieces were swollen in a digestion buffer containing 50 mM  $\text{NH}_4\text{HCO}_3$  and 12.5 ng/ $\mu\text{L}$  of porcine trypsin (Promega, Madison, WI, US) in an ice bath. After 30 min the supernatant was removed and discarded, 20  $\mu\text{L}$  of 50 mM  $\text{NH}_4\text{HCO}_3$  were added to the gel pieces and digestion allowed to proceed at 37 °C overnight. The supernatant containing tryptic peptides was dried by vacuum centrifugation. Prior to mass spectrometric analysis, the peptide mixtures were redissolved in 10  $\mu\text{L}$  of 5% formic acid.

## 2.7 Peptide sequencing by nano HPLC-ESI-MS/MS

Peptide mixtures were separated by using a nanoflow-HPLC system (1200 series Agilent Technologies, CA). A sample volume of 10  $\mu\text{L}$  was loaded by the auto-sampler onto a 2 cm fused silica pre-column (75  $\mu\text{m}$  I.D.; 375  $\mu\text{m}$  O.D.) at a flow rate of 2  $\mu\text{L}/\text{min}$ . Sequential elution of peptides was accomplished by using a flow rate of 200 nl/min and a linear gradient from Solution A (2% acetonitrile; 0.1% formic acid) to 50% of Solution B (98% acetonitrile; 0.1% formic acid) in 40 minutes over the pre-column in-line with a homemade 15 cm resolving column (75  $\mu\text{m}$  I.D.; 375  $\mu\text{m}$  O.D.; Zorbax 300-SB C18, Agilent Technologies, CA). Peptides were eluted directly into a ion Trap (model Esquire 6000, Bruker-Daltonik, Germany). Capillary voltage was 1.5-2 kV and a dry gas flow rate of 10 L/min was used with a temperature of 230 °C. The scan range used was from 300 to 1800 m/z. Protein identification was performed by searching in the National Center for Biotechnology Information non-redundant database (NCBI-nr) using the Mascot program (<http://www.matrixscience.com>). The following parameters were adopted for database searches: complete propionamide formation on cysteines and partial oxidation of methionines, peptide Mass Tolerance  $\pm 1.2$  Da, Fragment Mass Tolerance  $\pm 0.9$  Da, missed

cleavages 2. For positive identification, the score of the result of  $[-10 \times \text{Log}(P)]$  had to be over the significance threshold level ( $p < 0.05$ ).

## 2.8 Protein Categorization

Gene ontology (GO) lists were downloaded using web tools for the functional analysis of groups of genes in high-throughput experiments along with the use of information on Gene Ontology terms. Each protein was classified with respect to its biological process and molecular function using GO annotation. When no GO annotation was available, proteins were annotated manually based on literature searches and closely related homologues.

## 3. RESULTS AND DISCUSSION

### 3.1 Growth kinetics

*Ga. hansenii* AAB0248 can grow indistinctly in both culture media used. The adaptation phase to the environmental conditions is almost the same and last approximately 20-24 hours both in the pH 4 medium and in the pH 5.8 medium (Fig. 1).

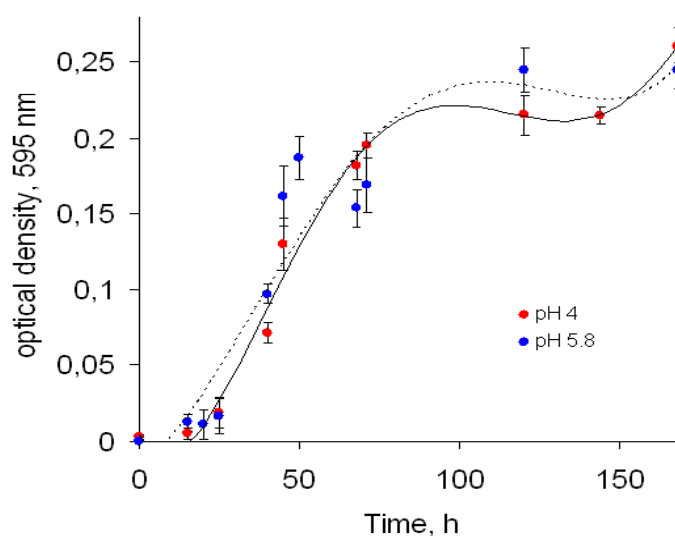


**Fig 1.** Growth kinetics of *Ga. hansenii* AAB0248 in pH 4 medium and in pH 5.8 medium.

The two growth curves are almost overlapped and this suggest a good adaptation of *Ga. hansenii* AAB0248 to both growth conditions applied. Besides we calculated the maximum growth rates ( $\mu_{\max}$ ) (Fig. 2) both in the pH 4 medium ( $\mu_{\max} = 0,0037 \text{ h}^{-1}$ ) and in the pH 5.8 medium ( $\mu_{\max} = 0,0027 \text{ h}^{-1}$ ). The acidophilic nature of *Ga. hansenii* AAB0248 emerges from the comparison of the two  $\mu_{\max}$  obtained.

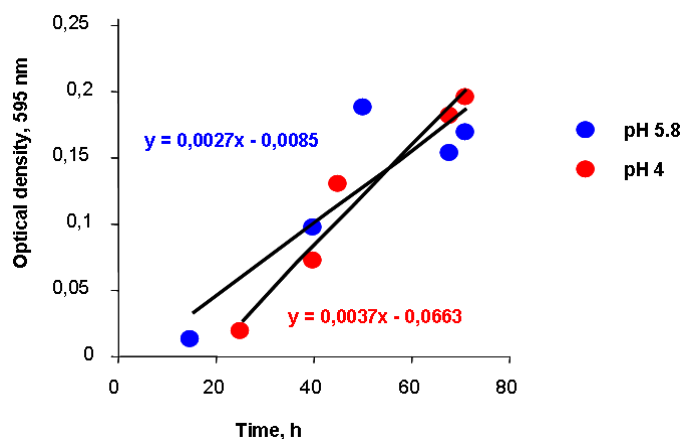


**Fig 2.** Maximum growth rates ( $\mu_{\max}$ ) of *Ga. hansenii* AAB0248 in pH 4 medium and in pH 5.8 medium.

### 3.2 *Ga. hansenii* AAB0248 2-DE Protein Pattern Analysis

To analyze the effect of the acetic acid on the growth of *Ga. hansenii*, the proteome profiles of cells grown in medium supplemented with acetic acid (pH 4) or normal GYP (pH 5.8), were evaluated by 2D-PAGE. Protein spots showing a statistically significant differential expression in pH 4-grown cells were analyzed at 5 days by means of 2-DE in the pH range of 3 to 10. Figure 3 shows all the 2D maps obtained for acetic acid (pH 4) medium and control (pH 5.8) medium grown cells.

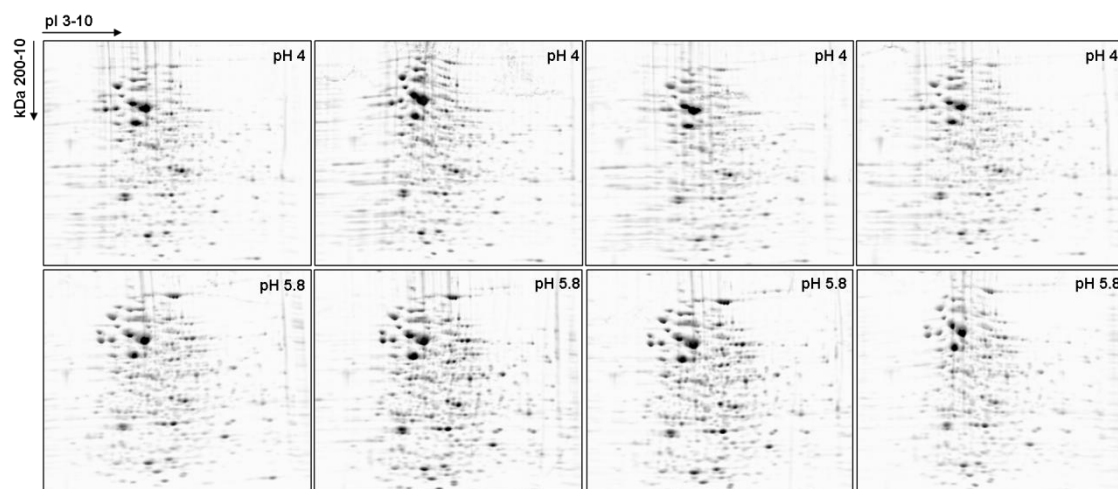


**Fig 3.** *Ga. hansenii* AAB0248 2D maps of pH 4 and pH 5.8 grown cells. The proteins (about 800 $\mu$ g) were first separated in a linear pH gradient of 3-10, then followed by separation in an SDS-PAGE (10-20%) and Sypro Ruby fluorescent staining.

By PDQuest analysis we detected protein spots and measured differential protein expression by analyzing the 4 replica of 2D maps obtained for each group. The average number of spots detected was  $552 \pm 11$  and  $578 \pm 7$  for 2D maps of pH 4 and pH 5.8 grown cells respectively. A total of 79 different spots (matched across all the replica 2D maps) were found to be differentially expressed in cells grown in medium supplemented with acetic acid: in particular 34 spots were found up-regulated and 45 down-regulated.

Figure 4 shows the typical high resolution 2-DE protein pattern (master map) obtained from *Ga. hansenii* AAB0248.

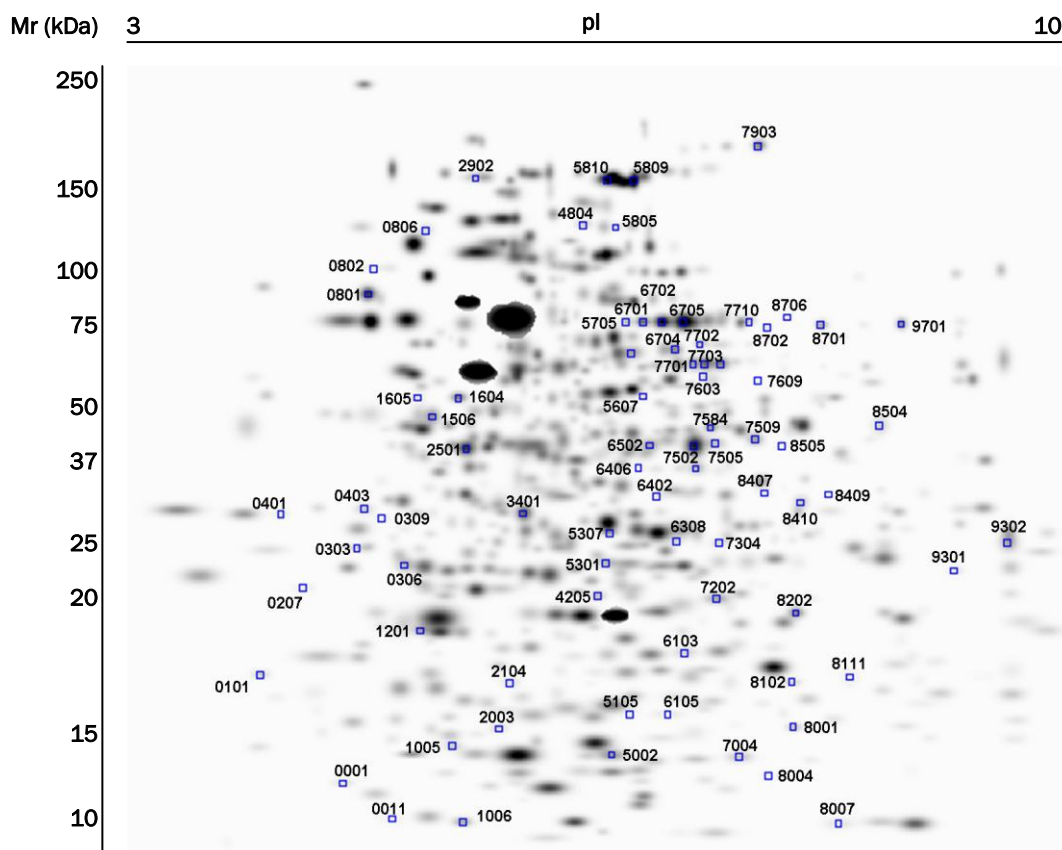


**Fig 4.** The standard map is represented with all 79 spots (marked by blue squares) found to be differentially expressed in *Ga. hansenii* AAB0248 grown in presence of acetic acid.

We identified 86 single polipeptidic chains that belong to proteins involved in whole cellular processes. In table 1, the successfully identified proteins corresponding to up- or down regulated spots are shown, together with the gene names, the spot number, the identification parameters and the indication of their gene ontology (GO) annotation (biological process and molecular function). Since the complete genome of *Ga. hansenii* has not been sequenced yet, the identification were obtained by using protein sequences of *Gluconacetobacter europaeus*, *Gluconobacter oxydans*, *Magnetospirillum magnetotacticum*, *Gluconacetobacter diazotrophicus*, *Blastopirellula marina*, *Deinococcus geothermalis*, *Zymomonas mobilis*, *Gloeobacter violaceus*, *Sinorhizobium meliloti* and *Escherichia coli*. Most of the spots were identified as proteins involved in sugar metabolism (28%) and translation/transcription (22%). But were also identified proteins involved in lipid metabolism (14%), cell redox homeostasis (8%), proteins turnover (7%), nucleic acid metabolism (7%), membrane transport (4%) and aminoacid metabolism (3%). Figure 5

shows a pie chart with the distribution of the identified proteins catalogued according to the biological process in which they are involved.

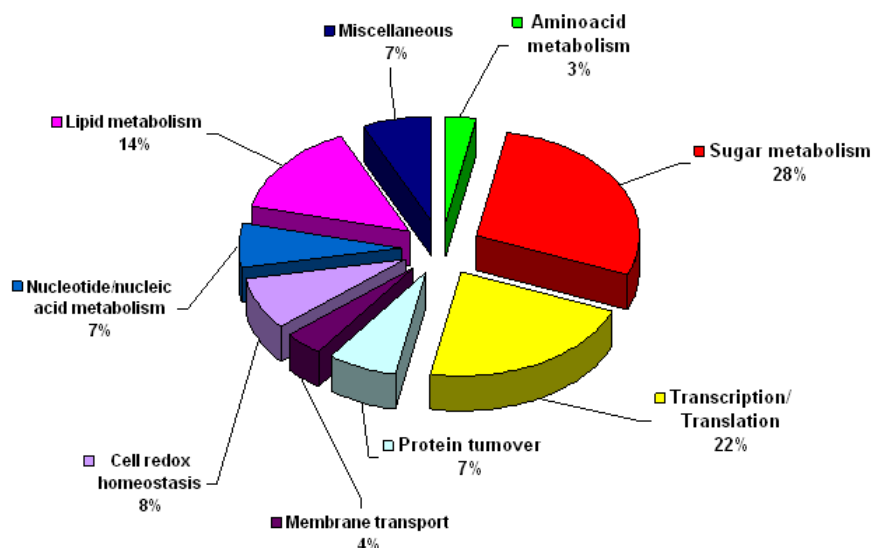


**Fig 5.** Distribution of the identified proteins according to the biological function. Assignments were made on the basis of information provided by gene ontology (GO) lists downloaded using FatiGO from Babelomics (<http://fatigo.bioinfo.cipf.es/>). The absolute number of proteins to which the distribution is referred is: 3 (aminoacid metabolism), 24 (sugar metabolism), 19 (transcription/translation), 5 (proteins turnover), 4 (membrane transport), 7 (cell redox homeostasis), 6 (nucleotide/nucleic acid metabolism), 12 (lipid metabolism), 6 (others cellular and metabolic processes).

Our data suggest that acetic acid have a global effect on protein expression and alter the expression of a relatively high number of proteins belonging to important cellular and metabolic pathways.

### ***Sugar metabolism***

Bacteria are able to live in environmental conditions that change frequently and, most often, rapidly. For doing so, they have evolved a series of adaptive mechanisms through which they constantly monitor their surroundings and adjust their physiology accordingly. In particular, they possess an array of regulatory devices that facilitate the conversion of available nutrients into components of central metabolic pathways and, thereby, the production of precursors of new cell material as well as energy for substrate uptake, biosynthesis, and growth (Cozzone, 1998). One of these pathways is the tricarboxylic acid cycle, or Krebs cycle, which plays two essential roles. First, it is responsible for the total oxidation to CO<sub>2</sub>, of acetyl coenzyme A, which is derived mainly from the pyruvate produced by glycolysis. Second, it provides intermediates that are required for the biosynthesis of amino acids, and therefore of cellular macromolecules, as well as heme biosynthesis. Bacteria must continuously replenish the pools of these intermediates in order to maintain them at

sufficient levels for active metabolism (Cozzzone, 1998). Surprisingly the cells of *Ga. hansenii* grown in presence of acetic acid, down-regulates the enzymes belonging to Krebs cycle and in particular we found a negative variation of isocitrate dehydrogenase (SSPs 6502, 7502, 7504, 7505, 7509, respectively down regulated of 2.44, 2.38, 2.50, 4.76, 3.70 folds), citrate synthase (SSP 7701, ↓2.27 folds, SSP 7703, ↓2.78 folds and SSP 7706, ↓3.03 folds), aconitate hydratase (SSP 5809, ↓3.45 folds and SSP 5810, ↓2.50 folds) and 2-oxoglutarate dehydrogenase (SSP 6704, ↓2.94 folds). The down regulation of the enzymes of Krebs cycle and of pyruvate dehydrogenase (SSP 2501, ↓4.54 folds) correspond to a simultaneous up regulation of glycolytic enzymes such as D-3-phosphoglycerate dehydrogenase (SSP 5607, ↑2.59 folds), enolase (SSP 1604, ↑2.49 folds) and pyruvate phosphate dikinase (SSP 2902, ↑2.10 folds). The result of this regulation is an excess of pyruvate that could be transformed in acetate from aldehyde dehydrogenase, that we found up regulated at pH 4.0 (SSP 5805, ↑5.77 folds and SSP 4804, ↑2.32 folds). Perhaps the acetate produced by fermentation of pyruvate may be utilized from bacteria during cellulose synthesis. In fact *Ga. hansenii* AAB0248 was selected not only for his resistance to acetic acid but also for his capacity of cellulose production: we found up regulated in cells grown in presence of acetic acid the enzyme dTDP-6-deoxy-3,4-keto-hexulose isomerase (SSP 4205, ↑2.16 folds) that is fundamental in cellulose synthesis (Ross et al., 1991). Bacterial cellulose appears to fulfil a structural role in the sense that it may confer mechanical, chemical, or biological protection within the natural habitat or facilitate cell adhesion processes necessary for symbiotic or infectious interactions. Presumably, the purpose of this extracellular material is to provide a firm surface matrix in which the embedded cells may benefit from close contact with the atmosphere. In addition cellulose pellicles provided protection from competitors which used the same substrate and were also observed to protect cells from the killing effects of UV light. Thus, cellulose pellicles may have multiple functions in the growth and survival of the organisms in nature (Ross et al., 1991) and may be implicated also in the resistance of *Ga. hansenii* AAB0248 to high acetic acid concentrations.

### ***Lipid metabolism***

As a consequence of the fermentation of pyruvate to acetate, there is a low production of acetyl-CoA and simultaneously there is the down regulation of the majority of the enzymes belonging to lipid metabolism. In fact we found a negative variation of 3-oxoacyl-(acyl carrier protein) synthase II (SSP 8202, ↓2.22 folds), acetyl-CoA carboxylase carboxyl transferase (SSP 8410, ↓2.13 folds), acetyl-CoA hydrolase (SSPs 6701, 6702, 6705, 5705, respectively down regulated of 2.17, 3.57, 3.70, 2.50 folds), dihydrolipoamide acetyltransferase (SSP 1506, ↓5.0 folds) and lipoyl synthase (SSP 8504, ↓2.70 folds). When acetate is the sole source of carbon and energy, it must first be activated to acetyl coenzyme A (acetyl CoA) to

become usable for replenishing intermediates of the tricarboxylic acid cycle via the glyoxylate bypass. This activation is also required when acetate is used for oxidation, for lipid synthesis, or for amino acid synthesis (Clark and Cronan, 1996). Nevertheless our data show that *Ga. hansenii* AAB0248 employed the acetate for cellulose synthesis instead of lipid synthesis.

### **Membrane transport**

Our data indicate that membrane functions, possibly including acetate transport and respiration, are involved in the acetate resistance mechanism of *Ga. hansenii*. Because the substrate, ethanol, and the product, acetic acid, of acetic acid fermentation are both toxic to the cell, acetic acid bacteria synthesize ATP by oxidative fermentation under extremely unfavourable conditions. It is conceivable that acetic acid bacteria have developed the GinI/GinR system to control the GmpA (an outer membrane protein) expression via GinA. In particular we found two outer membrane proteins (SSP 5307, ↑2.16 and SSP 6406, ↑2.12 folds) up-regulated in cells grown in presence of acetic acid. The OmpA (outer membrane proteins) family proteins play a structural role in the maintenance of gram-negative bacterial membrane integrity by embedding their N-terminal transmembrane strands into the outer membrane and providing their C-terminal domains in the periplasmic space as a physical linkage between the outer membrane and the peptidoglycan layer (Iida *et al.*, 2008). It is possible that *Ga. hansenii* could reduce acetic acid production from ethanol, because the outer membrane containing OmpA prevents the passage of ethanol into the periplasm, where alcohol dehydrogenase and aldehyde dehydrogenase, both of which are anchored to the inner membrane and are required for ethanol oxidation into acetic acid, are present.

### **Stress response**

It is noteworthy that acetic acid in its undissociated form is capable of diffusing into the cell, thus reducing the intracellular pH and this, in turn, may elicit the expression of several stress proteins including alkyl hydroperoxide reductase (SSP 1201, ↑2.53 and SSP 5105, ↑7.70 ) and radical SAM family Fe-S protein (SSP 8706, ↑2.13). In particular iron-sulfur (Fe/S) cluster-containing proteins perform central tasks in electron transport, catalysis, and the regulation of environmental responses. The complex bacterial biosynthetic systems that assist in the assembly of Fe/S clusters and their transfer into apo-proteins fall into three classes: the house-keeping ISC system, which is widely distributed across taxa; the NIF machinery dedicated to the assembly of the Fe/S clusters of nitrogenase from nitrogen-fixing bacteria; and the SUF machinery, which is required under oxidative stress and iron-limiting conditions (Gelling *et al.*, 2007). Besides our data indicate that *Ga. hansenii* AAB0248 synthesises a complete battery of molecular chaperones and proteins involved in translation and transcription to contrast the stress conditions. For example the main function of chaperone protein dnaK (SSP 1806, ↑2.57 folds) and GroEL (SSP 5705, ↓2.50



folds) appears to be prevention of accumulation of unfolded protein intermediates during stress (Di Cagno *et al.*, 2009). The increase in the expression of EF-Tu (SSP 0403, ↑3.71 and SSP 1605, ↑2.87) might also be related to its behavior as a chaperone (Caldas T *et al.*, 2000). Also ribosomal proteins, used in ribosome assembly or stability, were involved in sensing stress (Di Cagno R *et al.*, 2007). For instance ribosomal protein S2 is required for the recruitment of ribosomal protein S1 to the 30S ribosomal subunit during translation initiation, the appropriate interaction of S1 with S2 being required for translation of bulk mRNA in prokaryotes (El-Fahmawi and Owttrim, 2007). Our data indicate that there are three isoforms of S2 that are differentially regulated from *Ga. hansenii*: SSP 0401 and SSP 0403 are up regulated respectively of 3.98 and 3.71 folds and SSP 3401 that is down regulated of 7.14 folds. This is a unique observation as relatively little is known regarding the expression or regulation of S2 function in any other system. The different expression of the isoforms of S2 might be related to the combination of 2 post-translational modifications, phosphorylation and polyphosphate addition, that may synergistically reduce or induce the level of functional S2 and translation initiation.

The ribosomal protein S19 (SSP 0001, ↑3.35 folds) acts indirectly by altering the cytoplasmic translation. In *E. coli*, at the structural level, S19 has been involved in the binding of initiation factors on the ribosome and is the major protein cross-linked to the central part of an amino acid-tRNA bound in the ribosomal A site. Moreover S19 forms a complex with S13 that strongly binds the 16S RNA. Thus, S19 could play a role in initiation of translation and decoding (Dequard-Chablat and Sellem, 1994).

Finally ribosomal protein L7/L12, that we found down regulated (SSP 1005, ↓2.08 and SSP 5002, ↓2.33) is one of a few bacterial ribosomal proteins of which accumulated evidence points to its functional roles in protein synthesis, whereas other ribosomal proteins appear to play structural roles in folding and modulating the conformations of the ribosomal RNAs, which catalyze peptide bond formation and decoding. Recent *in vitro* studies have demonstrated that L7/L12 interact with the G protein factors EF-Tu, EF-G, RF3, and IF2 (Nechifor *et al.*, 2007). The simultaneous down regulation of L7/L12 and of the translation initiator factor IF-2 (SSP 7903, ↓6.67) might slow down the translation process.

### **Cells division**

Bacteria normally divide at the midpoint of the long axis of the cell (midcell). How the division machinery selects this site over other sites in the cell is not well understood. Surprisingly we found the new induction of cell division topological factor MinE (SSP 8004, ↑20.30 folds) in *Ga. hansenii* grown in presence of acetic acid. MinE is a small protein (88 aa) with at least two function. The protein not only suppresses MinC/D mediated division inhibition, but also appears capable of distinguishing midcell from the cell poles. Over expression of MinE causes suppression of MinC/D action at all potential division sites in the

cell and, therefore, loss of topological specificity (de Boer *et al.*, 1989). Studies on *E. coli* demonstrated that MinE is present in young cells and is necessary in the selection of the proper division site and may be involved in maintaining or establishing polarity in the cells (Raskin and de Boer, 1997). In the light of these considerations, our results indicate that *Ga. hansenii*, in this environment, has a renewed metabolic force.

#### 4. CONCLUSIONS

In conclusion, this study represented the first contribution to understand the mechanism involved in acetic acid resistance of *Ga. hansenii*. The data obtained indicate that the 2D-PAGE based protocol is a sensitive and accurate method to identify protein pattern changes and can provide fascinating contributions to the understanding of complex mechanisms, such as resistance of a bacterium to a cyto-toxic molecule. Summarizing, the response to acetic acid seems to involve cellulose synthesis and simultaneously the suppression of Krebs cycle and lipid metabolism. Our data shows that also the process of translation is slow down. Besides, cells grown in presence of acetic acid demonstrate a good adaptation to the acidic environment through the new induction of MinE.

**Tab. 1** Identification of the differentially expressed proteins in acetic acid-grown cells of *Ga. hansenii* AAB0248 strain.

Protein name	Gene name	Spot no.	SwissProtTrEMBL acc. #	NCBI acc. #	Mr. (Da) theor.	pI theor.	No. of peptides identified	Mascot score	Sequence Coverage (%)	microorganism	Molecular function GO term	Fold of variation at pH 4.0 <sup>d)</sup>
<b>Amino acid metabolism</b>												
acetolactate synthase 3 regulatory subunit	ilvH	8111	<b>A9GZJ1</b>	gi 162145865	/18452	/6.75	2	66	11		acetolactate synthase activity	Down 2.38
ketol-acid reductoisomerase	ilvC	6406	<b>B2R335</b>	gi 162145866	/36465	/5.69	3	131	8		ketol-acid reductoisomerase activity	Up 2.12
Serine hydroxymethyltransferase	glyA	7609	<b>A9HRP5</b>	gi 162148783	/46976	/6.29	8	401	15		glycine hydroxymethyltransferase activity	Up 4.44
<b>Sugar metabolism</b>												
2-oxoglutarate dehydrogenase E2 component	sucB	6704	<b>A9HFG9</b>	gi 162147212	/49848	/8.72	2	82	2		transferase activity	Down 2.94
aconitate hydratase	acnA	5809	<b>A9HEZ2</b>	gi 162147150	/97168	/6.30	13	681	16		4 iron, 4 sulfur cluster binding	Down 3.45
aconitate hydratase	acnA	5810	<b>A9HEZ2</b>	gi 162147150	/97168	/6.30	9	537	12		4 iron, 4 sulfur cluster binding	Down 2.5
adenylosuccinate lyase	GbCGDNIH1_1658	5706	<b>Q0BRJ6</b>	gi 114328322	/49363	/5.96	2	97	5		adenylosuccinate lyase activity	Down 2.94
adenylosuccinate lyase	purB	7603	<b>A9HJE7</b>	gi 162147738	/49363	/5.96	4	180	10		adenylosuccinate lyase activity	Up 2.68
adenylosuccinate synthetase	purA	5607	<b>A9HLQ1</b>	gi 162148039	/46329	/5.80	5	214	12		adenylosuccinate synthetase activity	Up 2.59
aldehyde dehydrogenase	aldH	5805	<b>O30329</b>	gi 2598224	/84053	/6.86	13	589	18	Gluconacetobacter europaeus	oxidoreductase activity	Up 5.77
aldehyde dehydrogenase	aldH	4804	<b>O30329</b>	gi 2598224	/84053	/6.86	15	635	19	Gluconacetobacter europaeus	oxidoreductase activity	Up 2.32
citrate synthase	GDI1830	7701	<b>A9HII7</b>	gi 162147614	/47427	/6.32	6	211	17		citrate (Si)-synthase activity	Down 2.27
citrate synthase	GDI1830	7703	<b>A9HII7</b>	gi 162147614	/47427	/6.32	4	153	11		itrate (Si)-synthase activity	Down 2.78
citrate synthase	GDI1830	7706	<b>A9HII7</b>	gi 162147614	/47427	/6.32	5	176	13		itrate (Si)-synthase activity	Down 3.03
D-3-phosphoglycerate dehydrogenase	serA	5607	<b>A9HIU7</b>	gi 162147658	/45320	/6.43	4	169	8		catalytic activity	Up 2.59
enolase protein	eno	1604	<b>B2QW92</b>	gi 162147711	/44781	/4.70	4	185	12		phosphopyruvate hydratase activity	Up 2.49
fructose 1,6-bisphosphatase II	glpX	2501	<b>A9HCQ2</b>	gi 162146849	/40891	/8.46	2	106	6		fructose-1,6-bisphosphatase activity	Down 4.54
Isocitrate dehydrogenase	GDI1991	0309	<b>A9HJQ1</b>	gi 162147775	/36255	/5.93	2	65	3		isocitrate dehydrogenase (NAD <sup>+</sup> ) activity	Up 5.85
isocitrate dehydrogenase	GDI1991	6502	<b>A9HJQ1</b>	gi 162147775	/36255	/5.93	8	328	14		isocitrate dehydrogenase (NAD <sup>+</sup> ) activity	Down 2.44

isocitrate dehydrogenase	GDI1991	7502	<b>A9HJQ1</b>	gi 162147775	/36255	/5.93	6	319	15		isocitrate dehydrogenase (NAD+) activity	Down 2.38
isocitrate dehydrogenase	GDI1991	7504	<b>A9HJQ1</b>	gi 162147775	/36255	/5.93	2	66	6		isocitrate dehydrogenase (NAD+) activity	Down 2.5
isocitrate dehydrogenase	GDI1991	7505	<b>A9HJQ1</b>	gi 162147775	/36255	/5.93	8	318	14		isocitrate dehydrogenase (NAD+) activity	Down 4.76
isocitrate dehydrogenase	GDI1991	7509	<b>A9HJQ1</b>	gi 162147775	/36255	/5.93	5	183	10		isocitrate dehydrogenase (NAD+) activity	Down 3.70
isocitrate dehydrogenase	GDI1991	8505	<b>A9HJQ1</b>	gi 162147775	/36255	/5.93	5	249	10		isocitrate dehydrogenase (NAD+) activity	Up 2.62
putative NAD-dependent aldehyde dehydrogenase	GOX1122	7710	<b>Q5FRV6</b>	gi 58039582	/50498	/5.69	5	275	12	Gluconobacter oxydans 621H	oxidoeductase activity	Up 2.51
putative pyruvate dehydrogenase E1 component subunit beta	pdhB	2501	<b>A9HHP7</b>	gi 162147505	/36882	/5.00	2	115	5		catalytic activity	Down 4.54
pyruvate phosphate dikinase	podA	2902	<b>A9HEP2</b>	gi 162147113	/96121	/5.22	3	139	3		kinase activity	Up 2.10
<b>Transcription/Translation</b>												
DNA-directed RNA polymerase subunit alpha	rpoA	1506	<b>B2QY59</b>	gi 162149150	/37384	/4.89	3	115	10		DNA-directed RNA polymerase activity	Down 5
electron transfer flavoprotein subunit beta	etfB	6308	<b>A9HEE6</b>	gi 162147074	/26296	/6.45	3	124	15		electron carrier activity	Up 4.51
elongation factor Tu	tufB	0403	<b>B2QY33</b>	gi 162149176	/42982	/5.33	3	121	9		motor activity	Up 3.71
elongation factor Tu	tufB	1605	<b>B2QY33</b>	gi 162149176	/42982	/5.33	12	506	33		translation elongation factor activity	Up 2.87
prolyl-tRNA synthetase	proS	5706	<b>A9HRR5</b>	gi 162148795	/53065	/5.07	3	122	6		ATP binding	Down 2.94
Ribosomal protein L4	rplD	0207	<b>B2QY36</b>	gi 162149173	/21758	/10.03	4	178	12		structural constituent of ribosome	Up 5.61
Ribosomal protein L7/L12	rplL	1005	<b>B2QY27</b>	gi 162149181	/12910	/4.90	5	245	33		structural constituent of ribosome	Down 2.08
Ribosomal protein L7/L12	rplL	5002	<b>B2QY27</b>	gi 162149181	/12910	/4.90	1	69	14		structural constituent of ribosome	Down 2.33
Ribosomal protein L10	rplJ	9302	<b>A9H3S7</b>	gi 162149182	/19224	/10.40	1	57	7		Protein binding	Up 3.25
Ribosomal protein L33	amb3569	0011	<b>Q2W1A2</b>	gi 23012441	/6390	/10.12	3	97	40	Magnetospirillum magnetotacticum MS-1	structural constituent of ribosome	Up 2.03
Ribosomal protein S2	Gdia_3347	0401	<b>B2R098</b>	gi 209545460	/28117	/6.09	6	281	31		structural constituent of ribosome	Up 3.98
Ribosomal protein S2	Gdia_3347	0403	<b>B2R098</b>	gi 209545460	/28117	/6.09	5	197	18		structural constituent of ribosome	Up 3.71
Ribosomal protein S2	Gdia_3347	3401	<b>B2R098</b>	gi 209545460	/28117	/6.09	11	508	47		structural constituent of	Down 7.14

											ribosome	
Ribosomal protein S19	rpsS	0001	<b>B2QY39</b>	gi 162149170	/10253	/10.54	3	118	35	Gluconacetobacter diazotrophicus PAI 5	structural constituent of ribosome	Up 3.35
translation-associated GTPase	GDI0937	1605	<b>A9HC06</b>	gi 162146759	/39269	/4.93	7	438	21		GTP binding	Up 2.87
transcription elongation factor NusA	nusA	0801	<b>A9HF12</b>	gi 162147158	/58182	/4.64	8	306	15		transcription factor activity	Down 2.08
transcription elongation factor NusA	nusA	0802	<b>A9HF12</b>	gi 162147158	/58182	/4.64	6	222	12		transcription factor activity	Up 7.33
translation initiation factor IF-2	GDI1365	7903	<b>B2QZ86</b>	gi 162147160	/97805	/7.24	13	616	13		translation initiation factor activity	Down 6.67
tRNA pseudouridine synthase B	DSM3645_06384	7202	<b>A4A2R8</b>	gi 87312284	/30557	/5.30	2	72	2	Blastopirellula marina DSM 3645	RNA binding	Down 2.78
<b>Protein turnover</b>												
ATP-dependent Clp protease proteolytic subunit	clpP	0306	<b>A9HCR1</b>	gi 162146853	/24688	/5.44	2	69	9		endopeptidase Clp activity	Down 2.04
chaperone protein dnaK	dnaK	1806	<b>A9HEA3</b>	gi 162147057	/67139	/4.89	6	278	12		ATP binding	Up 2.57
chaperonin GroEL	groL	5705	<b>B2QWL8</b>	gi 162147833	/57881	/5.43	3	99	8		protein binding	Down 2.5
cold shock-like protein cspE	cspE	9301	<b>A9HIW8</b>	gi 162147665	/23316	/9.51	4	228	15		DNA binding	Down 7.14
lipoprotein signal peptidase	Dgeo_2580	1006	<b>Q1J3C0</b>	gi 94972048	/18159	/10.21	1	63	6	Deinococcus geothermalis DSM 11300	aspartic-type endopeptidase activity	Down 2.04
<b>Membrane transport</b>												
electron transfer flavoprotein beta-subunit	etfB	7304	<b>Q5NMF6</b>	gi 56552376	/27257	/5.53	1	103	6	Zymomonas mobilis subsp. mobilis ZM4	electron carrier activity	Up 3.42
FeS assembly protein SufC	sufC	5301	<b>A9HRY6</b>	gi 162148829	/25885	/5.90	9	472	42		ATP binding	Down 2.13
Outer membrane protein	GDI0041	5307	<b>A9GZP4</b>	gi 162145880	/40378	/7.18	3	120	8		protein binding	Up 2.16
Outer membrane protein	GDI0041	6406	<b>A9GZP4</b>	gi 162145880	/40378	/7.18	2	111	6		cell outer membrane	Up 2.12
<b>Cell redox homeostasis</b>												
Alkyl hydroperoxide reductase subunit C	GOX1332	1201	<b>Q5FRB2</b>	gi 58039776	/20535	/4.98	6	391	36	Gluconobacter oxydans 621H	oxidoreductase activity	Up 2.53
Alkyl hydroperoxide reductase subunit C	GOX1332	5105	<b>Q5FRB2</b>	gi 58039776	/20535	/4.98	2	88	14	Gluconobacter oxydans 621H	oxidoreductase activity	Up 7.70
putative glyoxalase	GDI0871	2003	<b>A9HBG9</b>	gi 162146693	/14115	/4.80	2	87	13		oxidoreductase activity	Down 3.57
putative oxidoreductase	GDI2680	7402	<b>A9HPR5</b>	gi 162148460	/28942	/6.32	2	126	7		oxidoreductase activity	Down 8.33
putative oxidoreductase	GDI0555	7702	<b>A9H878</b>	gi 162146380	/34036	/6.19	1	66	4		oxidoreductase activity	Down 4.76
radical SAM family Fe-S protein	GDI0718	7903	<b>A9HA97</b>	gi 162146542	/54411	/6.94	8	224	16		catalytic activity	Down 6.67

radical SAM family Fe-S protein	GDI0718	8706	<b>A9HA97</b>	gi 162146542	/54411	/6.94	10	373	24		catalytic activity	Up 2.13
<b>Nucleotide/nucleic acid metabolism</b>												
Adenylate kinase	adk	4201	<b>B2QY56</b>	gi 162149153	/23784	/6.62	2	94	10		adenylate kinase activity	Down 4.54
histidine triad (HIT) protein	Gdia_1625	6105	<b>B2R2Y2</b>	gi 209543789	/13345	/6.12	1	84	12		catalytic activity	Up 7.55
inosine-5'-monophosphate dehydrogenase	guaB	8702	<b>A9HID1</b>	gi 162147595	/53289	/6.23	4	135	11		IMP dehydrogenase activity	Down 2.78
phosphoribosylaminoimidazole-succinocarboxamide synthase	purC	0303	<b>B2QWC4</b>	gi 162147740	/28945	/5.67	1	58	6		phosphoribosylaminoimidazole succinocarboxamide synthase activity	Up 2.91
phosphoribosylformylglycinamide synthase II	purL	1806	<b>A9HJG3</b>	gi 162147744	/77655	/4.89	6	279	8		phosphoribosylformylglycinamide synthase activity	Up 2.57
sulfate adenyltransferase subunit 2	cysD	8407	<b>A9H0V9</b>	gi 162149006	/30554	/6.35	3	100	13		sulfate adenyltransferase (ATP) activity	Down 2.17
<b>Lipid metabolism</b>												
3-oxoacyl-(acyl carrier protein) synthase III	fabH	8202	<b>Q7NF35</b>	gi 37523261	/34675	/5.81	1	55	3	Gloeobacter violaceus PCC 7421	3-oxoacyl-[acyl-carrier-protein] synthase activity	Down 2.22
Acetyl-CoA carboxylase carboxyl transferase	accD	8409	<b>A9HE81</b>	gi 162147048	/33855	/8.93	4	166	9		transferase activity	Up 2.01
Acetyl-CoA carboxylase carboxyl transferase	accD	8410	<b>A9HE81</b>	gi 162147048	/33855	/8.93	7	293	14		transferase activity	Down 2.13
Acetyl-CoA hydrolase	GDI1836	6701	<b>A9HIK2</b>	gi 162147620	/54894	/6.04	2	128	5		hydrolase activity	Down 2.17
Acetyl-CoA hydrolase	GDI1836	6702	<b>A9HIK2</b>	gi 162147620	/54894	/6.04	3	186	11		hydrolase activity	Down 3.57
Acetyl-CoA hydrolase	GDI1836	6705	<b>A9HIK2</b>	gi 162147620	/54894	/6.04	3	200	11		hydrolase activity	Down 3.70
Acetyl-CoA hydrolase	GDI1836	5705	<b>A9HIK2</b>	gi 162147620	/54894	6.04	2	132	5		transferase activity	Down 2.5
dihydrolipoamide acetyltransferase	acoC	1506	<b>A5YJ12</b>	gi 148530006	/36174	/4.94	3	115	8		hydrolase activity	Down 5
enoyl-[acyl-carrier-protein] reductase	fabI	6402	<b>A9H0U5</b>	gi 162149001	/37070	/6.80	3	126	8		oxidoreductase activity	Up 2.17
FAD dependent oxidoreductase	Gdia_3531	9701	<b>A9HMF9</b>	gi 209545640	/58994	/9.21	4	124	5		oxidoreductase activity	Down 4.35
glycerol-3-phosphate dehydrogenase	glpD	8701	<b>Q9PB78</b>	gi 15838857	/57273	/7.79	2	120	3		glycerol-3-phosphate dehydrogenase activity	Down 3.85
lipoyl synthase	lipA	8504	<b>A9HJB7</b>	gi 162147727	/36459	/7.15	5	189	14		lipoate synthase activity	Down 2.70
<b>Others (cellular and metabolic processes)</b>												
hypothetical protein GDI0701	GDI0701	6103	<b>A9H9B9</b>	gi 162146525	/22418	/6.33	1	86	5		unknown function	Down 2.44
hypothetical protein SMC01723	SMC01723	2104	<b>Q92SF7</b>	gi 15964195	/18704	/4.84	1	91	7	Sinorhizobium meliloti 1021	phosphatase activity	Up 5.47

putative carboxymuconolactone decarboxylase protein	GDI1413	8007	<b>A9HFF9</b>	gi 162147208	/11695	/5.33	2	118	12		peroxidase activity	Down 2.04
putative cell division topological specificity factor	minE	8004	<b>A9HLY4</b>	gi 162148068	/10393	/6.73	2	71	11		protein binding	Up 20.30
putative dTDP-6-deoxy-3,4-keto-hexulose isomerase	wbtA	4205	<b>Q6QNC8</b>	gi 45644919	/15663	/5.26	1	64	6	Escherichia coli	isomerase activity	Up 2.16
putative flagellar motor switch protein fliN	fliN	0101	<b>A9HHD1</b>	gi 162147463	/12701	/4.59	1	73	9		motor activity	Up 4.92





## BIBLIOGRAPHY

- Allen G.C.**, M.A. Flores-Vergara, S. Krasynanski, S. Kumar, W.F. Thompson, *Nature. Protocols*. 1 (2006) 2320.
- Alvarez O.M.**, M. Patel, J. Booker, L. Markowitz, *Wounds*. 16 (2004) 224.
- Anderson L.** and J. Seilhamer, *Electrophoresis*. 18 (1997) 533.
- Antonoli P.**, G. Zapparoli, P. Abbruscato, C. Sorlini, G. Ranalli, P.G. Righetti, *Proteomics*. 5 (2005) 2453.
- Berkelman T.**, *Methods. Mol. Biol.* 424 (2008) 51.
- Bekesiova I.**, J.P. Nap, L. Mlynarova, *Plant. Mol. Biol. Rep.* 17 (1999) 269.
- Bossi A.**, S. Rinalducci, L. Zolla, P. Antonoli, P.G. Righetti, G. Zapparoli, *J. Appl. Microbiol.* 102 (2007) 787.
- Caldas T.**, S. Laalami, G. Richarme, *J. Biol. Chem.* 275 (2000) 855.
- Carey K.L.**, A.M. Jongco, K. Kim, G.E. Ward, *Eukaryot. Cell*. 3 (2004) 1320-1330.
- Celestino P.B.**, L.R. de Carvalho, L.M. de Freitas, F.A. Dorella, N.F. Martins, L.G. Pacheco, *Genet. Mol. Res.* 3 (2004) 421.
- Chang L.**, Z. Zhang, H. Yang, H. Li, H. Dai, *J. Phytopathol.* 155 (2007) 431.
- Chang S.**, J. Puryear, J. Cairney, *Plant. Mol. Biol. Rep.* 11 (1993) 113.
- Clark D.P.** and J.E. Cronan, *Escherichia coli and Salmonella typhimurium: Cellular and Molecular Biology*, ed. FC Neidhardt, Washington, (1996) 343.
- Cozzone A.J.**, *Annu. Rev. Microbiol.* 52 (1998) 127-164.
- Czaja W.**, D. Romanovicz, R. M. Brown, *Cellulose*. 11 (2004) 403.
- Davies D.**, *Nat. Rev. Drug. Discov.* 2 (2003) 114.
- De Angelis M.** and M. Gobbetti, *Proteomics*. 4 (2004) 106.
- De Boer L.**, J.W. Brouwer, C.W. Van Hassel, P.R. Levering, L. Dijkhuizen, *Antonie. Van. Leeuwenhoek*. 56 (1989) 221.
- De Vero L.** and P. Giudici, *Int. J. Food. Microbiol.* 125 (2008) 96.
- Dequard-Chablat M.** and C.H. Sellem, *J. Biol. Chem.* 269 (1994) 14951.
- Di Cagno R.**, M. De Angelis, A. Limitone, F. Minervini, M.C. Simonetti, S. Buchin, M. Gobbetti, *Proteomics*. 7 (2007) 2430.
- Di Cagno R.**, M. De Angelis, R. Coda, F. Minervini, M. Gobbetti, *Res. Microbiol.* 160 (2009) 358.
- Doyle J.J.** and J.L. Doyle, *Phytochem. Bull.* 19 (1987) 11.
- Du Toit W.J.** and I.S. Pretorius, *Ann. Microbiol.* 52 (2002) 155.
- Ebner H.**, S. Sellmer, H. Follmann, *Biotechnology: A Multi-Volume Comprehensive Treatise*, eds. VCH, Weinheim, Germany (1996) 381.
- El-Fahmawi B.** and G.W. Owttrim, *Can. J. Microbiol.* 53 (2007) 551.
- Flagel L.**, J.R. Christensen, C.D. Gustus, K.P. Smith, P.M. Olhoft, D.A. Somers, P.D. Matthews, *Crop. Sci.* 45 (2005) 1985.
- Fontana J.D.**, A.M. de Sousa, C.K. Fontana, I.L. Torriani, J.C. Moreschi, B.J. Gallotti, S.J. de Sousa, G.P. Narcisco, J.A. Bichara, L.F. Farah, *Appl. Biochem. Biotechnol.* 25 (1990) 253.
- Francis M.**, H. Lin, J.C.-L. Rosa, H. Doddapaneni, E.L. Civerolo, *Eur. J. Plant Pathol.* 115 (2006) 203.
- Galante E.**, T. Caravaggio, P.G. Righetti, *Biochim. Biophys. Acta*. 442 (1976) 309.
- Gelling C.**, I.W. Dawes, N. Richhardt, R. Lill, U. Mühlenhoff, *Mol. Cell. Biol.* 28 (2008) 1851.
- Gonzalez A.**, J.M. Guillamon, A. Mas, M. Poblet, *Int. J. Food. Microbiol.* 108 (2006) 141.
- Gullo M.**, C. Caggia, L. De Vero, P. Giudici, *Int. J. Food Microbiol.* 106 (2006) 209.
- Gupta A.**, V.K. Singh, G.N. Qazi, A. Kumar, *J. Mol. Microbiol. Biotechnol.* 3 (2001) 445.
- Gygi S.P.**, Y. Rochon, B.R. Franza, R. Aebersold, *Mol. Cell. Biol.* 19 (1999a) 1720.
- Hancock R.D.** and R. Viola, *Trends. Biotechnol.* 20 (2002) 2002.
- Harjua V.A.**, A. Skeltona, G.R.G. Clover, C. Rattib, N. Boonhama, C.M. Henrya, R.A. Mumforda, *J. Virol. Methods*. 123 (2005) 73.
- Herbert B.R.**, J. Grinyer, J.T. McCarthy, M. Isaacs, E.J. Harry, H. Nevalainen, M.D. Traini, S. Hunt, B. Schulz, M. Laver, A.R. Goodall, J. Packer, J.L. Harry, K.L. Williams, *Electrophoresis*. 27 (2006) 1630.
- Hren M.**, J. Boben, A. Rotter, P. Kralj, K. Gruden, M. Ravnikar, *Plant. Pathol.* 56 (2007) 785.

- Hu J.S.**, M. Wang, D. Sether, W. Xie, K.W. Leonhardt, *Ann. Appl. Biol.* 128 (1996) 55.
- Husale S.**, W. Grange, M. Karle, S. Bürgi, M. Hegner, *Nucleic. Acids. Res.* 36 (2008) 1443.
- Iida A.**, Y. Ohnishi, S. Horinouchi, *J. Bacteriol.* 190 (2008) 5009.
- Incamps A.**, F. Hély-Joly, P. Chagvardieff, J.C. Rambourg, *Biotechnol. Bioeng.* 91 (2005) 447.
- Jaakola L.**, A.M. Pirttilä, M. Halonen, A. Hohtala, *Fruit. Mol. Biotech.* 19 (2001) 201.
- Josic D.** and J.G. Clifton, *Proteomics* 7 (2007) 3010.
- Kim S.-H.** and T. Hamada, *Lam. Biotech. Lett.* 27 (2005) 1841.
- Kim H.J.**, J.H. Kim, C.S. Shin, *Process. Biochem.* 35 (1999) 243.
- Konat G.**, H. Offner, J. Mellah, *Cell. Mol. Life. Sci.* 40 (1984) 304.
- Kubicek C.P.** and L. Karaffa, *Basic Biotechnology*, eds. Cambridge, University Press, New York, (2006) 359.
- Lee S.-O.**, G.-W. Hong, D.-K. Oh, *Biotechnol. Prog.* 19 (2003) 1081.
- Li R.**, R. Mock, Q. Huang, J. Abad, J. Hartung, G. Kinard, *J. Virol. Methods.* 154 (2008) 48.
- Li W.**, J.S. Hartung, L. Levy, *J. Microbiol. Methods.* 66 (2006) 104.
- Lopez R.**, C. Asensio, M.M. Guzman, N. Boonham, *J. Virol. Methods.* 136 (2006) 24.
- Mel'nikov S.M.**, V.G. Sergeyev, K. Yoshikawa, *J. Am. Chem. Soc.* 117 (1995) 2401.
- Möller E.M.**, G. Bahnweg, H. Sandermann, H.H. Geiger, *Nucleic. Acids. Res.* 20 (1992) 6115.
- Mumford R.**, K. Walsh, N. Boonham, *Bull. OEPP/EPPO Bull.* 30 (2000) 431.
- Murray M.G.** and W.F. Thompson, *Nucleic. Acids. Res.* 8 (1980) 4321.
- Nechifor R.**, M. Murataliev, K.S. Wilson, *J. Biol. Chem.* 282 (2007) 36998.
- Park J.K.**, J.Y. Jung, Y.H. Park, *Biotechnol. Lett.* 25 (2003) 2055.
- Park Y.S.**, S. Ohtake, K. Toda, M. Fukaya, H. Okumura, Y. Kawamura, *Biotechnol. Bioeng.* 33 (1989) 918.
- Parmessur Y.**, S. Aljanabi, S. Saumtally, A. Dookun-Saumtally, *Plant. Pathol.* 51 (2002) 561.
- Pedersen S.K.**, J.L. Harry, L. Sebastian, J. Baker, M.D. Traini, J.T. McCarthy, A. Manoharan, M.R. Wilkins, A.A. Gooley, P.G. Righetti, N.H. Packer, K.L. Williams, B.R. Herbert, *J. Proteome. Res.* 2 (2003) 303.
- Phillips C.I.** and M. Bogyo, *Cell. Microbiol.* 7 (2005) 1061.
- Piñeiro C.**, J. Barros-Velázquez, J. Velázquez, A. Figueras, J.M. Gallardo, *J. Proteome. Res.* 2 (2003) 127.
- Polati R.**, G. Zapparoli, P. Giudici, A. Bossi, *J. Chromatogr. B Analyt. Technol. Biomed. Life. Sci.* 877 (2009) 887.
- Puchooa D.**, *Sonn. African. J. Biotech.* 3 (2004) 253.
- Rabilloud T.**, *Electrophoresis* 17 (1996) 813.
- Raskin D.M.**, P.A. de Boer, *Cell.* 181 (1997) 685.
- Raspor P.** and D. Goranovic, *Crit. Rev. Biotechnol.* 28 (2008) 101.
- Righetti P.G.**, R.P. Brown, A.L. Stone, *Biochim. Biophys. Acta.* 542 (1978) 244.
- Ross P.**, R. Mayer, M. Benziman, *Microbiol. Rev.* 55 (1991) 35.
- Saghai-Maroofo M.A.**, K.M. Soliman, R.A. Jorgenson, R.W. Allard, *Proc. Natl. Acad. Sci. U.S.A.* 81 (1984) 8014.
- Silva P.**, H. Cardoso, H. Geros, *Am. J. Enol. Vitic.* 55 (2004) 65.
- Shalon D.**, S.J. Smith, P.O. Brown, *Genome. Res.* 6 (1996) 639.
- Shevchenko A.** and A. Shevchenko, *Anal. Biochem.* 296 (2001) 279.
- Stefanova S.**, M. Kosseva, I. Tepavicharova, V. Beschov, *Biotechnol. Lett.* 9 (1987) 475.
- Steiner P.** and U. Sauer, *Appl. Environ. Microbiol.* 67 (2001) 5474.
- Takai M.** and T. Erata, *Biosci. Ind.* 56 (1998) 808.
- Wang T.**, N. Zhang, L. Du, *Biotech. Lett.* 27 (2005) 629.
- Wang W.**, J. Sun, M. Hartlep, W.-D. Deckwer, A.P. Zeng, *Biotechnol. Bioeng.* 83 (2003) 525.
- Wyatt S.D.** and J.K. Brown, *Phytopathology* 86 (1996) 1288–1293.
- Yamaguchi Y.**, Y. Miyagi, H. Baba, *J. Neurosci. Res.* 86 (2008) 755.

**Yamaguchi Y.**, Y. Miyagi, H. Baba, *J. Neurosci. Res.* 86 (2008) 766.

**Yolles R.S.** and G. Freeman, *Biochim. Biophys. Acta.* 138 (1967) 506.

**Zhang N.**, R. Chen, N. Young, D. Wishart, *Proteomics.* 7 (2007) 484.

**Zoubi-Hasona K.** and L.J. Brady, *Methods. Mol. Biol.* 425 (2008) 287.



## SESSION 3



# PROTEOMICS MEETS IRON

## IRON PROTEOMICS

A large number of cellular enzymes depend on iron for their biological function and, consequently, this metal is essential for basic physiological processes. Iron can shuttle between two thermodynamically stable oxidation states,  $\text{Fe}^{3+}$  or ferric iron and  $\text{Fe}^{2+}$  or ferrous iron. This makes it ideally suited to the catalysis of biochemical reactions, but it also means that it is able to catalyze reactions leading to the production of toxic oxygen radicals, particularly when it is present in excess. Besides hydrated ferric ions are relatively strong acids; protons in water coordinated to ferric ions have a  $\text{pK}_a \approx 3$ . The conjugate bases of hydrated ferric ions form rapidly multinuclear species, accounting for the low solubility of aqueous ferric ions (10<sup>-18</sup> M) and for rust formation (Theil and Goss, 2009).

The chemical properties of iron makes it a fundamental element for life, complexing active sites of many crucial enzymes, while free iron leads to the formation of damaging free radicals via the Fenton series of reactions. As a result, individual cells and whole organisms must tightly regulate their iron influx and efflux to keep iron levels within the optimal physiological optimal range, enough to sustain metabolic functions, while preventing its accumulation in potentially toxic excesses (Anderson and Vulpe, 2009). Thus the organisms have evolved complex biochemical mechanisms for maintaining a balance between iron as an essential element and iron as a cytotoxic agent (Bleackley *et al.*, 2009).

Mechanisms to regulate iron homeostasis are most likely billions of years older than those for oxygen homeostasis. It could be hypothesised that contemporary microbes regulate iron in the absence of oxygen by modelling ancient organisms that lived before atmospheric oxygen appeared (Boyd *et al.*, 2009). Moreover, proteins that manage iron and oxidants such as the mini-ferritins in contemporary bacteria, also called Dps (DNA protection during stress) proteins, are expressed in anaerobic archaea (Wiedenheft *et al.*, 2005). Mini-ferritins are 12 subunit protein cages from archaea and bacteria that contrast with maxi-ferritins, the 24 subunit cages from bacteria, animals and plants, which use iron and dioxygen as substrates, by consuming iron and hydrogen peroxide as substrates to make the mineral inside protein nanocages. Such peroxide-consuming ferritins may be progenitors of modern ferritins and may have contributed to the transition from anaerobic to aerobic life with iron and oxygen. Iron and oxygen homeostasis, in animals, integrate DNA/mRNA controls; regulation of these two processes intersect along many pathways. Iron homeostasis occurs within cells and between cells to confer balance throughout tissues and the organism. Each

cell or tissue type will have a different iron set point for homeostasis that reflects the specific role of each cell type. For example, animal red blood cells need much more iron than epithelial cells because of the synthesis of haemoglobin (Wrighting and Andrews, 2008). Similarly, in plants, leaves contain much more iron than flowers because of the synthesis of ferredoxins important in photosynthesis (Kim and Guerinot, 2007).

Major steps in understanding iron metabolism were made over the last decade (Templeton, 2002). Peculiar is the discovery of iron role in regulating genes that involves its own metabolism and its trafficking at a post-transcriptional level (Cairo and Pietrangelo, 2000, Eisenstein, 2000, Theil and Eisenstein, 2000). Such role became textbook examples of such a mode of regulation. A perhaps reawakened interest in the metal saw classical molecular biological approaches such as differential display and subtraction cloning used to address more global effects of iron (Barisani, 2000, Ye and Connor, 2000). Recently, microarray technology has dominated such efforts (Liu *et al.*, 2005) and proteomics could provide new knowledge for understanding the iron metabolism or homeostasis.

In single-cell organisms without recognizable organelles, i.e., most bacteria and archaea, iron will be distributed relatively uniformly throughout the cytoplasm either in protein cofactors or in ferritins. The regulation of bacterial iron homeostasis is often controlled by the iron-sensing ferric uptake repressor (Fur). The *Bacillus subtilis* Fur protein acts as an iron-dependent repressor for siderophore biosynthesis and iron transport proteins. Through the use of proteomic techniques Gaballa *et al.* (2008) demonstrated that Fur also coordinates an iron-sparing response that acts to repress the expression of iron-rich proteins when iron is limiting.

The iron distribution in single-cell organisms with internal compartments, such as photosynthetic plastids in *Chlamydomonas* or mitochondria in *Saccharomyces* and *Chlamydomonas*, is uneven with much higher iron concentrations in the organelles. In plastids, for example, high concentrations of iron are needed for the electron transfer by iron sulfur ferredoxins for photosynthesis and, in mitochondria, for the electron transfer by heme proteins of mitochondrial oxidative metabolism. A study on *Saccharomyces cerevisiae* analyzed metabolic changes under iron deficiency via proteomic methods. The YGH2 yeast strain expressing H-ferritin, the YGH2-KG (E62K and H65G) mutant strain, and the YGT control strain were used. Comparative proteomic analysis showed that the synthesis of 34 proteins was at least stimulated in YGH2, whereas the other 37 proteins were repressed. The increased proteins included major heat-shock proteins and proteins related to endoplasmic reticulum-associated degradation (ERAD). On the other hand, the proteins involved in folate metabolism, purine and methionine biosynthesis, and translation were reduced. This suggests that intracellular iron depletion induces imperfect translation of proteins. This study is the first to present a molecular model for iron deficiency and may



provide valuable information on the regulatory network of iron metabolism (Seo *et al.*, 2008).

Finally the distribution of iron among tissues or cells in multicellular organisms is not uniform. When the specialized role of a tissue requires large amounts of iron, the cellular iron concentration can be an order of magnitude higher than in a more average tissue or cell. Extracellular iron transport molecules can recognize cell or tissue iron need, which is often communicated by the total number of surface receptors that bind extracellular iron complexed to protein or chelator transporters.

The most iron-rich parts of plants are the leaves, seeds and roots. For instance the proteome data analysis provided an integrated view of the adaptive metabolism change of tomato roots to iron deficiency, especially a clear configuration of the carbohydrate metabolism network. Most of the altered proteins in iron-deficiency roots of tomato are associated closely with iron uptake and delivery, sulfur metabolism, alleviating redox damage, root phenotypical change, signal reception, transduction, *etc.* (Li *et al.*, 2008).

In animals, tissues with specialized functions in iron or oxygen homeostasis have the highest iron concentrations. The most iron-rich part of animals is the blood, followed by spleen, liver, and kidney. Changes in gene expression maintain iron homeostasis during iron deficiency or iron excess. For instance the iron-low diet affected the epithelial cell proteome and inhibited the development of chronic intestinal inflammation, suggesting a critical role for nutritional factors in the pathogenesis of inflammatory bowel disease (Werner *et al.*, 2009). The hormone that coordinates whole body responses to changes in iron is hepcidin propeptide (Wrighting and Andrews, 2008, Ganz, 2008, Nemeth, 2008, De Domenico, 2008), secreted by the liver. A proteomic study of Kartikasari *et al.* (2008) demonstrated for the first time that secretion of bioactive hepcidin-25 by liver cells correlates with its gene transcription and points towards synergism between iron and inflammation signaling pathways. The uncovered synergistic interaction between iron and inflammation pathways in hepcidin regulation holds potential implications especially in the management of iron disorder conditions. Two pathological conditions with altered iron homeostasis, the anemia of chronic disease and hereditary hemochromatosis, can be traced to abnormal hepcidin metabolism. The anemia of chronic disease is caused by increased hepcidin and reflects an innate immune response thought to protect the host by diminishing both transferrin bound iron and pathogen iron acquisition. This response has the side effect of causing a mild anemia in the host, an anemia due to a change in the iron distribution within the body. The result is that the red cells are iron-deficient but macrophages have excess iron. Hereditary hemochromatosis (HH) is associated with a decrease in serum hepcidin that leads to continued efflux of absorbed iron by enterocytes (gut epithelial cells) mediated by the efflux protein ferroportin on the basolateral (serum) surface of the intestine and a defect in

sensing body iron accurately. In particular hereditary hemochromatosis type I is an autosomal-recessive iron overload disease associated with a mutation in *HFE* gene. Petrak *et al.* (2007) undertook a proteomic study comparing protein expression in the liver of *HFE* deficient mice with control animals. They found 11 proteins that were differentially expressed in the *HFE*-deficient liver using two-dimensional electrophoresis and mass spectrometry identification. Of particular interest were urinary proteins 1, 2 and 6, glutathione-S-transferase P1, selenium binding protein 2, sarcosine dehydrogenase and thioredoxin-like protein 2. This data suggest possible involvement of lipocalins, TNF-alpha signaling and PPAR-alpha regulatory pathway in the pathogenesis of hereditary hemochromatosis and suggest future targeted research addressing the roles of the identified candidate genes in the molecular mechanism of hereditary hemochromatosis. All this studies mapping iron metabolism-specific protein expression pattern offers new directions to put the pieces of iron homeostasis puzzle together, nevertheless iron remains still somewhat enigmatic.

# CHAPTER 1

## HIGH RESOLUTION PREPARATION OF MONOCYTE-DERIVED MACROPHAGES (MDM) PROTEIN FRACTIONS FOR CLINICAL PROTEOMICS

### 1. INTRODUCTION

Macrophages are involved in a number of key physiological processes and complex responses such as inflammatory, immunological, infectious diseases and iron homeostasis. Iron homeostasis is mainly controlled by the liver-produced hepcidin peptide (Nemeth *et al.*, 2004). This small hormone synchronizes systemic iron fluxes by binding to the iron export channel ferroportin located on the surface of macrophages, hepatocytes and intestinal enterocytes to cause its internalization and proteolysis (Andrews, 2008). Ferroportin, the only known cellular iron exporter, is highly expressed on cells involved in iron export, including the duodenal mucosa, macrophages and cells of the placenta. In macrophages, ferroportin is required for the efficient recycling of iron from ingested erythrocytes (De Domenico *et al.*, 2008). *In vivo*, tissue macrophages are derived from circulating monocytes recruited in the tissues by constitutive or inflammatory signals (Hansson, 1999, Dale *et al.*, 2008). Primary cultures of monocyte-derived macrophages (MDMs) constitute a good model for studying the biological activities of macrophages, and are excellent candidates for a proteomic approach; in fact they can be easily obtained and cultured within 12 days. During this period they acquire many of the characteristics of *in vivo* activated tissue macrophages, such as CD14 (LPS receptor)-expression (Schlegel *et al.*, 1999), and the secretion of proteases involved in remodelling the extracellular matrix (Lepidi *et al.*, 2001). Proteomic analysis is the most powerful method to elucidate the proteic effectors of cellular processes (O'Farrel, 1975, Van den Bergh and Arckens, 2005, Yang and Huang, 2007). Two dimensional electrophoresis allows to map protein populations, to identify and underpin proteins whose expression levels correlate with particular responses or with pathological states (Hanash, 2003), generating information to designate protein markers specific for the disease. Sometime, the analysis of total cell proteome poses practical challenges, due to its complexity (a thousand of proteins expressed in a cell), to the great dynamic range of protein expression and to the different protein properties (pI, molecular mass, hydrophobicity, post-translational modifications). Suitable strategies to decrease such high complexity are aimed at analysing subsets of the proteome, e.g. by narrowing the pH range used for the first dimension (Westbrook *et al.*, 2001), or by the sub-fractionation of proteins

into more homogeneous classes (Righetti *et al.*, 2001). The analysis of single cellular compartments, fractionating the proteins into common localisation categories, e.g. secreted components, membrane, nuclear, organelle's proteins and cytosol, has given important practical advantages and results offer a better insight into the protein expression of each cell fraction considered (Yates *et al.*, 2005, Komatsu, 2007, Fischer *et al.*, 2006, Song *et al.*, 2006, Guimarães de Araújo and Huber, 2007). Sometimes the isolation of proteome sub-sets has been achieved with selective tagging methods for proteins, as in the case of surface proteins, membrane-associated components (Sabarth *et al.*, 2002). Alternatively, sequential extraction methods are used to collect proteins with physico-chemical properties in-common (Cordwell, 2008). Aimed at understanding the molecular mechanisms occurring during the physiological responses of macrophages to different stimuli/environment/pathological conditions, the proteome of such cells has been submapped in secretome, cytosol and membrane proteomes (Dupont *et al.*, 2004, Slomianny *et al.*, 2006). Further optimisation of the protein extraction method would results in higher resolution of the 2D maps, with benefit in terms of comparative proteome studies, thus permitting to expand significantly our knowledge on macrophages and on their role in iron dealing. MDMs are a good model for macrophages proteomic studies, being easy to recruit, grow and mimicking well tissues differentiated ones. Here we report on the effective fractionation of cytosol and membrane proteins of MDMs, by the adaptation of a protocol that uses the neutral detergent Triton X-114, whose peculiarity is the temperature-dependent solubility.

The treatment proved to be very effective for fractionating proteins on the basis of their hydropathicity (Santoni *et al.*, 2000). Membrane, cytosol and secretome proteins have been run on 2D gels. Mini gels allowed to count over 500 protein spots, with very sharply focused spots. MS/MS on sampled spots was used for deciphering the maps, indicating good correlation between the fraction analysed and the protein spot identified in the fraction. In preliminary experiments we also assessed the obtained fraction by SELDI-TOF-MS for hepcidin content, and we could detect a peptide with the same mass as hepcidin only in the cytosolic fraction, as expected.

## **2. MATERIALS AND METHODS**

### **2.1 Monocyte Derived Macrophages Cultures**

Peripheral blood mononuclear cells were isolated from healthy human blood donors attending to the Transfusion Service, University Hospital of Verona.

Primary cultures of human MDMs were prepared as described by Pinet *et al.* (2003) with minor changes. Monocytes were left to differentiate in a RPMI medium, containing 2 mM

streptomycin, 2 mM Gln, and 10% FCS. Monocytes purity was tested by flow cytometer, according to Pinet *et al.* (2003) quality criteria.

## 2.2 Cell lysis

After the differentiation, cells were lysed as suggest by Slomianny *et al.* (2006) with some modifications. Lysis solution was 10 mM HEPES, 10 mM KCl, protease inhibitor (Mini-Complete Roche). Cell were washed 4–5 times with 10 ml DPBS at room temperature. The washes were collected and pooled for secretome analysis. Three ml of cold lysis buffer were added and incubate 10 min. Cells were scraped from the surface and centrifuged 25 min at  $16000 \times g$ . Cytoplasm was recovered as supernatant, membranes as pellet.

## 2.3 Extraction of secreted proteins

The culture media were pooled and the proteins precipitated for 1 h at 0 °C by adding 15% TCA. The protein pellets were collected by centrifuging at  $13000 \times g$  for 10 minutes at 4 °C and washed two times with 1 ml of cold acetone. The pellets were then resuspended in buffer containing 2 M thiourea, 7 M urea, 3% CHAPS, 20 mM Tris, and protein concentration was determined by Bradford assay using BSA as standard.

## 2.4 Extraction of intracellular (cytosol) proteins

The supernatant was precipitated overnight at -20 °C with acetone : methanol (8:1 vol/vol), then centrifuged 20 minutes at  $18300 \times g$ ; the pellet was recovered, let dry and re-suspended in 7 M urea, 2 M thiourea, 3% CHAPS, 20 mM Tris, 1% ampholytes and centrifuged 40 minutes at  $18300 \times g$  to precipitate DNA contaminants (dark pellet on the bottom of the eppendorf).

## 2.5 Extraction of membrane proteins

The extraction buffer is prepared with 2% Triton X-114 in TBS (150 mM NaCl, 10 mM Tris-HCl pH 7.6). The extraction is conducted on ice. The membrane pellet is re-suspended in 100 µl MilliQ water and added of 500 µl extraction buffer, then 1) homogenised with a small syringe, 2) let stand in ice for 1 min, 3) vortex for 1 min, 4) let stand in ice for 1 min. The four steps are repeated five times and then the sample is kept on ice for 10 min, vortexed, and finally put 1 hour at 37 °C. The sample is then centrifuged for 5 minutes at  $16000 \times g$  at room temperature. The lower phase contains Triton X-114 with the membrane proteins, the upper phase contains the aqueous phase and proteins. The two phases are collected and each one is precipitated overnight at -20 °C with acetone : methanol (8:1 vol/vol), then centrifuged 20 minutes at  $18300 \times g$ . Each pellet was recovered, let dry and re-suspended in 7 M urea, 2 M thiourea, 3% CHAPS, 20 mM Tris.

## 2.6 Extraction of membrane-associated proteins

The upper phase, expected to be enriched in hydrophilic proteins, collected during the extraction of membrane proteins, was precipitated overnight with cold acetone : methanol (8:1 vol/vol) at -20 °C. The protein pellets were recovered by centrifugation at  $18300 \times g$  for 20 minutes at 4 °C. The pellets were then resuspended in buffer containing 2 M thiourea, 7 M urea, 3% CHAPS, 20 mM Tris, and protein concentration was determined by Bradford assay.

## 2.7 Control of fraction purity by western immunoblotting

Protein fractions were separated by SDS-PAGE and immunodetected with antibody specific for a cytosolic protein (PGK I) and a membrane bound protein (MMP 9) by Western blot to verify the efficiency of separation protocol. Protein extracts were diluted 1:1 with Laemmli's sample buffer (62.5 mM Tris-HCl, pH 6.8, 25% glycerol, 2% SDS, 0.01% bromophenol blue, 5%  $\beta$ -mercaptoethanol), boiled for 3 minutes and separated by SDS-PAGE on 12% T acrylamide gels in Tris/glycine/SDS buffer. Proteins were then electroblotted onto PVDF membranes (Biorad) at 60 V for 2 h at 4 °C. Non specific sites were blocked by incubating with 3% non-fat dried milk and 0.05% Tween-20 (Sigma-Aldrich) in Tris-buffered saline (TBS-T) for 1 h at 37 °C. Membranes were incubated overnight at room temperature with the primary antibody for PGK-I (Sigma-Aldrich) diluted 1:500, in 3% non-fat dried milk and 0.05% Tween-20 (Sigma-Aldrich) in TBS and with the primary antibody for MMP 9 (Sigma-Aldrich) diluted 1:1000 in 3% non-fat dried milk and 0.05% Tween-20 (Sigma-Aldrich) in TBS. Membranes were washed four times for 15 min with TBS-T and then were incubated for 1 h at room temperature with the appropriate horseradish peroxidase-conjugated secondary antibody: ECL anti-goat IgG horseradish peroxidase-linked (Sigma-Aldrich) at 1:20000 dilution for PGK I and ECL anti-rabbit IgG horseradish peroxidase-linked (Sigma-Aldrich) at 1:5000 dilution for MMP-9. Membranes were washed three times for 15 min with TBS-T and once for 15 min with TBS. Finally the immunocomplexes were detected by chemiluminescence (ECL, GE Healthcare,) on X-ray XOMat AR (Kodak, Rochester, NY, USA) films. The Western-blot image was obtained by scanning films using Quantity One software Version 4.4 (Biorad).

## 2.8 2-DE electrophoresis

Proteins samples (100  $\mu$ g for intracellular proteins, 100  $\mu$ g for membrane proteins, 100  $\mu$ g for membrane-associated proteins and 100  $\mu$ g for secreted proteins) were mixed with solubilization buffer (2 M thiourea, 7 M urea, 3% CHAPS, 20 mM Tris) to obtain a final volume of 150  $\mu$ l. Each sample was reduced and alkylated with 5 mM tributylphosphine and

10 mM acrylamide. The mixture was then applied to the dry gel strip (IPG 70 mm, pH 3–10 non linear gradient) for reswelling. Focusing was performed at 300 V for 2 h, 400 V for 1 h, 1000 V for 6 h, 2000 V for 2 h, 3500 V for 5 h, 5000 V until the complete focalization (25000 V x h). The current was limited to 50  $\mu$ A *per* strip, and the temperature was kept at 20 °C for all IEF steps. For SDS-PAGE, the IPG strips were incubated in equilibration buffer (6 M urea, 2% SDS, 20% glycerol, 0.375 M Tris-HCl pH 8.8) for 26 min and then transferred to the second dimension onto 10%–20% T gradient acrylamide gels. The gels were run 5 mA *per* gel for 1 h, 10 mA *per* gel for 1 h and 20 mA *per* gel until the bromophenol blue front had reached the bottom of the gel. The 2-DE gels were stained in Sypro Ruby: the proteins were first fixed in a solution of 7% acetic acid and 10% methanol for 1 h, then incubated in Sypro Ruby overnight and finally destained in 7% acetic acid and 10% methanol for 2 h. Sypro Ruby stained 2-DE gels were digitized using VersaDoc (BioRad, Hercules, CA) and bioinformatic analysis was performed with PDQuest 7.3.0 (BioRad).

## 2.9 Mass spectrometry analysis

### *In-Gel-Digestion*

Protein spots were carefully cut out from Sypro Ruby stained gels and subjected to in-gel trypsin digestion according to Shevchenko *et al.* (2006) and colleagues with minor modifications. The gel pieces were swollen in a digestion buffer containing 50 mM  $\text{NH}_4\text{HCO}_3$  and 12.5 ng/ $\mu$ l of trypsin (modified porcine trypsin, sequencing grade, Promega, Madison, WI) in an ice bath. After 30 min, the supernatant was removed and discarded, 20  $\mu$ l of 50 mM  $\text{NH}_4\text{HCO}_3$  was added to the gel pieces, and digestion was allowed to proceed at 37 °C overnight. The supernatant containing tryptic peptides was dried by vacuum centrifugation. Prior to mass spectrometric analysis, the peptide mixtures were redissolved in 10  $\mu$ L of 5% formic acid.

### *Protein Identification by nano-HPLC-MS/MS*

Peptide mixtures were separated using a nanoflow-HPLC system (Ultimate; Switchos; Famos; LC Packings, Amsterdam, The Netherlands). A sample volume of 10  $\mu$ l was loaded by the autosampler onto a homemade 2 cm fused silica precolumn (75  $\mu$ m i.d.; 375  $\mu$ m o.d.; Reprosil C18-AQ, 3  $\mu$ m (Ammerbuch-Entringen, DE)) at a flow rate of 2  $\mu$ l/min. Sequential elution of peptides was accomplished using a flow rate of 200 nl/min and a linear gradient from solution A (2% acetonitrile and 0.1% formic acid) to 50% of solution B (98% acetonitrile and 0.1% formic acid) in 40 min over the precolumn in-line with a homemade 10–15 cm resolving column (75  $\mu$ m i.d.; 375  $\mu$ m o.d.; Reprosil C18-AQ, 3  $\mu$ m (Ammerbuch-Entringen, Germany)). Peptides were eluted directly into a High Capacity ion Trap (model HCTplus, Bruker-Daltonik, Germany). Capillary voltage was 1.5–2 kV and a dry gas flow rate of 10 l/min was used with a temperature of 230 °C. The scan range used was

from 300 to 1800  $m/z$ . Protein identification was performed by searching in the National Center for Biotechnology Information non-redundant database (NCBI nr) using the Mascot program <http://www.matrixscience.com>. The following parameters were adopted for database searches: complete carbamidomethylation of cysteines and partial oxidation of methionines, peptide mass tolerance  $\pm 1.2$  Da, fragment mass tolerance  $\pm 0.9$  Da, missed cleavages 2. For positive identification, the score of the result of  $(-10 \log(P))$  had to be over the significance threshold level ( $P < 0.05$ ). Even though high MASCOT scores are obtained with values greater than 60, when proteins were identified with only one peptide, a combination of automated database search and manual interpretation of peptide fragmentation spectra was used to validate protein assignments. In this manual verification, the mass error, the presence of fragment ion series, and the expected prevalence of C-terminus containing (Y-type ions) in the high mass range were all taken into account. Moreover, replicate measurements have confirmed the identity of these protein hits.

### 2.10 Method for SELDI-TOF analysis

Hepcidin-25 measurements in the MDM fractions were performed by SELDI-TOF-MS, using a Ciphergen Protein Biosystem IIc mass spectrometer (model PBSIIc, Ciphergen Biosystems, Freemont, CA) and IMAC 30 ProteinChip arrays (Bio-Rad Laboratories, Hercules, CA), according to the manufacturer's instructions with some modifications. A similar protocol was used for semi-quantitative detection of urinary hepcidin (Bozzini *et al.*, 2008). Finally, 1  $\mu$ l of a saturated solution of sinapinic acid in 0.5% (vol/vol) trifluoroacetic acid and 50% (vol/vol) acetonitrile, used as energy-absorbing matrix (EAM), was applied to each spot surface, allowed to air-dry, and reapplied. Mass-to-charge ( $m/z$ ) spectra were generated using the PBSIIc TOF mass spectrometer at laser intensity 180, detector sensitivity 9; high mass limit 50 kDa; and optimization interval 1500 to 10000 Da. Synthetic 25-hepcidin (Peptides International, Louisville, KY) was used for external mass calibration and, spiked into the cytosolic fraction sample, for peak confirmation. Peak annotation was performed with ProteinChip Software after baseline subtraction.

## 3. RESULTS AND DISCUSSION

Primary cultures of human MDMs were prepared by differentiation of monocytes from blood donors according to literature (Pinet *et al.*, 2003). Optical microscope analysis showed a good differentiation of MDMs in 12 days. The purity of the cultures was evaluated as in Pinet *et al.* (2003); the flow cytometry analysis permitted to assess the purity of the cultures by testing positivity of macrophages to CD14 and CD45 (Fig. 1).



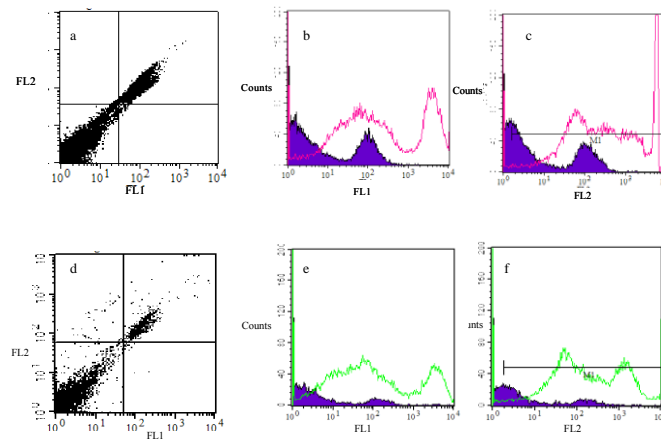


**Fig 1.** Analysis of macrophages purity by with flow cytometry: positivity control to CD14 and CD45.

Iron metabolism and macrophages are closely linked; these specialized cells are devoted to iron storage and recycling, expressing crucial proteic effectors on the cell membrane such as ferroportin (the only known iron-exporting-channel) and other soluble iron-related proteins (Iron Regulatory Proteins -IRPs, Ferritin, etc.) (Pinet *et al.*, 2003). While most of the genes and RNAs involved in iron homeostasis have been described, still little is known on the proteins deputed to such function. To unravel protein candidates of clinical interest, proteome analysis appears as the reference technology for such investigations. Due to the complexity of an entire cell lysate from a proteomic point of view, and willing to gain a wide range of information, we decided to fractionate the sample prior to 2D electrophoresis. Protein extraction from MDMs was obtained using a lysis and fractionation protocol which distinguished proteins on the basis of their hydrophaticity. This method partially derives from what achieved in (Slomianny *et al.*, 2006, Santoni *et al.*, 2000) but was optimized for MDM cell and allowed the sub-fractionation of the total proteome of MDMs into intracellular proteome, membrane proteome, membrane associated proteome and secretome. In Figure 2, 2D maps of the 4 fractions are compared with the total lysate normally obtained with a single step sample preparation, clearly showing the increase in resolution and amount of information obtainable.

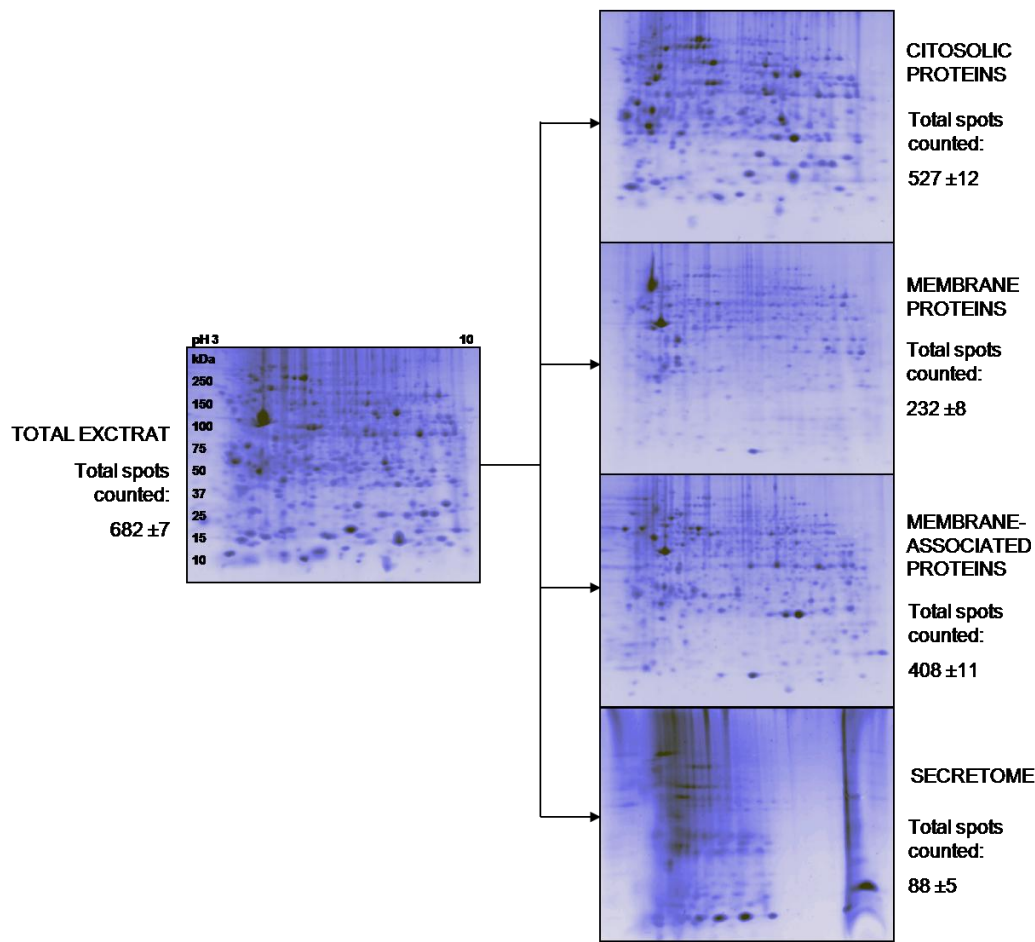


**Fig 2.** 2D-Maps representing total protein extract from macrophages and protein fractions derived from the proposed protocol. 2D mini gels of a total protein extract from macrophages cells and the 4 fractions obtained by applying the extraction protocol with Triton X-114 (cytosolic fraction, membrane fraction, membrane associated fraction and secretome fractions, from the top to the bottom). All the 2D-PAGE are run on a 3–10 non linear IPG strip and an equal amount of total protein content was loaded on each gel. For each 2D map the spots count, as obtained with PDQuest software, is indicated.

For each fraction the number of protein spots detected is also reported. Being most interested in the membrane fraction, we extracted membrane proteins of macrophages using the neutral detergent Triton X-114. The fractionation protocol exploits the temperature dependent solubility of Triton X-114. Fractionation steps include mixing Triton X-114 with cell lysates at 0 °C, where it is freely soluble and where it forms complexes associating hydrophobic proteins, followed by a step-wise change in temperature, reaching Triton X-114 cloud point (23 °C), that induce the detergent precipitation, causing the trapping of the protein complexes in an insoluble phase. The treatment proved to be simple and very effective for fractionating membrane and cytosol proteins, permitting to obtain high resolution 2D gels. A fraction of "membrane associated" proteins was also recovered. The use of neutral detergent Triton X-114 for MDM membrane protein extraction was already demonstrated to give better results in comparison to solvent extraction (Slomianny *et al.*, 2006), even if it was used only in conjunction with liquid chromatography separations. Here

we employed Triton X-114 and analysed extracted proteins by 2D electrophoresis and MS. Upon lysis of human MDMs, the intracellular fraction was recovered by precipitation of the supernatant. The pellet of the lysis, containing the membranes was treated with the neutral detergent Triton X-114 for protein extraction. The protocol was adjusted for MDMs: the re-iteration in sequence of the mixing steps with the detergent and incubation steps ameliorated the protein-detergent complexation. Fractions were run on 2D-PAGE (Minigel of 8 cm length) and maps were analysed, after staining with Sypro Ruby, by PDQuest software. After images digitalization it was possible to highlight the presence of an elevated number of spots in all the maps representative of the fractions (i.e.  $527 \pm 12$ ,  $232 \pm 8$ ,  $408 \pm 11$  in the intracellular, membrane and membrane associated fraction, respectively). These spots number accounts for a good quality and high resolution protein profiles. The quality of the fractions recovered (intracellular and membrane) was assessed by SDS-PAGE electrophoresis followed by MS-MS or Western blotting. Intracellular fraction was assayed for the presence of the cytosolic enzyme phosphoglycerate kinase (PGK I), a protein typical of the glycolytic pathway and for the absence of membrane protein contamination, (Fig. 3, panels A-B), by incubating the same Polyvinylidene Fluoride (PVDF) membrane with an antibody against the matrix metalloproteinase 9 (MMP 9).

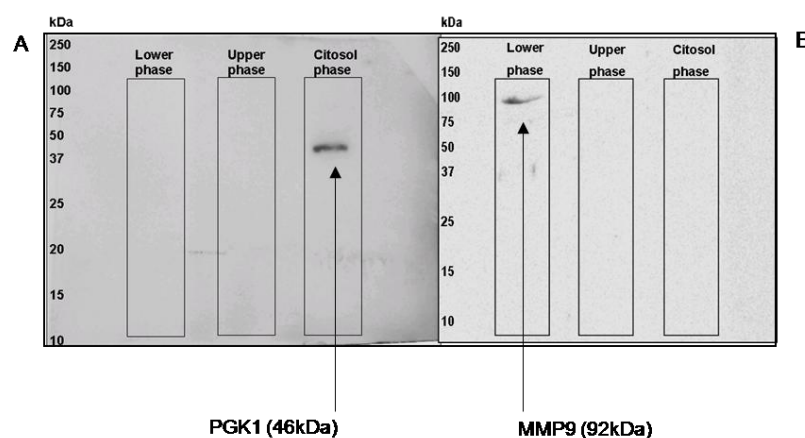


**Fig 3.** Western blot analysis for PGK-1 presence in the obtained fractions. Western blot analyses for the cytosolic enzyme phosphoglycerate kinase (PGK I), typical of the glycolysis, panel A, and for the membrane bound protein Metalloproteinase 9 (MMP9), panel B. The three fractions were run together on the same SDS-PAGE loading an equal amount of total protein. The same PVDF membrane was used. Film image with the relative protein bands only in the lane corresponding to the cytosolic compartment and to the membrane fraction are reported. Western blot images were captured by GS710 densitometer (Bio-Rad) and analyzed by QuantityOne software.

The three main fraction were run on the same SDS-PAGE and equal amount of total protein were loaded in each lane. Only the lane referring to the cytosolic fraction showed a distinct band when developed with the anti-PGK 1 antibody, being clear the presence of the enzyme only in there and thus indicating no major contamination between fractions. In addition, only the lane referring to the membrane fraction showed a distinct band when developed with

the anti MMP 9 antibody, indicating no contamination of the cytosolic fraction by membrane proteins. Figure 3 shows some comparisons between selected zones of the total extract and the corresponding zone on 2D gels of fractions, highlighting the different resolution achieved when proteins were fractionated prior to the 2D run. In analogy with membrane proteome literature (Churchward *et al.*, 2005), the recovery of integral and membrane associated proteins was successfully obtained with the use of detergents, because their lipophilic character mimics the native lipid membrane environment. A quantitative evaluation of the 2D maps was performed by comparing the results of spots image analysis of the membrane fraction with those of the total extract. It was evident that, in the selected zones (Fig. 4), the increase in spot density resulted 2.1 fold, thus indicating the substantial improvement in density gained with the fractionation. The membrane fraction was also subjected to qualitative studies. MS analysis of a sample of 21 spots from the membrane fraction gave the identifications shown in Table 1 (the cut spots are indicated with circles in the map in Fig. 5). Among these proteins, 10 are integral membrane proteins and the remaining proteins are all associated to the plasma membrane or to membrane proteins, being 90% the total recovery percentage. These results support the Triton X-114 extraction method for MDMs membrane protein studies. Figure 3D reports the number of protein counted in each fraction and the count of the map of the total extract. The number of proteins doubles in case of fractionation, also indicating the great advantage of the chosen protocol. The fractionation of the samples enabled to increase the amount of information achievable on the protein effectors in macrophages. All the four compartments analysed can be further studied and evaluated in terms of specific enzymes or antigens. Being interested in iron metabolism we also evaluated the fractions in term of hepcidin content (Fig. 6).

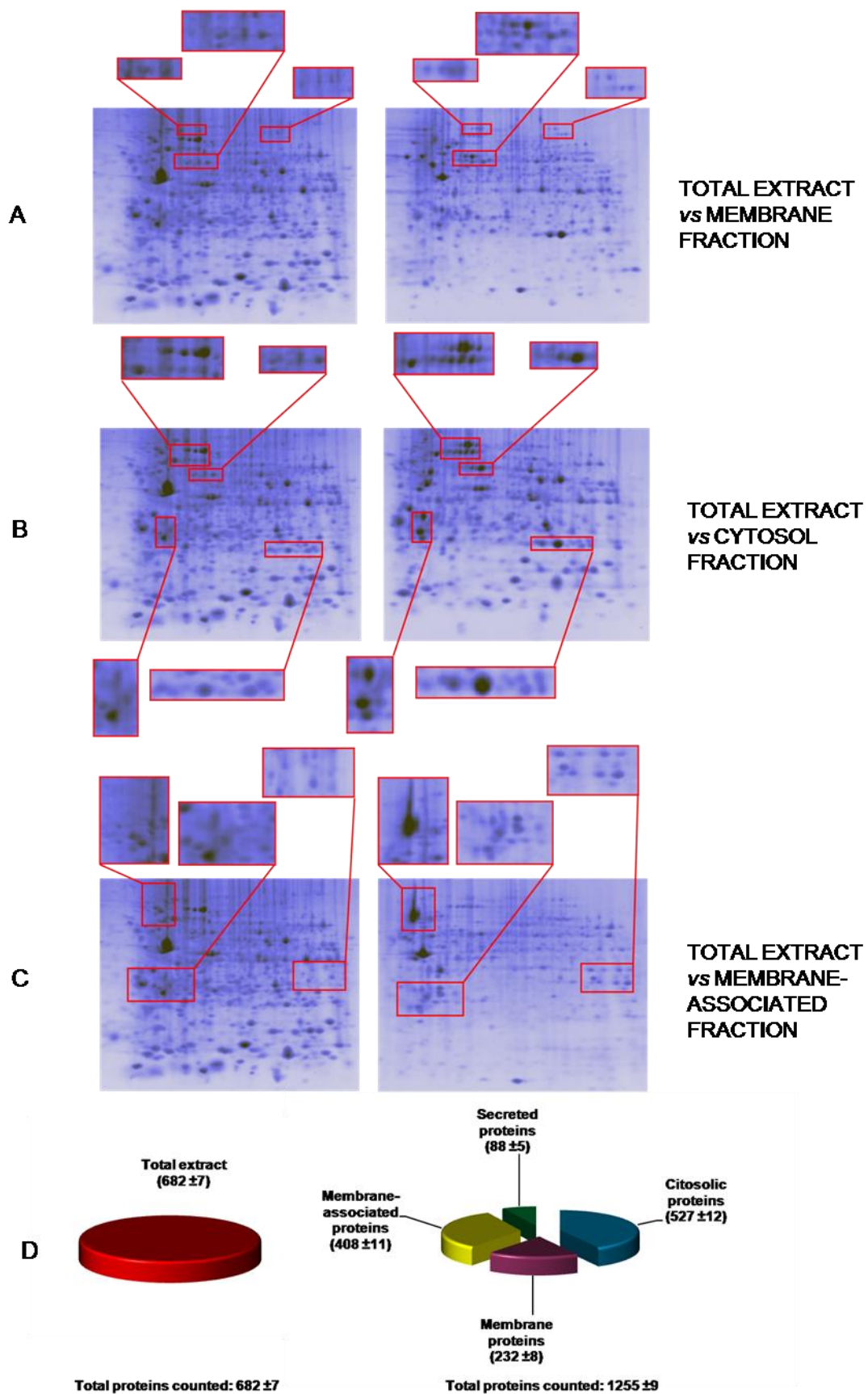


**Fig 4.** Comparison between total extract 2D map and fractions 2D maps. 2D gels of total extract and fractions with enlargements of specific zones and a diagram reassuming the numerical data obtained. A) total extract versus membrane fraction. B) total extract versus cytosolic fraction. C) total extract versus membrane associated fraction. D) Pie chart representing the Spots counts relative to the total extract (left panel) and the summary of the 4 fractions obtained with the proposed protocol.

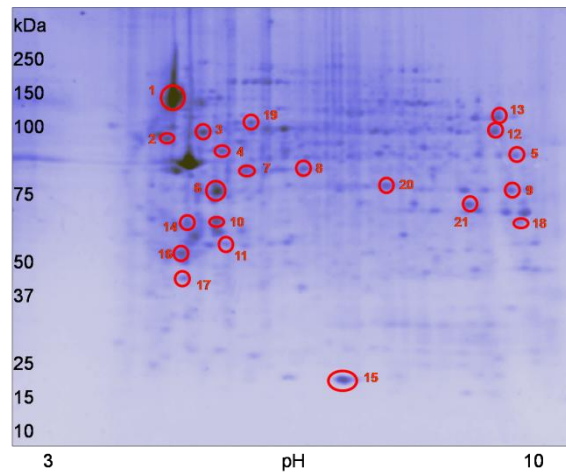


**Fig 5.** 2D map of the membrane fraction used for spot excision and ID. 2D gel of the membrane fraction showing the cut spots as red circles numbered from 1 to 21.

Hepcidin is the master regulator of iron homeostasis and acts by tuning iron influx into plasma from tissues dedicated to iron storage or transport. In particular macrophages recycle iron from senescent enterocytes. Our interest was to monitor hepcidin presence in the fraction in order to study its behavior in cultured macrophages. In preliminary experiments, a peptide matching the mass of hepcidin was detectable only in the cytosol but not in the other compartments (Fig. 6).

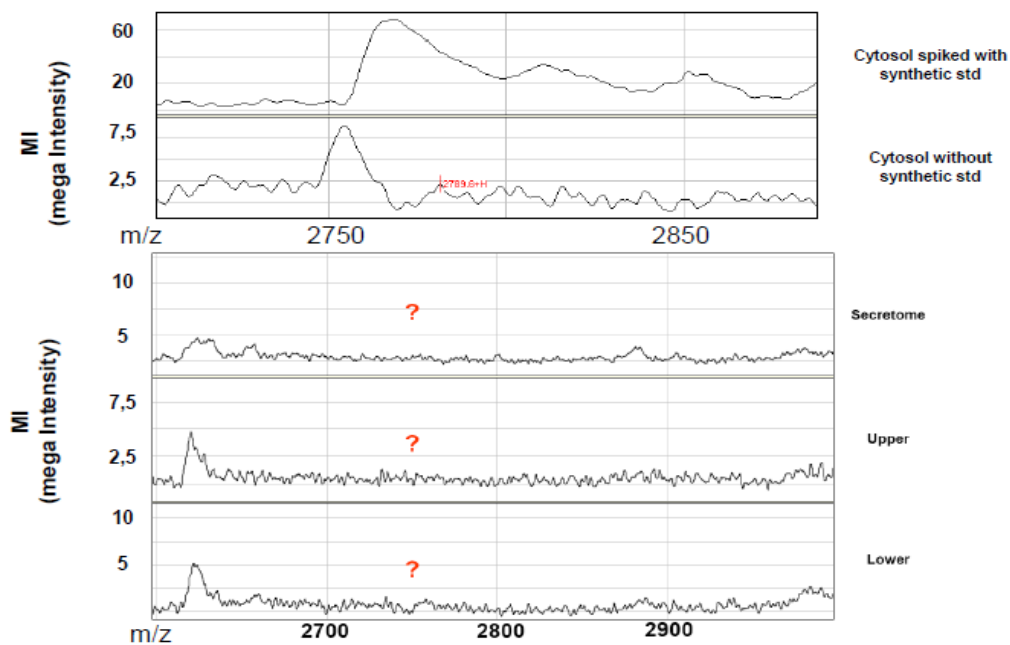


**Fig 6.** SELDI analysis of the fractions. SELDI-TOF spectra representing the four fractions analysed on IMAC 30 chip arrays. The peak of a peptide matching the mass of hepcidin 25 is shown when present. A spectrum containing the hepc 25 synthetic standard spiked into the cytosolic fraction is also shown.

Notwithstanding recent progress, much work remains to be done in defining the role of hepcidin in both healthy and diseased states. However, to date, few investigative tools are available (Ganz *et al.*, 2008, Swinkels *et al.*, 2008, Murphy *et al.*, 2007, Murao *et al.*, 2007). By means of SELDI-TOF-MS technology, we and others were successful to detect hepcidin and its isoforms in urine and serum (Nemeth *et al.*, 2004, Kemna *et al.*, 2008, Bozzini *et al.*, 2008). Our preliminary results appear to confirm the presence of hepcidin in macrophages also as protein, extending the data reported by Theurl and colleagues about hepcidin mRNA in monocyte/macrophages (Theurl *et al.*, 2008). The presence of a peptide of the same mass as hepcidin in the cytosolic fraction is in agreement with the known cycle of hepcidin from liver to cells, by means of binding to ferroportin and internalization (Nemeth *et al.*, 2004, Andrews, 2008, De Domenico *et al.*, 2007). We are going to validate this approach investigating other MDMs under different conditions. Further experiments are needed for a better understanding of the peptide behavior regarding its binding to membrane proteins. The mutual interaction of hepcidin with ferroportin is essential for the understanding of iron homeostasis in the cells (De Domenico *et al.*, 2008) and the study of MDMs from patients and/or animal models of ferroportin disease (Pietrangelo, 2004) could give new insights into this field.

#### 4. CONCLUSION

The purpose of this work was to find a feasible method for the study of cytosolic, integral membrane, membrane associated and secreted proteins in comparative proteomics experiments of clinically relevant samples. This technique, based on Triton X-114, allowed us to obtain high resolution 2D maps for all the fractions. The fractionation and extraction method gave as an improvement in spots number detectable and amount of information achievable. In particular the results obtained mapping membrane proteins are remarkable: the maps show high quality spots and no streaks. In fact membrane proteins, due to their hydrophobicity, usually focus poorly using the conventional isoelectrofocusing (IEF) procedure, often leading to horizontal streaks. Mapping separately the protein population of macrophages, in healthy and disease conditions, would allow a deeper understanding of Hereditary Hemochromatosis and iron related disorders.



**Table 1.** Membrane fraction identified proteins.

SSP	Mw, kDa theor.	pI predict.	No. of peptides identified	Mascot Score	NCBI Accession Number	Protein ID
5	51372	8.88	11	592	gi 872121	isocitrate dehydrogenase (NADP+) [Homo sapiens]
21	38780	7.57	21	1301	gi 18645167	Annexin A2 [Homo sapiens]
	38639	6.32	3	162	gi 190200	Porin [Homo sapiens]
17	42128	5.22	4	198	gi 28336	mutant beta-actin (beta'-actin) [Homo sapiens]
	18537	5.21	2	70	gi 5453559	ATP synthase, H <sup>+</sup> transporting, mitochondrial F0 complex [Homo sapiens]
13	58411	7.58	17	1101	gi 35505	pyruvate kinase [Homo sapiens]
	59828	9.16	2	113	gi 4757810	ATP synthase, H <sup>+</sup> transporting, mitochondrial F1 complex [Homo sapiens]
1	53738	5.03	36	1940	gi 340219	Vimentin [Homo sapiens]
14	42080	5.37	6	317	gi 62897625	beta actin variant [Homo sapiens]
15	12905	5.77	3	70	gi 34616	beta-2 microglobulin [Homo sapiens]
12	59785	9.07	20	1136	gi 127798841	ATP synthase, H <sup>+</sup> transporting, mitochondrial F1 complex, alpha subunit 1 [Homo sapiens]
10	29843	5.57	9	485	gi 4505773	prohibitin [Homo sapiens]
3	50810	5.02	25	651	gi 37492	alpha-tubulin [Homo sapiens]
18	30737	8.63	7	420	gi 238427	Porin 31HM [human, skeletal muscle membrane] [Homo sapiens]
11	30337	6.99	3	178	gi 4758788	NADH dehydrogenase (ubiquinone) Fe-S protein 3, 30kDa (NADH-coenzyme Q reductase) [Homo sapiens]
20	49851	7.70	20	710	gi 704416	elongation factor Tu [Homo sapiens]
16	42052	5.29	5	131	gi 4501885	beta actin [Homo sapiens]
7	42080	5.37	8	398	gi 62897625	beta actin variant [Homo sapiens]
2	48083	4.95	17	1052	gi 89574029	mitochondrial ATP synthase, H <sup>+</sup>



						<b>transporting F1 complex beta subunit</b> <b>[Homo sapiens]</b>
<b>8</b>	53559	5.93	4	189	gi 32709	IFP53 [Homo sapiens]
<b>6</b>	42080	5.37	8	371	gi 62897625	<b>beta actin variant</b> <b>[Homo sapiens]</b>
<b>4</b>	53297	5.94	6	241	gi 46593007	<b>ubiquinol-cytochrome c reductase core protein I</b> <b>[Homo sapiens]</b>
<b>19</b>	53809	6.03	19	1278	gi 40889610	Chain A, Crystal Structure Of Human Tryptophanyl-Trna Synthetase [Homo sapiens]



## CHAPTER 2

# PROTEOMIC RESPONSE TO IONIC-IRON IN MURINE MACROPHAGES

### 1. INTRODUCTION

Iron is a trace element essential for life, as it is required for erythropoietic function, oxidative metabolism and cellular immune responses (Munoz *et al.*, 2009). A distinctive feature of iron metabolism is the degree to which body iron is conserved and hence recycled. The body of a normal adult human contains typically 3 to 4 g of iron. Most of the iron is distributed within red blood cells (RBC) hemoglobin (65%; 2300 mg). Approximately 10% is present in muscle fibers (in myoglobin) and other tissues (in enzymes and cytochromes) (350 mg). The remaining body iron is stored in the liver (200 mg), macrophages of the reticuloendothelial system (RES; 500 mg), and bone marrow (150 mg). Only about 0.03% (or ~1-2 mg) is lost per day (Munoz *et al.*, 2009). To replace the basal losses and remain in iron balance, a roughly equivalent amount of iron should be absorbed from the diet (1-2 mg absorbed from the ~15-20 mg of iron introduced with the diet). Thus, the daily exchange of iron between body and environment is relatively small and contrasts sharply with the comparatively large exchange of this metal between internal organs (Knutson and Wessling-Resnick, 2003). For example, each day the bone marrow utilizes approximately 24 mg of iron to produce over 200 billion new erythrocytes. To meet the demand for heme production necessary for erythropoiesis, iron must be recycled from senescent red cells; this process is carried out by macrophages of the RES.

Highly sophisticated strategies should be in place to acquire and regulate iron, also as consequence of the lack in the body of effective iron excretory routes (Siah *et al.*, 2006). Particular attention should be given to the role of macrophages at the interface between iron and immunity, both in producing highly toxic hydroxyl radicals through iron-mediated oxydation, and by being at the same time the major site for iron storage.

Under inflammatory conditions, iron uptake and/or release in macrophages is modulated by cytokines, radicals produced by macrophages themselves and acute phase proteins from the liver (Theurl *et al.*, 2005). An increase in iron retention within macrophages is observed during inflammation. At the same time iron modulates macrophage effector pathways by regulating cytokine activities, the induction of anti-microbial effector pathways of macrophages and indirectly via regulating lymphocyte proliferation and activities which then affect macrophage differentiation and activation. Since iron is an essential compound for microbial growth and proliferation the control over iron homeostasis is a central battlefield

deciding about the fate of an infection. Thus, it is not surprising that proteins (e.g. phagolysosomal proteins) associated with resistance towards infections with intracellular pathogens also have been discovered to act as iron transporters (Porto *et al.*, 1994, Roy and Andrews, 2001, Meyer *et al.*, 2002, Weiss, 2002b).

Despite the importance of iron physiology, iron recycling by macrophages has remained one of the least well-understood area of iron metabolism (Aisen, 1990). Information on genes involved in iron metabolism (Vidal *et al.*, 1993, Feder *et al.*, 1996, Fleming *et al.*, 1997, Gunshin *et al.*, 1997, Abboud and Haile, 2000, Kristiansen *et al.*, 2001) and mostly –if not exclusively- expressed in the RES, and the identification of the serum peptide Hepcidin and of its role in iron metabolism offered a key contribute towards a better understanding of iron physiology (Nicolas, 2001), but still the dynamic character of such process is to be clarified. It is known that iron acquisition pathways by macrophages proceed through two alternative ways: either via phagocytosis or via endocytosis. Plus, a distinguish should be made between free iron form and heme iron acquisition. Dietary iron (non-heme) is prevalently absorbed in the non-bioavailable oxydised form ( $\text{Fe}^{3+}$ ). Ferrous ions are first reduced to  $\text{Fe}^{2+}$  by a ferrireductase (McKie *et al.*, 2000) and then transported across metal transmembrane ion channels. Transporters are Nramp1 which is expressed exclusively in monocyte and macrophages and Nramp2, ubiquitous, this latter better known as divalent metal ion transporter 1 (DMT-1) (Fleming *et al.*, 1997, Gunshin *et al.*, 1997). Nramp1 localizes to lysosomes and late endosomes and is rapidly recruited to membranes of maturing phagosomes (Gruenheid *et al.*, 1997, Searle *et al.*, 1998, Govoni *et al.*, 1999). DMT-1 localizes to recycling endosomes (Tabuchi *et al.*, 2000). Interestingly, macrophage DMT-1 mRNA levels lack of iron responsiveness, as indicated from studies of cultured fibroblasts and erythroleukemic cells (Wardrop and Richardson, 1999) and consistently by results on macrophage cell lines (RAW264.7 and J774) where the levels of DMT-1 transcripts did not change in parallel with changes in transferrin receptor mRNA (Wardrop and Richardson, 2000).

The major pathway by which macrophages acquire heme-iron is erythrophagocytosis. Senescent erythrocytes are taken up via phagocytosis and are then degraded within the phagolysosome (Maines, 1997). Alternative iron acquisition pathways seems to be occasionally activated, as in case of bacterial infections; in the case, iron seems to be sequestered via a siderophore-like uptake pathway, mediated by the protein lipocalin-2, as a innate immune response, but the role of this pathway still need deeper investigations (Theurl *et al.*, 2005). Another particular case of iron acquisition happens when erythrocytes are destroyed intravascularly (Garby and Noyes, 1959), the released hemoglobin is complexed by haptoglobin and goes mainly to liver clearance (Deiss, 1999). However,

studies have identified a hemoglobin scavenger receptor, CD163, expressed exclusively on monocytes and macrophages (Kristiansen *et al.*, 2001).

Once iron enters cells it is either stored within ferritin or utilized upon incorporation into iron containing enzymes. An estimate of 10–20% percent remain in the labile iron pool which is important for macrophage effector functions and the regulation of cellular iron homeostasis (Oppenheimer, 2001). Iron homeostasis is maintained mainly at the postranscriptional/translational level by interaction of cytoplasmic proteins, so called iron regulatory proteins (IRP)-1 and 2, with RNA stem loop structures, iron responsive elements (IRE) (Muckenthaler *et al.*, 2008 ).

Iron export is effected by Ferroportin (also called Ireg1 or SLC11A3), a transmembrane iron exporter, implicated in the basolateral transfer of ferrous iron to the circulation (Pietrangelo, 2002). After being transported by ferroportin ferrous iron undergoes oxidation which is maintained by the membrane bound ferrioxidase hephaestin, and ferric iron release from cells can then be transferred for incorporations to transferrin (Vulpe *et al.*, 1999).

Besides the above mentioned molecular effectors, a comprehensive understanding of iron homeostasis, would offer a preferential point of view for gaining information on the proteins involved in cellular iron handling and on their interplay in iron tuning. Macrophages are identified as ideal candidates for such investigation, through a holistic approach that would help to unravel the complex responses associated to iron levels. The study proposed takes advantage of the proteomic approach, one of the most powerful method to elucidate the proteic effectors of cellular processes (O'Farrel, 1975, Clarke *et al.*, 2008, Zichi *et al.*, 2008). A comparative proteomic analysis was carried out on cultured murine macrophages challenged with iron (ferric ammonium citrate) at a near physiological concentration (10  $\mu$ M).

We report the mapping of iron-stimulated protein expression versus un-stimulated in its entire complexity. The comparison of the two proteomes helped in defining stimulus-expressed or stimulus-suppressed proteins, identifying molecular candidates involved in the physiological handling of elemental iron and therefore suggesting potential implication for immunity and control of infections.

## **2. MATERIALS AND METHODS**

### **2.1. Cell culture and protein extraction**

Mouse Bone Marrow macrophages isolated from C3H WT mice were maintained in culture for 7 days. Macrophages were incubated with ferric ammonium citrate (FAC) (10 nM Fe) for 24 h in serum-free media. Intracellular, membrane, membrane associated fractions were obtained as described by Polati *et al.* (2009) and analysed on 2-DE.

## 2.2. 2-DE and statistical analysis

Proteins samples (800 µg for intracellular proteins, 600 µg for membrane proteins, 300 µg for membrane-associated proteins) were mixed with solubilization buffer (2 M thiourea, 7 M urea, 3% CHAPS, 20 mM Tris) to obtain a final volume of 450 µl. Each sample was reduced and alkylated with 5 mM tributylphosphine and 10 mM acrylamide (Hamdan *et al.*, 2001). The mixture was then applied in gel for reswelling with a dry IPG 170 mm, pH 3-10 non linear gradient. Focusing was performed at 300 V for 2 h, 400 V for 1 h, 1000 V for 6 h, 2000 V for 2 h, 3500 V for 5 h, 10000 V until the complete focalization (65000 Vh). The current was limited to 50 µA *per strip*, and the temperature was kept at 20 °C for all IEF steps. For SDS-PAGE, the IPG strips were incubated in equilibration buffer (6 M urea, 2% SDS, 20% glycerol, 0.375 M Tris-HCl pH 8.8) for 26 min and then transferred for the second dimension onto 10%-20% gradient acrylamide gels. The gels were run overnight (10 mA *per gel*) until the bromophenol blue front had reached the bottom of the gel (20 mA *per gel*). The 2-DE gels were stained in Sypro Ruby: the proteins were first fixed in a solution of 7% acetic acid and 10% methanol for 1 h, then incubated in Sypro Ruby overnight and finally destained in 7% acetic acid and 10% methanol for 2 h. Sypro Ruby stained 2-DE gels were digitized using Versadoc (BioRad) and bioinformatic analysis was performed with PDQuest 7.3.0 (BioRad). Experimental results were compared by one-way analysis of variance (ANOVA) and the data were expressed as means  $\pm$  6 SE. Group means were considered to be significantly different at  $p < 0.05$ , as determined by the technique of protective least-significant difference (LSD) when ANOVA indicated an overall significant treatment effect,  $p < 0.05$ .

## 2.3. Mass Spectrometry Analysis

### *In-Gel-Digestion*

Protein spots were carefully cut out from Sypro Ruby stained gels and subjected to in-gel trypsin digestion according to Shevchenko and colleagues with minor modifications (Shevchenko *et al.*, 1996). The gel pieces were swollen in a digestion buffer containing 50 mM  $\text{NH}_4\text{HCO}_3$  and 12.5 ng/µL of trypsin (modified porcine trypsin, sequencing grade, Promega, Madison, WI) in an ice bath. After 30 minutes, the supernatant was removed and discarded, 20 µL of 50 mM  $\text{NH}_4\text{HCO}_3$  was added to the gel pieces, and digestion was allowed to proceed at 37 °C overnight. The supernatant containing tryptic peptides was dried by vacuum centrifugation. Prior to mass spectrometric analysis, the peptide mixtures were redissolved in 10 µL of 5% formic acid.

### *Protein Identification by nano-HPLC-MS/MS*

Peptide mixtures were separated using a nanoflow-HPLC system (Ultimate; Switchos; Famos; LC Packings, Amsterdam, The Netherlands). A sample volume of 10 µL was loaded

by the autosampler onto a homemade 2 cm fused silica precolumn (75  $\mu\text{m}$  i.d.; 375  $\mu\text{m}$  o.d.; Reprosil C18-AQ, 3  $\mu\text{m}$  (Ammerbuch-Entringen, DE)) at a flow rate of 2  $\mu\text{L}/\text{min}$ . Sequential elution of peptides was accomplished using a flow rate of 200 nL/min and a linear gradient from solution A (2% acetonitrile and 0.1% formic acid) to 50% of solution B (98% acetonitrile and 0.1% formic acid) in 40 minutes over the precolumn in-line with a homemade 10–15 cm resolving column (75  $\mu\text{m}$  i.d.; 375  $\mu\text{m}$  o.d.; Reprosil C18-AQ, 3  $\mu\text{m}$  (Ammerbuch-Entringen, Germany)). Peptides were eluted directly into a High Capacity ion Trap (model HCTplus, Bruker-Daltonik, Germany). Capillary voltage was 1.5–2 kV and a dry gas flow rate of 10 L/min was used with a temperature of 230 °C. The scan range used was from 300 to 1800  $m/z$ . Protein identification was performed by searching in the National Center for Biotechnology Information non redundant database (NCBI nr) using the Mascot program (<http://www.matrixscience.com>). The following parameters were adopted for database searches: complete carbamidomethylation of cysteines and partial oxidation of methionines, peptide mass tolerance  $\pm 1.2$  Da, fragment mass tolerance  $\pm 0.9$  Da, missed cleavages 2. For positive identification, the score of the result of ( $-10 \log(P)$ ) had to be over the significance threshold level ( $P < 0.05$ ). Even though high MASCOT scores are obtained with values greater than 60, when proteins were identified with only one peptide, a combination of automated database search and manual interpretation of peptide fragmentation spectra was used to validate protein assignments. In this manual verification, the mass error, the presence of fragment ion series, and the expected prevalence of C-terminus containing (Y-type ions) in the high mass range were all taken into account. Moreover, replicate measurements have confirmed the identity of these protein hits.

## 2.4. Western Blotting

### ***Control of different expression by western immunoblotting***

Protein fractions were separated by 2-DE (Polati *et al.*, 2009) and immunodetected with antibody specific for a cytosolic protein (ferritin - FTH) and a membrane bound protein (Glyceraldehyde 3 phosphate dehydrogenase - GAPDH) by Western blot to confirm their different expression. After the separation by bidimensional electrophoresis, proteins were electroblotted onto PVDF membranes (Biorad) at 60 V for 2 h at 4 °C. Non specific sites were blocked by incubating with 3% non-fat dried milk and 0.05% Tween-20 (Sigma-Aldrich) in Tris-buffered saline (TBS-T) for 1 h at 37 °C rocking. Membranes were incubated overnight at room temperature with the primary antibody for GAPDH (Sigma-Aldrich) diluted 1:1000 in 3% non-fat dried milk and 0.05% Tween-20 (Sigma-Aldrich) in TBS and with the primary antibody for FTH (Santa Cruz) diluted 1:500 in 3% non-fat dried milk and 0.05% Tween-20 (Sigma-Aldrich) in TBS. Membranes were washed four times for 15 min with TBS-T and then were incubated for 1 h at room temperature with the appropriate horseradish

peroxidase-conjugated secondary antibody: ECL anti-rabbit IgG horseradish peroxidase-linked (Sigma-Aldrich) at 1:5000 dilution for both GAPDH and FTH. Membranes were washed three times for 15 min with TBS-T and one time for 15 minutes with TBS. Finally the immunocomplexes were detected by chemiluminescence (ECL, Amersham Biosciences) on X-ray X-Omat AR (Kodak, Rochester, NY, USA) films. The image of the western-blot were obtained by scanning films using Quantity One software Version 4.4 (Biorad).

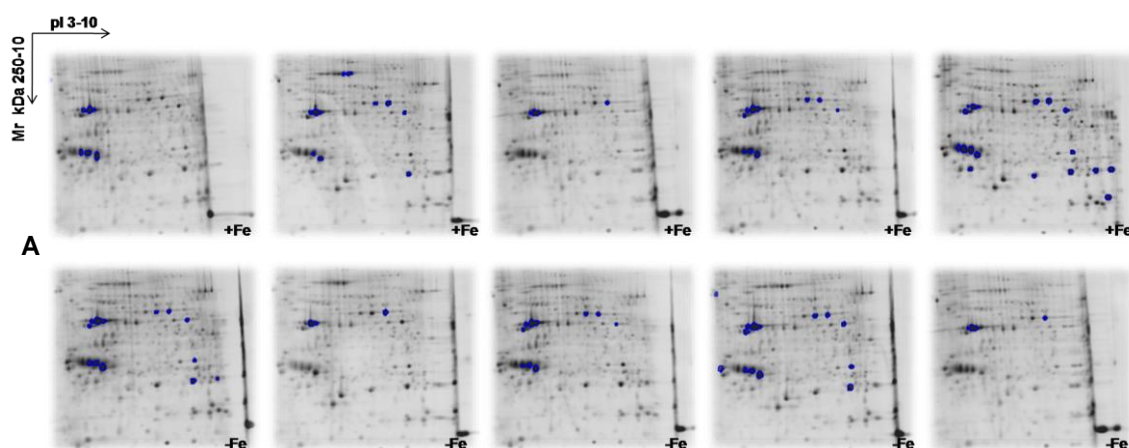
### 3. RESULTS

#### 3.1. Proteic pattern before and after iron stimulus: 2-DE

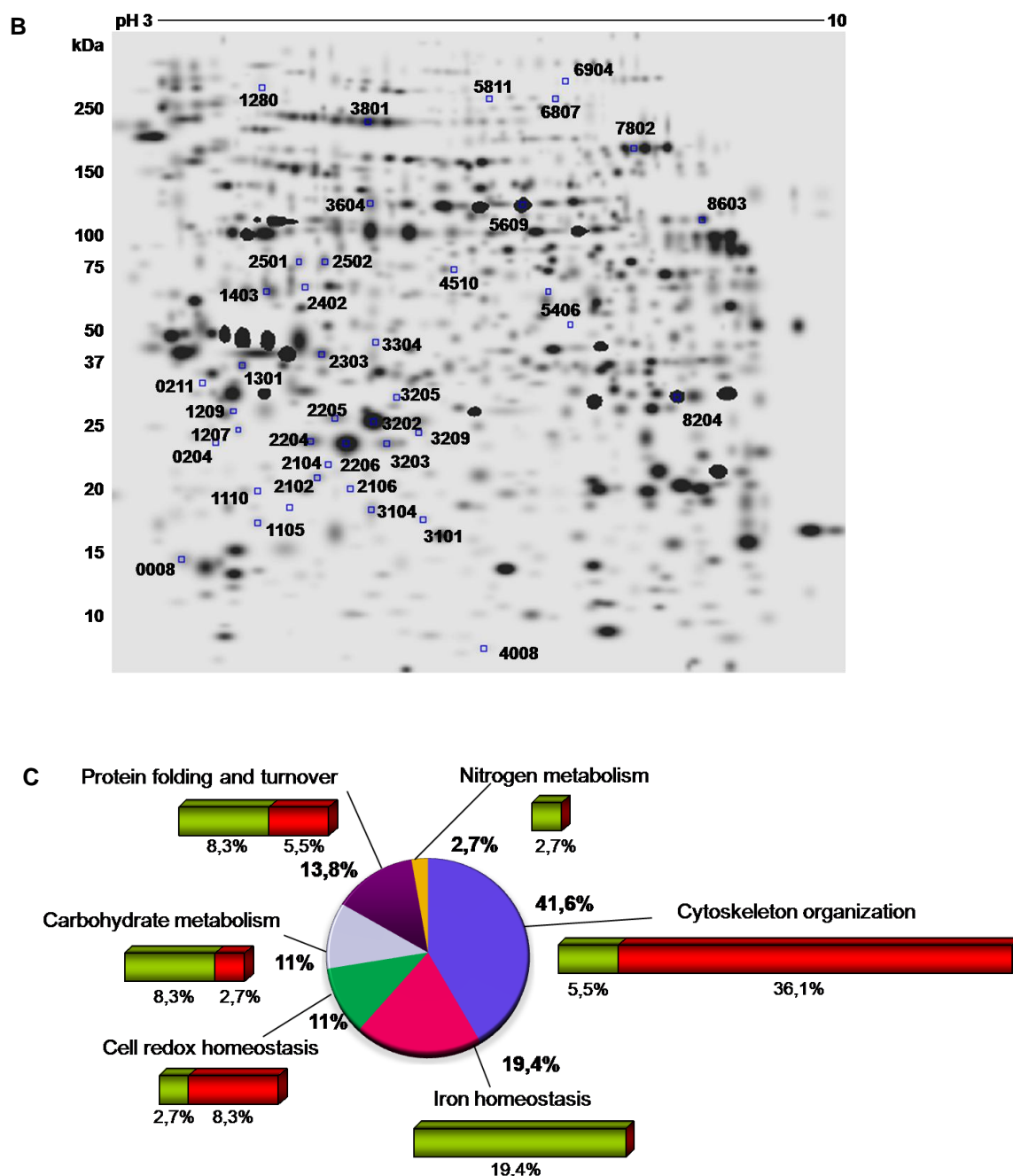
Proteins extracted from  $10 \times 10^6$  cells were fractionated with a method set up for obtaining high resolution 2D maps from monocytes/macrophages (Polati *et al.*, 2009). Three discrete fractions, indicated as intracellular proteins, membrane proteins and membrane associated proteins were recovered, quantified and analysed by 2-DE (5 replica gels for each fraction).

##### 3.1.1. Intracellular proteome

2-DE gels of the intracellular fraction of cells treated with Fe and control cells (i.e. non-treated) were run each in five replicas. The images of the gels, analysed by the software PDQuest 7.3.0 (BioRad), were used to develop a master map (Fig. 1) on which were counted a number of 913 protein spots representative of all the proteins of the two experimental groups analyzed. The comparative analysis highlighted the spots differentially expressed with statistical significance (minimum ratio accepted  $>1.5$  fold) on the master map. The comparison of the cytosol fraction of treated cells versus control cells evidenced 19 proteins over-expressed and 20 proteins under-expressed.



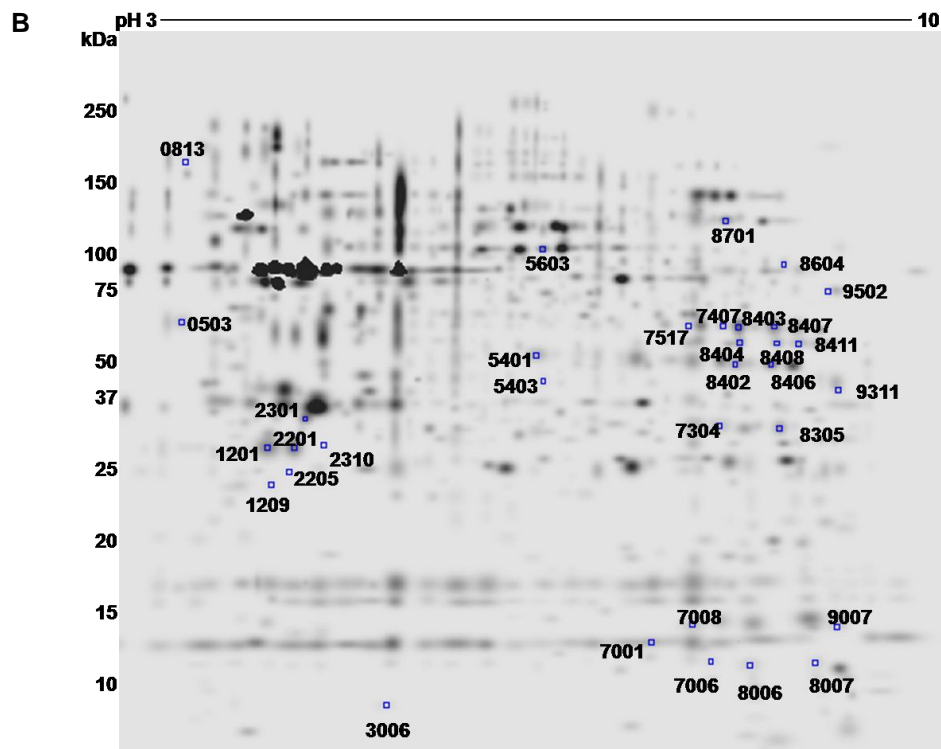
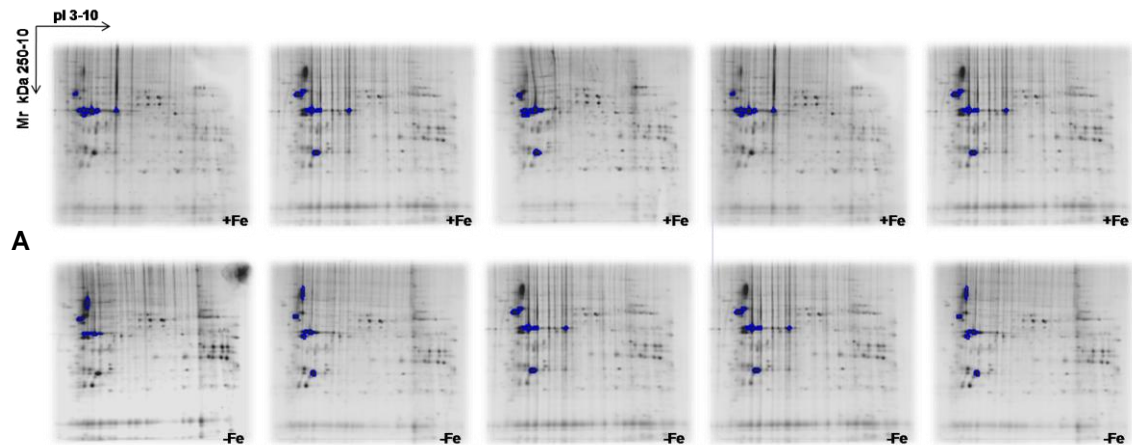


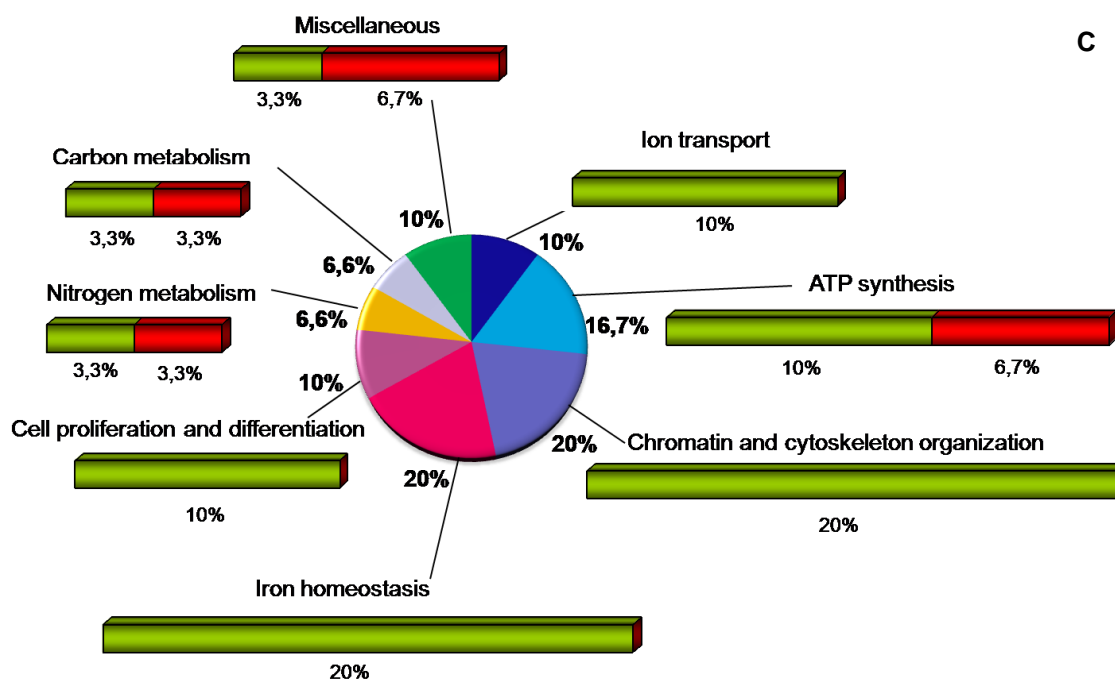


**Fig 1. A.** Replica maps of intracellular proteome of macrophages treated with iron (+Fe) and not treated (-Fe). **B.** Master map of intracellular proteome of macrophages. Blue squares highlight proteins differentially expressed in macrophages. **C.** Protein GO categorization. Distribution of the identified proteins according to the biological function. Assignments were made on the basis of information provided by gene ontology (GO) lists downloaded using the tool FatiGO30 from Babelomics (<http://fatigo.bioinfo.cipf.es/>). The absolute number of proteins to which the distribution is referred is 15 proteins (2 up and 13 down) (cytoskeleton organization), 1 (1up) (nitrogen metabolism), 5 (3 up and 2 down) (protein folding and turnover), 4 (3 up and 1 down) (carbohydrate metabolism), 4 (1 up and 3 down) (cell redox homeostasis), 7 (7 up) (iron homeostasis).

### 3.1.2. Membrane proteome

Similarly to 3.1.1., the master map of membrane proteins was elaborated (Fig. 2). A total of 813 spots were counted, of which 24 were over-expressed and 9 were under-expressed upon Fe treatment.

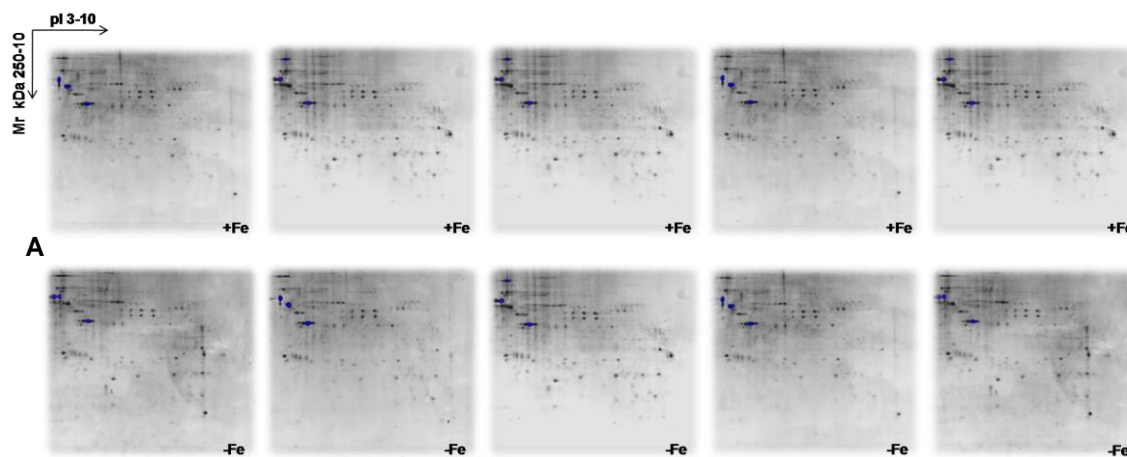




**Fig 2. A.** Replica maps of membrane proteome of macrophages treated with iron (+Fe) and not treated (-Fe). **B.** Master map of membrane proteome of macrophages. Blue squares highlight proteins differentially expressed in macrophages. **C.** Protein GO categorization. Distribution of the identified proteins according to the biological function. Assignments were made on the basis of information provided by gene ontology (GO) lists downloaded using the tool FatiGO30 from Babelomics (<http://fatigo.bioinfo.cipf.es/>). The absolute number of proteins to which the distribution is referred is 6 proteins (6 up) (chromatin and cytoskeleton organization), 6 (6 up) (iron homeostasis), 3 (3 up) (cell proliferation and differentiation), 2 (1 up and 1 down) (nitrogen metabolism), 2 (1 up and 1 down) (carbon metabolism), 3 (2 up and 1 down) (miscellaneous), 3 (3 up) (ion transport).

### 3.1.3. Membrane associated proteome

Finally, 2-DE gels of the membrane-associated fraction of mouse macrophages treated with Fe and control were performed as well in five replica. The master map, shown in Figure 3, showed a total of 316 spots. Regarding this fraction, the spots that resulted differentially expressed upon the Fe treatment were respectively 15 (over-expressed) and 3 (under-expressed).



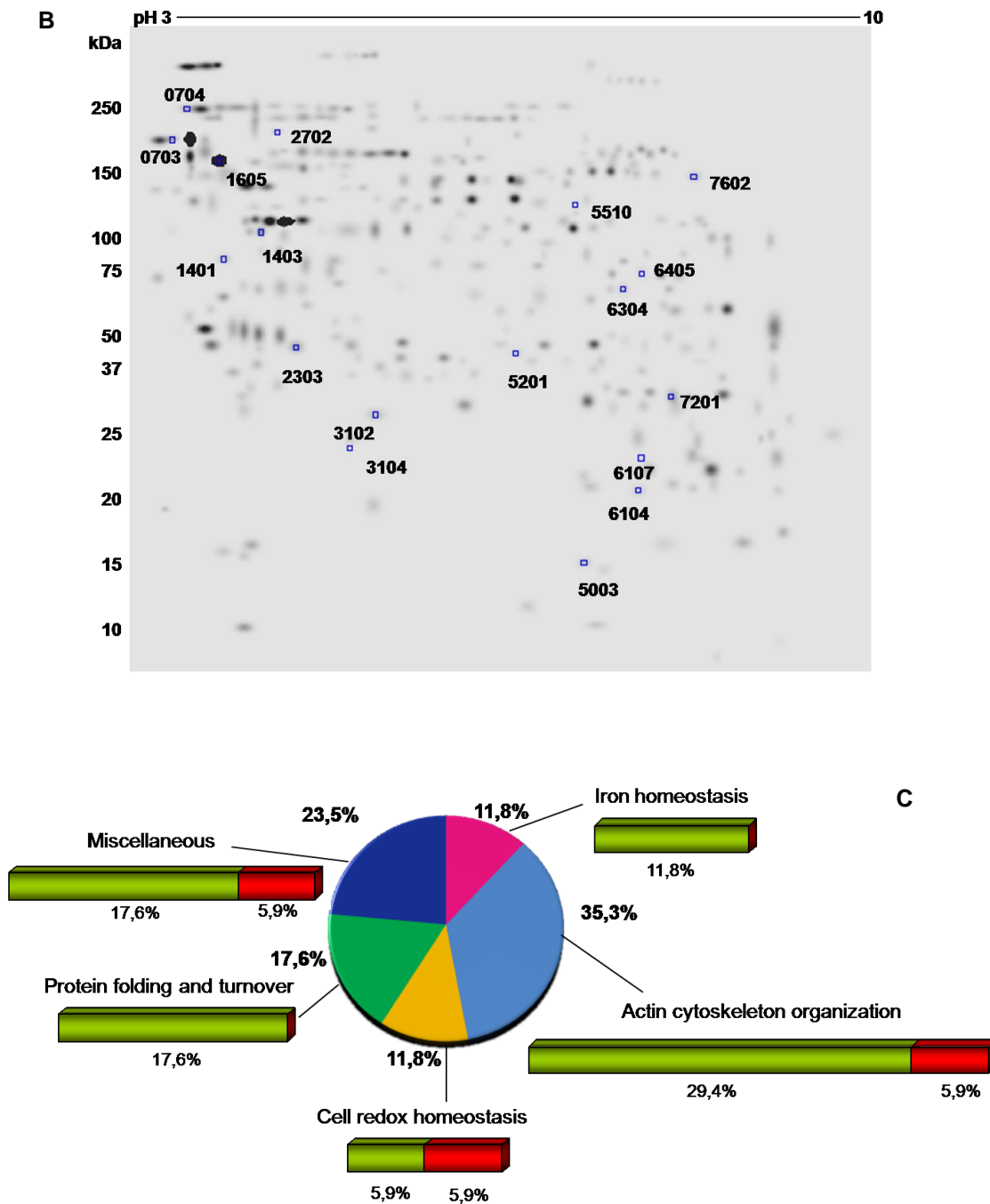


**Fig 3. A.** Replica maps of membrane-associated proteome of macrophages treated with iron (+Fe) and not treated (-Fe). **B.** Master map of membrane-associated proteome of macrophages. Blue squares highlight proteins differentially expressed in macrophages. **C.** Protein GO categorization. Distribution of the identified proteins according to the biological function. Assignments were made on the basis of information provided by gene ontology (GO) lists downloaded using the tool FatiGO30 from Babelomics (<http://fatigo.bioinfo.cipf.es/>). The absolute number of proteins to which the distribution is referred is 6 proteins (5 up and 1 down) (actin cytoskeleton organization), 2 (2 up) (iron homeostasis), 4 (3 up and 1 down) (miscellaneous), 3 (3 up) (protein folding and turnover), 2 (1 up and 1 down) (cell redox homeostasis).

### 3.2. Identification of iron-regulated proteins

Proteins that resulted significantly varied on the 2D-maps were identified by nano-HPLC/MS-MS and the complete lists are reported in Table 1 (intracellular proteins), Table 2 (membrane proteins) and Table 3 (membrane associated proteins).

#### 4. DISCUSSION

In this study, we were able to improve the understanding of the molecular effects produced by an iron challenge on macrophage cells by analyzing the differential protein expression in control and in macrophages treated with near-physiological concentrations of iron (10 ng/L FAC). The choice of this concentration was based on the aim to mimic the conditions of physiological milieu in presence of iron while avoiding toxic or extreme responses. Cytosol, membranes and membrane-associated proteins were analysed independently with comparative proteomics. The analysis of homogeneous sub-fractions of the proteome, allowed to achieve the optimisation in the 2D separation and favoured a better insights of the protein population induced by iron exposure.

The analysis of data in Table 1, 2 and 3, indicate that only few proteins in the different fractions are completely switched on/off (regulated >10 folds, i.e. ratio of normalized optical densities of treated samples vs. controls). In particular we found a protein (SSP 8603) over-expressed of 15.59 folds in the intracellular fraction of macrophages cultured with Fe; a protein (SSP 7006) newly induced in the membrane fraction of macrophages cultured with Fe and finally, in the membrane-associated fraction, we found a protein (SSP 3104) over-expressed of 22.08 folds in Fe-growth macrophages, while SSP7602 is completely switched off. All the other proteins differentially expressed, were regulated with quantitative ratios < 10 fold. These results seem in line with the *quasi*-physiological condition of the treatment, in fact only a small number of proteins were strongly induced or repressed. The localization/function of the regulated proteins is shown in panels C of Fig. 1-3 where the different categories are present with the respective % indicating the regulation of functions upon iron stimulus.

##### ***Basal metabolism supports stress conditions***

An overall enhancement of the metabolic rate was observed in presence of the Fe stimulus, as accounted by the up-regulation of several cytosolic enzymes: PGK1 (↑ 15.59 fold), Arginase (↑ 3.03 fold), Phosphopyruvate hydratase activity of LOC433182 hypothetical protein (↑ 1.74 fold). Fe induces also an increment in the levels of proteins related to oxidative stress, e.g. Peroxiredoxin 1, which is involved in the redox regulation of the cells, eliminating peroxides generated from metabolism. In parallel, protein folding and turnover result altered due to the presence of iron, as indicated by the increment of HSP proteins Hspd1 (↑ 1.75 fold) and Hspb1 (↑ 2.35 fold), the proteasome up-regulation (↑ 2.59 fold) and of components for RNA transcription (e.g. p100 co-activator, ↑ 3.96 fold). Changes in the expression of cystatin B (↑ 1.51 fold), and Peptidylprolyl-isomerase (↑ 1.70 fold) and of proteasome components (subunit alpha, type 6, ↑ 1.66 fold) were also found onto the membrane. Thus, the basal metabolic enhancement upon Fe stimulus seems to trigger a wider cellular defence mechanism, put in place by macrophages at both cytosolic and

membrane levels to contrast the oxidative environment, and which consists of redox-related responses, folding preservation mechanisms and misfolding clean-up mechanisms, all simultaneously activated in response to iron. Besides, the metabolic rate enhancement invokes increase in the available energy, thus ATP synthase components, known for their proton transport activity, are significantly increased in their expression levels at the mitochondrial membrane.

#### ***Iron homeostasis and iron uptake***

As expected, Fe induces the over-expression of storage proteins specific for iron, the ferritins, mainly localized within the cytosol. Ferritin takes up iron in a soluble, non-toxic, readily available form, in agreement with what reported on its induction by iron (Truty *et al.*, 2001). Western blot analysis of 2-DE with ferritin antibody confirmed ferritin over-expression in presence of iron stimulus (Fig. 4).

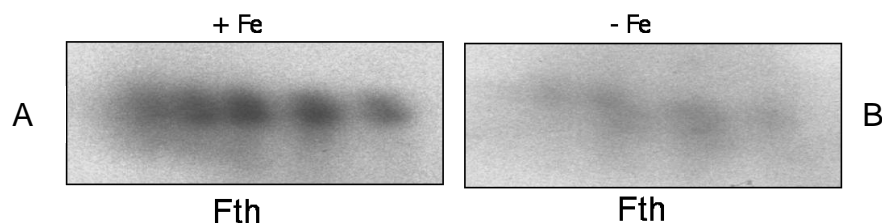


**Fig 4.** Bidimensional western blot of Ferritin. **A** Ferritin isoforms expressed in macrophages after treatment with FAC. **B** Ferritin isoforms physiologically expressed in macrophages.

Iron storage involves the uptake of iron (II) at the outer shell of ferritin, its oxidation by molecular oxygen at the dinuclear ferroxidase centers, and the movement of iron (III) into the cavity for deposition as ferrihydrite. The protein is formed by oligomers of 24 peptide chains, made of two types of subunits: L (light) chain and H (heavy) chain, that form a roughly spherical shell with a remarkable diameter of 12 nm and contains into the central cavity up to 4500 iron atoms deposited as insoluble mineral (Theil, 1990).

As to what concerns routes for the uptake of iron, it is interesting to note that our results clearly indicate glyceraldehyde-3-phosphate dehydrogenase (GADPH) among membrane proteins, and up-regulated in presence of iron ( $\uparrow 2.36$ ). GADPH role is normally associated with the glycolysis and localizes within the cytoplasm. However, the presence of GADPH on cell surfaces of human and murine macrophage and the link of its expression with the availability of iron in the medium was recently reported (Raje *et al.*, 2007). These authors demonstrated that GADPH is able to interact with transferrin and that the GADPH-transferrin complex is subsequently internalized into the early endosomes, leading to the hypothesis of GADPH acting as receptor for transferrin, in alternative to the well known receptors Trf 1 and Trf 2. Our experiments completely confirmed GADPH localization, as 2D gels indicate its expression on macrophage membranes, and GADPH modulated expression upon Fe

stimulus. Western immunoblot analysis of GADPH (Fig. 5) confirmed the data obtained with the comparative analysis indicating the diverse role of that protein: in presence of iron stimulus GADPH was prevalently localised on the membrane where it presumably acts as receptor for transferrin, whereas in non stimulated condition it is localised in the cytosol where it functions as a metabolic enzyme. Our data support the role of GADPH as a multifunctional protein within the cell and in particular as an alternative mechanism for iron acquisition.

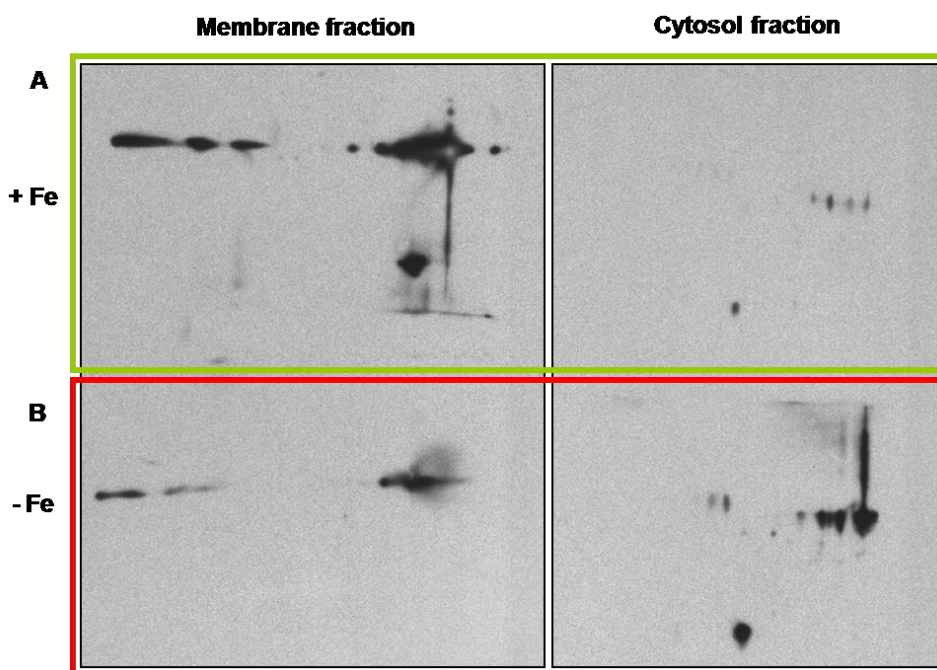


**Fig 5.** Bidimensional western blot of GADPH. **A.** GADPH isoforms expressed in macrophages after treatment with FAC in membrane and cytosol fraction. **B.** GADPH isoforms physiologically expressed in macrophages in membrane and cytosol fraction.

An incremented anion transport activity in presence of iron emerges from the up-regulation of the membrane voltage dependent anion channels (VDAC) 1, 2 and B-36. The voltage-dependent anion channels (VDAC), located to the mitochondrial outer membrane, function as gatekeeper for the entry and exit of mitochondrial metabolites, and thus controls cross-talk between mitochondria and the cytosol. VDAC was also identified as a site for the docking of cytosolic proteins, such as hexokinase, and was recognized as a key protein in mitochondria-mediated apoptosis in experiments conducted on tumor cells (Shoshan-Barmatz *et al.*, 2009). Key regions of VDAC1 functioning in apoptosis induction and regulation by hexokinase. It could be hypothesised that in macrophages challenged with iron the up-regulation of VDACs is consequence of the activation of intracellular defence mechanisms linked to iron homeostasis.



***Cytoskeleton: possible implications in iron uptake and delivery***

Iron uptake activity of challenged macrophages seems to influence cytoskeleton reorganization. Close to the membrane the Fe stimulus up-regulates vimentin ( $\uparrow$  4.54) and galectin-3 ( $\uparrow$  1.97), as indicated by our investigation on the expression of membrane associated protein fraction (Fig. 3); both proteins are involved in phagocytosis and in internalization processes (Sano *et al.*, 2006). Vimentin and galectin-3 localize on phagocytic structures, replacing actin (Sano *et al.*, 2003). The hypothetical role of vimentin and galectin-3 could be to increase the phagocytic activity of macrophages, induced by the Fe stimulus, absolving one of the main physiological roles of macrophages: iron internalization. In parallel, es1 protein is down-regulated ( $\downarrow$  2.94), its job relates with microtubule-organization of the mammalian cell; es1 protein is involved in the centrosome and plays many important roles during cell growth and organization (Manning *et al.*, 2008).

The actin cytoskeleton has been reported to be required also for the regulation of ion channel activity and in the intracellular trafficking; in particular data reports on the binding of VDAC channel to actin (Noda *et al.*, 2008) These findings are in agreement with our proteomic data on anion channel expression and on the actin increment next to membranes.

A different picture emerges from the cytosol, where data indicate the down-regulation of proteins of the cytoskeleton induced by the Fe stimulus: beta-actin ( $\downarrow$  2.15), gamma-actin-like protein ( $\downarrow$  2.88), A-X actin ( $\downarrow$  1.56), actin ( $\downarrow$  2.52). The down-regulation include also proteins with a role of control on signalling pathways the glia maturation factor gamma-isoform 1 ( $\downarrow$  2.42) and on the formation of vesicles, the vesicle mediated transport mKIAA3012 protein ( $\downarrow$  1.54) and Rho GDP dissociation inhibitor (GDI) beta ( $\downarrow$  1.56). The presence of higher iron levels seems to induce the de-structuration or the de-polymerisation of the cytosolic actin filaments.

Comparing the proteomic data of the cytoskeleton proteins upon iron challenge in cytosol and those of the membrane & membrane associate 2D maps, two apparently contrasting effects seem to take place in the macrophage cell: an increase in cytoskeleton elements next to the membrane and a depolymerisation of the cytoskeleton within the cytosol. A possible explanation to such a phenomenon comes from recent observations on the role of transport of internal proteins attributed to the microtubules and in general to the structures of the cytoskeleton (Noda *et al.*, 2008, Hasan *et al.*, 2006). A confirm of the cytoskeleton function in the transport of proteins to critical sites which is also of particular significance for iron homeostasis is in the discovery of the association of ferritin to microtubules that suggested these interaction plays a role in regulating the intracellular localization and/or release of ferritin under different physiological circumstances (Hasan *et al.*, 2005). Further works provided insights into the binding properties of ferritin with the microtubules in vitro,



indicating a dependence of the association on ferritin oligomerisation state (Hasan *et al.*, 2006). Our proteomic data are in agreement with the supposed microtubule-driven mechanisms for the intracellular distribution of ferritin, indicating the Fe stimulus induce incremented cytoskeletal proteins at the membrane, thus localized next to the iron transport structures. It could be foreseen that ferritin loaded with iron would be next delivered to destinations by an analogous mechanism (or driveway) of microtubules, which in this case would polymerize from the membranes across the cytosol to the recipient cell structures.

### ***Inflammatory***

Of particular interest is the newly induction ( $\uparrow >10$ ) of the Mif protein, also called macrophage migration inhibitory factor, whose presence was always described pivotal to induce a response to inflammation. MIF is a highly conserved cytokine which was originally described as a soluble factor expressed by T cells in delayed-type hypersensitivity responses exerting inhibitory effects on macrophages migration (David, 1966). More recently MIF has been acknowledged to play pleiotropic roles in the control of inflammatory “set-point” (Calandra, 1995), being so involved in acute and chronic inflammatory diseases such as septic shock, rheumatoid arthritis, atherosclerosis and ischemic heart (Bernhagen *et al.*, 1993, Burger-Kentischer *et al.*, 2002, Baugh *et al.*, 2002, Miller *et al.*, 2008). Moreover, MIF has gain great popularity especially in vascular diseases and myocardial damage being under investigation as a therapeutic target for plaque regression (Zernecke *et al.*, 2008, Noels *et al.*, 2009).

MIF was never found, before us, induced by iron exposure but, as iron can elicit oxidative stress, this result is also in agreement with recent reports; in fact MIF was identified in some proteomic studies for having a role in the response to oxidative stress in epithelial cells, T cells and neurons (Cha *et al.*, 2007, Nguyen *et al.*, 2003, Harrison and Sumners, 2009). In the context of macrophage cell, which is recognized as being at the interphase between iron and immunity for the control of infections (Theurl *et al.*, 2005), this new finding of MIF prompt induction can be of pivotal importance for the understanding and eventual treatment of inflammation and inflammatory related diseases.

## **5. CONCLUSIONS**

Comparative proteomic was a powerful tool for the analysis of iron regulated proteins in macrophage cells. The protein expression related to that stimulus can be very helpful for a better understanding of the role of this cell type in iron metabolism, immunity and infection. Moreover the information obtained on the molecular mechanism elicited can give new insight in the understanding of the pathophysiology of congenital and acquired disorders of iron homeostasis. It would be beneficial to compare the present results, in whose MDMs were stimulated with ionic iron at physiological concentrations, with data on MDMs

stimulated with senescent erythrocytes, in whose presumably a phagocytosis response would be elicited.

**Table 1.** Identification of the differentially expressed proteins of intracellular proteome in macrophages treated with iron.

Protein name	Gene name	Spot no.	NCBI acc. #	Mr. (Da) theor.	pI theor.	No. of peptides identified	Mascot score	Molecular function	Fold of variation
<b>Cytoskeleton organization</b>									
Gamma actin-like protein	Actg1	0211	gi 6425087	44029	5.11	7	378	Protein binding	Down 2.88
Moesin	Msn	6904	gi 70778915	67839	6.22	16	874	Protein binding	Up 3.96
Glia maturation factor, gamma isoform 1	Gmfg	1110	gi 11993950	16909	5.57	3	124	Actin binding	Down 2.42
A-X actin	Actb	2501	gi 309090	42009	5.21	10	586	Protein binding	Down 1.56
Actin	Actb	1403	gi 74187644	42053	5.23	10	536	Protein binding	Down 2.52
Gamma actin-like protein	Actg1	2303	gi 6425087	44029	5.11	9	498	Protein binding	Down 1.91
Rho, GDP dissociation inhibitor (GDI) beta	Arhgdib	2102	gi 33563236	22894	4.97	5	166	GTPase activator activity	Down 1.63
Annexin A3	Anxa3	2402	gi 5902786	36520	5.33	9	483	Calcium ion binding	Down 3.44
Rap1b	Rap1b	3209	gi 595280	21201	5.37	5	270	GTP binding	Down 1.91
Beta actin	Actb	2502	gi 74187644	42053	5.23	7	374	Protein binding	Down 2.15
Rho GDP dissociation inhibitor (GDI) alpha	Arhgdia	1301	gi 31982030	23450	5.12	7	402	GTPase activator activity	Down 1.56
Moesin	Msn	6807	gi 70778915	67839	6.22	4	163	Protein binding	Up 2.09
Chain A, Solution Structure Of Coactosin-Like Protein (Cofilin Family)	Cotl1	1105	gi 159163110	16621	5.13	9	348	Actin binding	Down 1.57
Lipocortin I	Anxa1	5406	gi 198845	38952	6.56	6	458	Calcium ion binding	Down 1.67
RAB1B, member RAS oncogene family	Rab1b	1207	gi 21313162	27717	5.55	2	149	GTP binding	Down 1.54
<b>Iron homeostasis</b>									
Ferritin light chain 1	Ftl1	3104	gi 120524	20847	5.66	9	505	Stores iron in a soluble, non-toxic, readily available form	Up 3.03
Ferritin heavy chain 1	Fth1	2204	gi 6753912	21224	5.53	11	498	Stores iron in a soluble, non-toxic, readily available form	Up 3.72
Ferritin light chain 1	Ftl1	2104	gi 120524	20847	5.66	8	478	Stores iron in a soluble, non-toxic, readily available form	Up 3.50
Ferritin heavy chain 1	Fth1	2206	gi 6753912	21224	5.53	13	618	Stores iron in a soluble, non-toxic, readily available form	Up 2.63
Ferritin light chain 1	Ftl1	3203	gi 120524	20847	5.66	12	720	Stores iron in a soluble, non-toxic, readily available form	Up 4.41

								readily available form	
mCG23169 Eukaryotic Ferritin	cd01056	3202	gi 148690909	20845	5.66	12	759	Stores iron in a soluble, non-toxic, readily available form	Up 4.28
Ferritin light chain 1	Ftl1	2205	gi 120524	20847	5.66	10	636	Stores iron in a soluble, non-toxic, readily available form	Up 3.79

#### Cell redox homeostasis

Peroxiredoxin 1	Prdx1	8204	gi 6754976	22390	8.26	14	722	Peroxiredoxin activity	Up 1.92
SH3-binding domain glutamic acid-rich protein like	Sh3bgrl	0008	gi 9910548	12917	4.87	6	301	Antioxidant activity	Down 3.44
type II peroxiredoxin 1	Prdx1	1209	gi 3603241	21949	5.20	2	80	Peroxiredoxin activity	Down 2.05

#### Carbohydrate metabolism

Phosphoglycerate kinase 1	Pgk1	8603	gi 40254752	44909	8.02	23	1189	ATP binding	Up 15.59
Hypothetical protein LOC433182	Eno1	5609	gi 70794816	47453	6.37	25	1419	Phosphopyruvate hydratase activity	Up 1.74
Hypothetical protein LOC433182	Eno1	3604	gi 70794816	47453	6.37	11	630	Phosphopyruvate hydratase activity	Up 1.67
Pyruvate kinase	Pkm2	7802	gi 31981562	58378	7.18	17	942	Pyruvate kinase activity	Down 2.56

#### Protein folding and turnover

Proteasome 28 subunit, alpha	Psme1	3304	gi 6755212	28826	5.73	11	511	proteasome activator activity	Up 2.59
p100 co-activator	Snd1	6904	gi 6009521	99934	6.64	5	288	Nuclease activity	Up 3.96
Proteasome subunit beta type-9 precursor	Psmb9	0204	gi 130856	23496	5.11	7	394	Threonine endopeptidase activity	Down 1.68
Heat shock protein	Hspd1	3801	gi 74211667	60878	6.04	7	322	ATP binding	Up 1.75
Heat shock protein 1, beta	Hspb1	1820	gi 40556608	83571	5.39	14	740	ATP binding	Up 2.35
Ubiquitin-conjugating enzyme E2N	Ube2n	3101	gi 12838544	17228	5.71	4	221	Ubiquitin-protein ligase activity	Down 2.26

#### Nitrogen metabolism

UMP-CMP kinase	Cmpk1	3205	gi 23821758	22379	5.68	8	414	ATP binding	Down 2.17
Arginase 1	Arg1	4510	gi 7106255	34957	6.51	7	346	Arginase activity	Up 3.03

**Table 2.** Identification of the differentially expressed proteins of membrane proteome in macrophages treated with iron.

Protein name	Gene name	Spot no.	NCBI acc.	Mr. (Da) theor.	pI exp./theor.	No. of peptides identified	Mascot score	Molecular function	Fold of variation
<b>Ion transport</b>									
Voltage-dependent anion channel 2	Vdac2	7407	gi 6755965	32340	7.48	4	193	ion channel	Up 1.68
Voltage-dependent anion channel 1	Vdac1	8406	gi 6755963	30851	8.62	8	502	ion channel	Up 1.60
B-36 VDAC=36 kda voltage dependent anion channel	Vdac2	5401	gi 299036	32327	7.44	9	489	ion channel	Up 1.76
<b>ATP synthesis</b>									
ATP synthase, H <sup>+</sup> transporting, mitochondrial F1 complex, O subunit	Atp5o	2205	gi 20070412	23406	10.00	4	174	Proton transport	Up 2.81
ATP synthase, H <sup>+</sup> transporting, mitochondrial F1 complex, alpha subunit, isoform 1	Atp5a	8411	gi 6680748	59830	9.22	7	537	Proton transport	Up 1.60
ATP synthase, H <sup>+</sup> transporting, mitochondrial F1 complex, alpha subunit, isoform 1	Atp5a	8701	gi 6680748	59830	9.22	21	1198	Proton transport	Up 2.06
F1F0 ATP synthase E subunit	Atp5k	8007	gi 1491942	8198	9.39	2	60	Proton transport	Down 2.70
Ubiquinol-cytochrome c reductase binding protein	Uqcrcq	9007	gi 13385726	13553	9.10	7	313	Electron transport	Down 5.55
<b>Chromatin and cytoskeleton organization</b>									
Histone cluster 1, H2ah	Hist1h2ab	7008	gi 30061327	13942	11.03	3	149	Core component of nucleosome	Up 2.19
Histone H4	Hist1h4a	7001	gi 94378251	17513	10.59	6	340	Core component of nucleosome	Up 2.49
Gamma actin-like protein	Actb	2310	gi 6425087	44029	5.11	6	334	Protein binding	Up 3.01
Actin, gamma	Actb	2301	gi 123298587	32941	5.15	8	443	Protein binding	Up 1.68
Vimentin	Vim	0813	gi 55408	53746	5.06	6	214	Protein binding	Up 4.54
rab7	Rab7a	2201	gi 1050551	23829	7.53	5	239	Endocytic transport	Up 1.78
<b>Iron homeostasis</b>									
Heme-binding protein	Hebp2	1201	gi 3724328	21165	5.18	2	109	heme binding	Up 1.72
Glyceraldehyde-3-phosphate dehydrogenase	Gapdh	7517	gi 55153885	36093	7.59	4	209	Protein binding	Up 2.36
Glyceraldehyde-3-phosphate dehydrogenase	Gapdh	8408	gi 55153885	36093	7.59	10	491	Protein binding	Up 1.55
Glyceraldehyde-3-phosphate dehydrogenase	Gapdh	8404	gi 55153885	36093	7.59	7	305	Protein binding	Up 1.60
Glyceraldehyde-3-phosphate dehydrogenase	Gapdh	8403	gi 55153885	36093	7.59	9	489	Protein binding	Up 1.55

Glyceraldehyde-3-phosphate dehydrogenase	Gapdh	8407	gi 55153885	36093	7.59	9	463	Protein binding	Up 1.51
--	-------	------	-------------	-------	------	---	-----	-----------------	---------

#### Cell proliferation and differentiation

RAS related protein 1b	Rap1b	1209	gi 52138628	21013	5.65	4	127	GTP binding	Up 2.23
Galectin-3	Lgals3	9311	gi 52851	27469	8.57	8	531	Sugar binding	Up 1.97
Macrophage migration inhibitory factor	Mif	7006	gi 6754696	12667	6.79	2	72	phenylpyruvate tautomerase activity	Newly induced

#### Nitrogen metabolism

Nit protein 2	Nit2	5403	gi 12963555	30825	6.44	8	410	Hydrolase activity	Down 2.32
Glutamate oxaloacetate transaminase 2, mitochondrial	Got2	9502	gi 6754036	47780	9.13	11	601	L-aspartate:2-oxoglutarate aminotransferase activity	Up 2.34

#### Carbon metabolism

Isocitrate dehydrogenase 2 (NADP+), mitochondrial	Idh2	8604	gi 27370516	51358	8.88	10	610	NAD or NADH binding	Up 1.71
Phosphopyruvate hydratase	Eno1	5603	gi 70794816	47453	6.37	13	822	Lyase	Down 6.25

#### Miscellaneous

es1 protein	D10Jhu81e	7304	gi 20070420	28415	9.00	7	284	unknown	Down 2.94
mCG15232, isoform CRA_b	Eef1a1	8305	gi 148694454	38315	9.13	10	384	GTPase activity	Down 3.45
RIKEN full-length enriched mouse cDNA	Rcan1	8402	gi 12848861	31398	7.72	2	134	Protein binding	Up 1.68

**Table 3.** Identification of the differentially expressed proteins of membrane-associated proteome in macrophages treated with iron.

Protein name	Gene name	Spot no.	NCBI acc. #	Mr. (Da) theor.	pI theor.	No. of peptides identified	Mascot score	Molecular function	Fold of variation
<b>Iron homeostasis</b>									
mCG23169	Fth	3102	gi 148690909	20845	5.66	12	746	Stores iron in a soluble, non-toxic, readily available form	Up 5.17
Ferritin heavy chain 1F	Fth	3104	gi 6753912	21224	5.53	8	399	Stores iron in a soluble, non-toxic, readily available form	Up 22.08
<b>Actin cytoskeleton organization</b>									
Annexin A2	Anxa2	6405	gi 6996913	38937	7.55	16	865	Cytoskeletal protein binding	Up 1.96
beta-actin	Actb	2303	gi 74191564	42066	5.30	10	452	Protein binding	Up 1.85
Vimentin	Vim	2702	gi 2078001	51590	4.96	14	765	Protein binding	Up 1.90
put. beta-actin (aa 27-375)	Actb	1403	gi 49868	39446	5.78	12	382	Protein binding	Up 1.59
CAP, adenylate cyclase-associated protein 1	Cap1	7602	gi 157951604	51875	7.16	1	150	Actin binding	Not detected
Calreticulin	Calr	0703	gi 6680836	48136	4.33	15	712	Actin binding	Up 9.26
<b>Cell redox homeostasis</b>									
Peroxioredoxin 1	Prdx1	7201	gi 6754976	22390	8.26	11	518	Hydroperoxide oxidoreductase	Up 2.01
Protein disulfide-isomerase precursor (PDI) (Prolyl 4-hydroxylase subunit beta) (Cellular thyroid hormone-binding protein) (p55) (Erp59)	P4hb	1605	gi 129729	57507	4.79	24	1170	Disulphide isomerase activity	Down 3.57
<b>Protein folding and turnover</b>									
Cystatin B	Cst2	5003	gi 6681071	11153	6.82	5	164	Cysteine-type endopeptidase inhibitor activity	Up 1.51
Peptidylprolyl isomerase A	Ppia	6104	gi 6679439	18131	7.74	7	345	Peptide binding	Up 1.70
Proteasome (prosome, macropain) subunit, alpha type 6, isoform CRA_b	Psme1	5201	gi 148704781	28353	6.99	6	372	Threonine-type endopeptidase activity	Up 1.66
<b>Miscellaneous</b>									
L-lactate dehydrogenase A	Lhda	6304	gi 6754524	36817	7.62	10	543	Dehydrogenase	Down 2.5
Vacuolar adenosine triphosphatase subunit D	Atp6v0a1	1401	gi 3955100	40749	4.39	10	517	Ion transport	Up 1.70
78 kDa glucose-regulated protein precursor (GRP 78) (Heat shock 70 kDa protein 5) (Immunoglobulin heavy chain-binding protein)	Hspa5	0704	gi 2506545	72492	5.07	32	1795	ATP binding	Up 2.42

Hypothetical protein LOC433182	Eno1	5510	gil70794816	47453	6.37	16	937	Lyase	Up 4.27
--------------------------------	------	------	-------------	-------	------	----	-----	-------	---------



## CHAPTER 3

# PROTEOMIC RESPONSE TO HEME-IRON IN MURINE MACROPHAGES

### 1. INTRODUCTION

The importance of well-defined amounts of iron for the survival, replication and differentiation of animals, plants and almost all microorganisms is well established (Chricton, 2001). Iron deficiency is a general problem in biology, and in human it is responsible for 400-500 million cases of anaemia, among the one-third of the world's population. However, iron in excess is toxic, particularly in human, where Hemochromatosis is one of the most frequent genetic disorders, with an estimated carrier frequency of 1 in 200 in the Caucasian population of Northern European descent for C282Y homozygotes (greater than that of cystic fibrosis and phenylketonuria together). It is therefore not surprising that iron homeostasis is a major concern in human health and well-being. Excess iron accumulation in the tissues, in cells and even in organelles, can result in toxicity and is associated with pathological disorders. In addition to the classic iron loading found in genetic haemochromatosis and in secondary iron overload disorders, such as the thalassaemias, with their associated dysfunctions (Chricton, 2001), there are many other diseases associated with excess of iron. For example, iron accumulation in the brain has been associated with Parkinson's disease, Alzheimer's disease, Huntington's chorea and HIV encephalopathy (Rouault, 2001) and more recently in basal ganglia disease (Curtis *et al.*, 2001) and Hallervorden Spatz syndrome (Zhou *et al.*, 2001), while Friedreich ataxia, excessive mitochondrial iron accumulation occurs particularly in brain and cardiac tissue (Kaplan, 1999). Thereby an adequate supply of iron is essential for good health. In human, more than 60% of total body iron is present in erythrocytes complexed with the heme of hemoglobin. After a life-span of 120 days, senescent red blood cells (RBCs) are specifically cleared from the circulation by tissue macrophages and heme iron is efficiently recycled. In mammals, this process is critical in iron homeostasis (Knutson and Wessling-Resnick, 2003). Macrophages play a critical role in body iron homeostasis by recovering iron from senescent red blood cells and returning it to the circulation for binding to transferrin, which delivers the metal to the cells that need it for various functions, thus contributing for more than 80% to the daily iron turnover (Recalcati *et al.*, 2009). However, the molecular mechanisms involved in macrophage iron handling are still poorly documented. After RBCs engulfment by macrophages in phagosomes, hemoglobin is degraded and iron is released from heme through the action of heme oxygenase, the rate-limiting enzyme of heme

degradation (Maines, 1997, Tenhunen *et al.*, 1969). Heme iron is subsequently recycled to the blood circulation to respond to the needs of the organism. Three isoforms of HO have been described in mammals, but only HO-1, an inducible form, appears to be largely responsible for heme catabolism in macrophage cells (Poss and Tonegawa, 1997). Due to the localization of HO-1 in the endoplasmic reticulum (ER) (Tenhunen *et al.*, 1969), heme freed from RBC inside the phagolysosome is assumed to reach the cytosol by diffusing across the phagosomal membrane. However, the more recent discovery of Desjardins and colleagues showing participation of ER in phagosome formation (Gagnon *et al.*, 2002) may suggest heme degradation inside the erythrophagolysosome. Iron transporters belonging to the Nramp family and localized in the phagosomal membrane may help subsequently to transport iron into the cytosol (Forbes and Gros, 2001). Heme iron is then either stored in macrophages, or exported into the circulation to respond to body iron needs. Ferritin seems to play an important role in macrophage iron storage secondary to the catabolism of red cell heme. In fact, ferritin has been shown to be strongly upregulated after erythrophagocytosis (Knutson and Wessling-Resnick, 2003). Interestingly, in splenic macrophages, iron deposition was observed in paracrystallin arrangements surrounded by membranes that likely correspond to intralysosomal formation of hemosiderin, an insoluble aggregated form of partially digested ferritin (Ferreira *et al.*, 2001). Ferroportin, the first cellular iron exporter identified in mammals (Abboud and Haile, 2000, McKie *et al.*, 2000, Donovan *et al.*, 2000), is highly expressed in tissue macrophages (Abboud and Haile, 2000, Donovan *et al.*, 2000, Yang *et al.*, 2002) and plays a key role in iron release from macrophages after EP (Pietrangelo, 2004, Donovan *et al.*, 2005, Knutson *et al.*, 2005, Knutson *et al.*, 2003). Recently, insight into ferroportin function came from the observation that hepcidin, a major systemic regulator of iron metabolism (Ganz, 2005), is able to bind to ferroportin and to lead to internalization and degradation of the iron exporter (Nemeth *et al.*, 2004). The iron export from macrophages seems to be also dependant of the activity of a ferroxidase, the ceruloplasmin (Harris *et al.*, 1999). However, despite several evidences that point out the importance of HO-1, ferritin, ferroportin or hepcidin in heme iron recycling, little is known about the molecular mechanisms involved in iron recovery from heme. The absence of a clear description regarding the process of heme iron recycling in macrophages may be due in part to the inherent difficulties in studying EP *in vivo* and of reproducing *in vitro* the natural clearance of RBCs by macrophages.

To date information on RBCs recognition, trapping and destruction from macrophages are highly complex and not completely understood (Bratosin *et al.*, 1998, Bratosin *et al.*, 1997). Two erythrophagocytosis pathways have been described in the literature: an immunoglobulin-dependant pathway that relies on opsonization of effete RBCs by natural antibodies as a primary signal for clearance and an immunoglobulin-independent pathway

that involves non-immune mediators for recognition and destruction of old RBCs. The importance of the latter pathway has been clearly demonstrated by the observation that erythrophagocytosis can occur in the absence of immunoglobulins (Bratosin *et al.*, 1997). A classical model of EP is the phagocytosis of IgG-coated erythrocytes by macrophages. However, it has to be kept in mind that this model does not take into account the major cellular changes observed in old RBC membranes. Indeed, numerous changes including appearance of new molecules (e.g. externalization of phosphatidylserine), modification of preexisting molecules (desialylation, exposure of h-galactosyl residues), occurring in the erythrocyte membrane have been identified as markers for phagocytes to bind and phagocytose a senescent RBC (Bratosin *et al.*, 1998). Here, we carried out a comparative proteomic analysis using artificially aged rabbit RBCs and primary culture of murine (C3H WT) bone marrow-derived macrophages (BMDMs) that tends to mimic the natural clearance of senescent RBCs. We report the mapping of heme-stimulated protein expression versus un-stimulated in its entire complexity. The comparison of the two proteomes helped in defining stimulus-expressed or stimulus-suppressed proteins, to precise the molecular mechanisms involved in heme iron recycling.

## **2. MATERIALS AND METHODS**

### **2.1. Cell culture and protein extraction**

Mouse Bone Marrow macrophages isolated from C3H WT mice were maintained in culture for 7 days. Macrophages were incubated with senescent RBCs accordingly to Delaby *et al.* (2005). Intracellular, membrane, membrane associated fractions were obtained as described by Polati *et al.* (2009) and analysed on 2-DE.

### **2.2. 2-DE and statistical analysis**

Differential proteomics analyses were performed as described by Polati *et al.* (2009) (session 3, chapter 1, paragraphs 2.2-2.5, 2.7-2.8).

### **2.3. Mass Spectrometry Analysis**

Differential proteomics analyses were performed as described by Polati *et al.* (2009) (session 3, chapter 1, paragraph 2.9).

## **3. RESULTS**

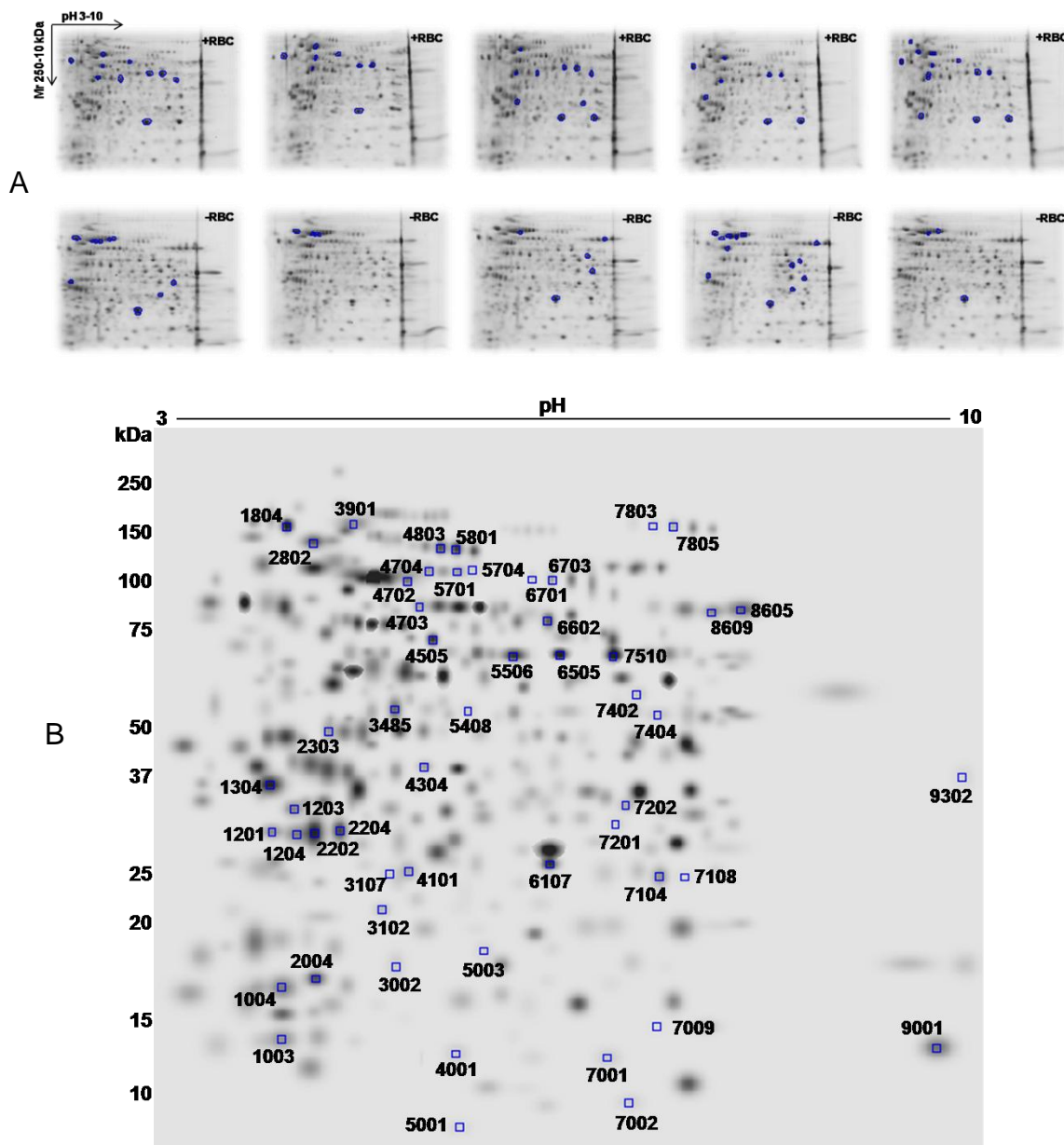
### **3.1. Proteic pattern before and after iron stimulus: 2-DE**

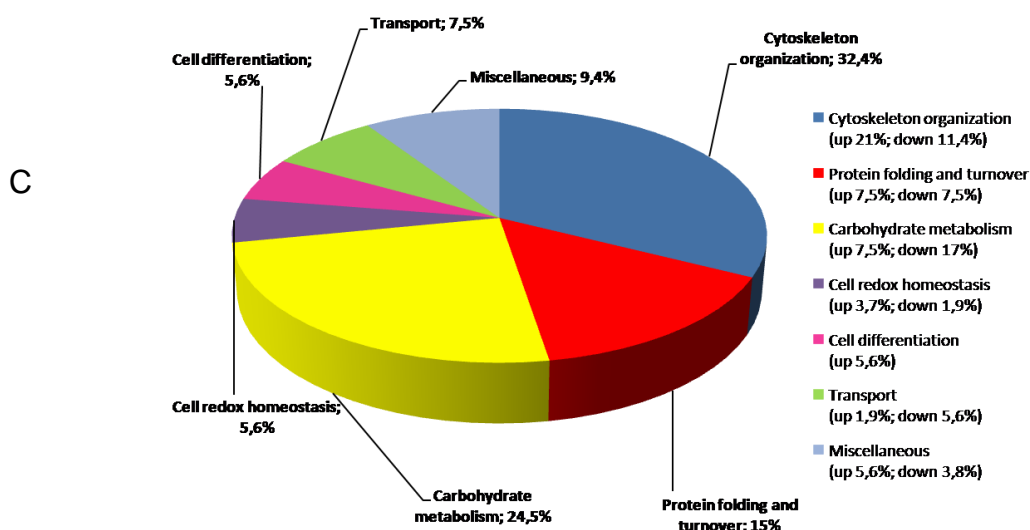
Proteins extracted from  $10 \times 10^6$  cells were fractionated with a method set up for obtaining high resolution 2D maps from monocytes/macrophages (Polati *et al.*, 2009). Two discrete

fractions, indicated as intracellular proteins and membrane proteins were recovered, quantified and analysed by 2-DE (5 replica gels for each fraction).

### 3.1.1. Intracellular proteome

2-DE gels of the intracellular fraction of cells treated with senescent RBCs and control cells (i.e. non-treated) were run each in five replicas. The images of the gels, analysed by the software PDQuest 7.3.0 (BioRad), were used to develop a master map (Fig. 1) on which were counted a number of 360 protein spots representative of all the proteins of the two experimental groups analyzed. The comparative analysis highlighted the spots differentially expressed with statistical significance (minimum ratio accepted >2.0 fold) on the master map. The comparison of the cytosol fraction of treated cells versus control cells evidenced 27 proteins over-expressed and 26 proteins under-expressed.

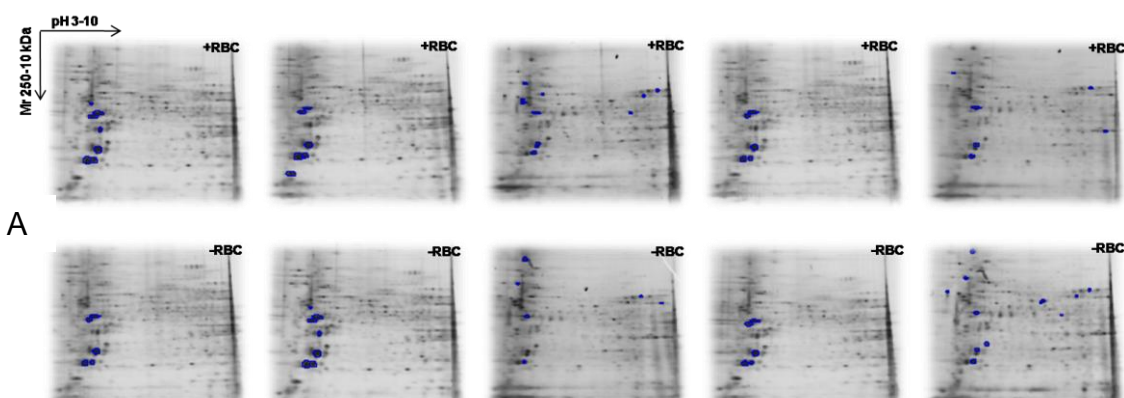




**Fig 1. A.** Replica maps of intracellular proteome of macrophages treated with RBC (+RBC) and not treated (-RBC). **B.** Master map of intracellular proteome of macrophages. Blue squares highlight proteins differentially expressed in macrophages. **C.** Protein GO categorization. Distribution of the identified proteins according to the biological function. Assignments were made on the basis of information provided by gene ontology (GO) lists downloaded using the tool FatiGO30 from Babelomics (<http://fatigo.bioinfo.cipf.es/>). The absolute number of proteins to which the distribution is referred is 17 proteins (11 up and 6 down) (cytoskeleton organization), 8 (4 up and 4 down) (protein folding and turnover), 13 (4 up and 9 down) (carbohydrate metabolism), 3 (3 up) (cell differentiation), 3 (2 up and 1 down) (cell redox homeostasis), 4 (1 up and 3 down) (transport), 5 (3 up and 2 down) (miscellaneous).

### 3.1.2. Membrane proteome

Similarly to 3.1.1., the master map of membrane proteins was elaborated (Fig. 2). A total of 336 spots were counted, of which 33 were over-expressed and 28 were under-expressed upon RBCs treatment.



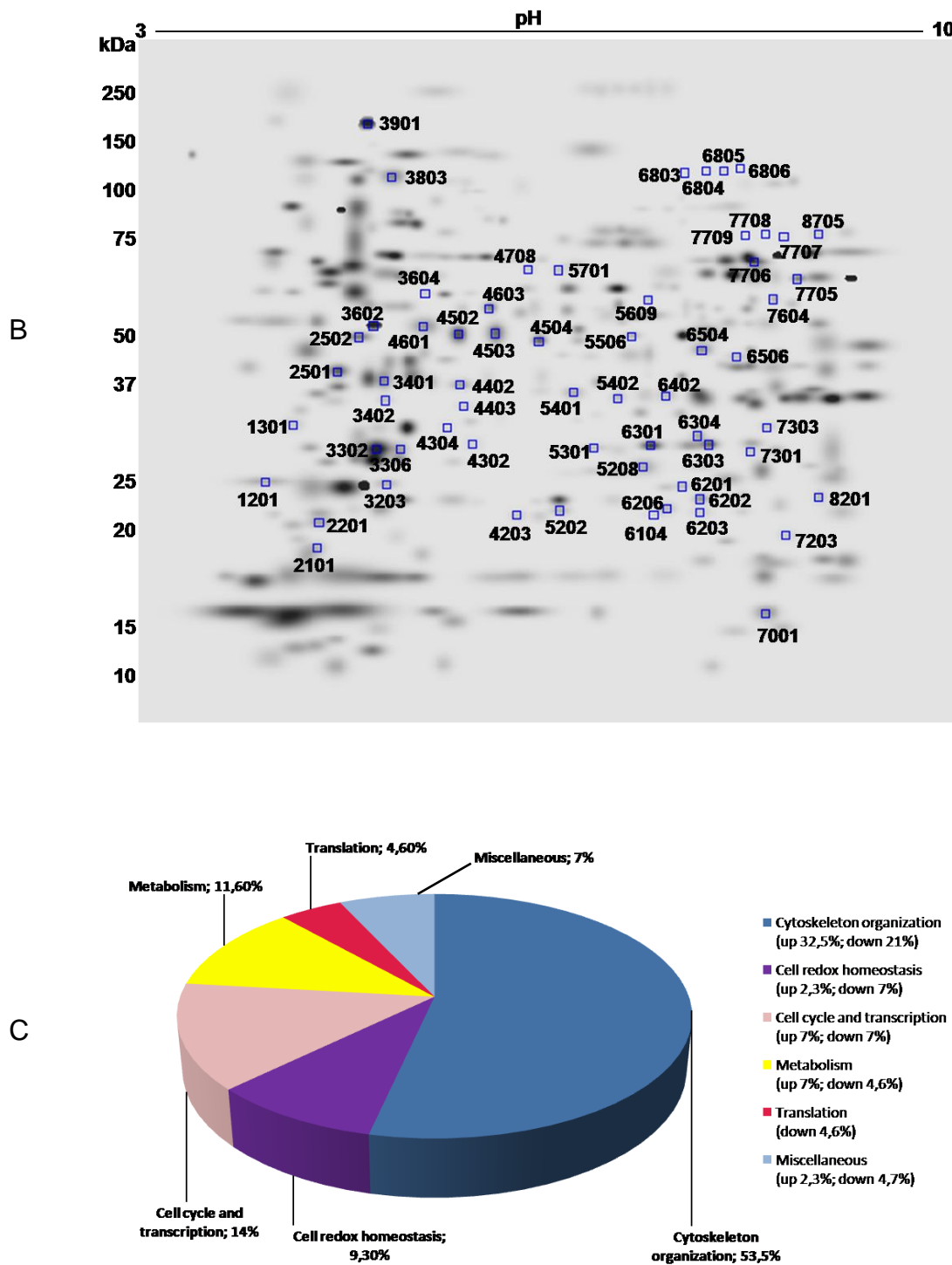


**Fig 2. A.** Replica maps of membrane proteome of macrophages treated RBC (+RBC) and not treated (-RBC). **B.** Master map of membrane proteome of macrophages. Blue squares highlight proteins differentially expressed in macrophages. **C.** Protein GO categorization. Distribution of the identified proteins according to the biological function. Assignments were made on the basis of information provided by gene ontology (GO) lists downloaded using the tool FatiGO30 from Babelomics (<http://fatiGO.bioinfo.cipf.es/>). The absolute number of proteins to which the distribution is referred is 23 proteins (14 up and 9 down) (cytoskeleton organization), 4 (1 up and 3 down) (cell redox homeostasis), 6 (3 up and 3 down) (cell cycle and transcription), 5 (3 up and 2 down) (metabolism), 2 (2 up) (translation), 3 (1 up and 2 down) (miscellaneous).

### 3.2. Identification of regulated proteins

Proteins that resulted significantly varied on the 2D-maps were identified by nano-HPLC/MS-MS and the complete lists are reported in Table 1 (intracellular proteins) and Table 2 (membrane proteins).

## 4. DISCUSSION

In this study, we were able to improve the understanding of the molecular effects produced by erythrophagocytosis on macrophage cells by analyzing the differential protein expression in control and in macrophages treated with artificially aged rabbit RBCs to mimic the natural clearance of senescent RBCs and to observe how heme-iron is recycled.

Cytosol and membranes were analysed independently with comparative proteomics, because the analysis of homogeneous sub-fractions of the proteome allows to optimise the 2D separations, thus favouring a better insight of the protein population induced by RBC phagocytosis.

The proteins found regulated are reported in Table 1 and 2. Results indicate that numerous proteins in the two fractions are regulated >10 folds (ratio of normalized optical densities of treated samples vs. Controls), such regulation threshold is conventionally defined as completely switched on/off. The list of spots switched on/off is reported in Figure 3.

A	Spots switched on/off in cytosol fraction	Spots switched on/off in membrane fraction	B
	SSP1004 - <i>on</i>	SSP2201 - <i>off</i>	
	SSP1204 - <i>on</i>	SSP3402 - <i>off</i>	
	SSP1804 - <i>on</i>	SSP5202 - <i>off</i>	
	SSP2802 - <i>on</i>	SSP6203 - <i>off</i>	
	SSP4505 - <i>on</i>	SSP6304 - <i>on</i>	
	SSP6107 - <i>off</i>	SSP6402 - <i>off</i>	
	SSP7002 - <i>on</i>	SSP6804 - <i>on</i>	
	SSP7104 - <i>on</i>		

**Fig 3.** List of SSP switched on (green background) and switched off (red background) after treatment of macrophages with senescent RBC. **A.** Spots switched on/off in cytosol fraction, **B.** spots switched on/off in membrane fraction.

It is interesting to note that the newly induced proteins are located mainly in the cytosolic fraction, while the majority of proteins switched off were found in the membrane fraction. All the other proteins differentially expressed, were regulated with quantitative ratios < 10 folds. The localization/function of the regulated proteins is shown in panels C of Fig. 1-2 where proteins are ordered for similar categories and are indicated with the respective % of regulation upon iron stimulus.

***Cytoskeletal alterations: implications of the erythrophagocytosis***

In mammals, macrophages are multifunctional cells. Apart from their crucial role in the regulation of both innate and acquired immunity, they play a fundamental role as scavenger in the clearance of non-self materials such as microorganisms and altered-self materials such as apoptotic cells, immune complexes, inflammatory products and senescent erythrocytes. Thus, whereas the immune-activity is based on phagocytosis and intracellular degradation, the clearance-activity largely depends on the production and secretion of a panel of regulatory molecules such as cytokines, chemokines, and nitrogen oxide (NO). The phagocytic activity involves substantial remodeling of the cytoskeleton. Our proteomics results highlighted changes in the cytoskeletal proteins involved in erythrophagocytosis. The majority of cytoskeletal proteins that we found regulated during erythrophagocytosis belong to the class of actin. Four different isoforms of beta-actin were up-regulated (SSP8705, ↑3.5; SSP4304, ↑4.99; SSP3302, ↑2.43; SSP1204, newly induced) and also gamma-actin (SSP2204, ↑3.54; SSP2101, ↑5.44; SSP2502, ↑2.85; SSP7604, ↑2.13) both in the cytosol fraction and in the membrane fraction. It was demonstrated by Stossel (1993) that the dynamic shifts in the concentration and length of actin filaments provide the force and structure for non-muscle cell motility and phagocytosis. It was estimated that phagocytosis is associated with a 40% increase in the content of filamentous actin in phagocytic cells (Greenberg *et al.*, 1991). In addition there are a myriad of actin-binding proteins that relate to temporal and spatial regulation of actin filaments assembly.

Actin filaments assemble with a fast-growing or barbed end. Which refers to the end of filaments decorated with fragments of myosin. Proteins capable of blocking exchange at the barbed end can prevent indiscriminate growth of actin filaments and control the localization of newly assembled actin filaments. Among the proteins assolving the function of actin regulatory proteins there are polypeptides of the gelsolin family (Kwiatkowski, 1999). Here, we found an up-regulation of gelsolin at the cytoplasmic level (SSP4803, ↑4.05; SSP5801, ↑4.50) and a simultaneous down-regulation of this protein (SSP6504, ↓5.53) in the membrane fraction of macrophages treated with senescent RBCs.

Another protein belonging to gelsolin family appears down-regulated at membrane level: the macrophage capping protein (CapG) (SSP6506, ↓2.16). CapG is the only member of gelsolin family that does not sever actin filaments (Southwick, 1995). It was proposed that active remodeling of the actin cytoskeleton by gelsolin family proteins might regulate the endo/exocytic activities in phagocytic cells (Beaulieu *et al.*, 2005). The regulation of actin family and gelsolin family proteins goes hand in hand with the differential expression of other cytoskeletal proteins such as coronins (SSP4402, ↓2.45; SSP4603, ↓3.73; SSP4708, ↑2.67), an ARP3 actin-related protein (SSP4505, newly induced) and a chaperonin containing TCP-1 (CCT) (SSP6602, ↑4.40). A classical function of coronins is in regulating



the actin cytoskeleton and the microtubule system. Furthermore coronins act in intracellular vesicle formation and trafficking (Rybakin and Clemen, 2005). In particular Yan and colleagues (2005) examined the role of coronin in the phagocytic process of macrophages. They demonstrated that coronin-1 transiently accumulates at the nascent phagosome in a temporal sequence similar to that of actin. Moreover they observed significant changes in macrophages adhesion properties and in phagocytic potential, with impaired accumulation of ARP3 and actin at the phagocytic cup. These results provide the first evidence for a requisite function of coronin-1 in macrophage phagocytosis and are perfectly in agreement with our proteomic data. Furthermore the complex ARP2/3 is considered the main driving force for the formation of pseudopod protrusions (i.e. phagocytic cup) around the target (May *et al.*, 2000). Interestingly CCT, that was here found up-regulated after erythrophagocytosis, is a molecular chaperone assisting protein folding in the cytosol of eukaryotes. CCT facilitates the folding of actin and tubulin in the presence of ATP and is bound to newly synthesized actin, tubulin and some other unidentified polypeptides (Yokota *et al.*, 2000). Ultimately, high and sudden energy demand is seen during cell-shape change: a process in which ATP fuels the cytoskeletal machinery that drives cell-morphology alteration. Indeed, due to the evidences, various studies now argues in favor of a model in which up to 50% of cellular energy expenditure via ATP hydrolysis is required for acto-myosin dynamics in cell types with a constantly changing morphology, like neurons, astrocytes and immune cells (Hertz *et al.*, 2007). Regarding ATP requirements, in macrophages treated with senescent RBCs we found over-expression of an ATP synthase (SSP7705,  $\uparrow 2.29$ ) and brain creatine kinase (CK-B), this latter results over expressed of 2.12 folds in the cytoplasm and completely switched off at the membrane level. Our data are in agreement with the results of Kuiper and colleagues (2008) who demonstrated that the metabolic ATP-supply activity of CK-B is of local importance and facilitates specific phagocytosis steps via effects on actin-based events early in the binding-ingestion process.

***ER stress: implications in inflammation, in attenuation of metabolism and in translation***

Interestingly our proteomics data suggest that erythrophagocytosis causes in macrophages the stress of endoplasmic reticulum (ER). ER stress is of particular interest because is involved in inflammation, neurodegeneration, diabetes mellitus, heart diseases, and kidney diseases (Han *et al.*, 2008, Lin *et al.*, 2008, Marciniak and Ron, 2006). ER stress has also been related to autoimmune diseases including rheumatoid arthritis (Gao *et al.*, 2008, Purcell *et al.*, 2003) and autoimmune myositis (Nagaraju *et al.*, 2005). Accordingly to these authors aberrant ER stress responses can contribute to disease.

ER stress is caused by perturbation of its homeostatic functions: accumulation of unfolded proteins in the ER lumen is a shared hallmark of the perturbation the physiological functions of the ER and results in the activation of a common response to such stress situation. The

ER chaperone BiP serves as a master controller of the stress response (Quinones *et al.*, 2008).

In unstressed cells, BiP is associated with the ER luminal domains of the stress sensors, thanks to the low concentration of unfolded proteins under these conditions. Accumulation of unfolded proteins triggers their interaction with BiP, which results in depletion of the free BiP pool, and sequestering of BiP from the ER luminal domains of the stress sensors, resulting the activation of these latter (Schröder, 2008). In our proteomics analysis we found the simultaneous down regulation of BiP (SSP5704, ↓6.37) and cathepsin D (SSP4503, ↓2.64), an aspartyl protease involved in the degradation of BiP (Shi *et al.*, 2009). Furthermore murine valosin-containing protein (SSP3901) results up-regulated of 2.45 folds in macrophages treated with senescent RBCs. The valosin-containing protein, also termed p97, belongs to the AAA superfamily, ATPases associated with a variety of cellular activities. In particular Wojcik *et al.* (2006) demonstrated a significant up-regulation of transcripts encoding for this protein associated with apoptosis, ER stress and oxidative stress.

To maintain ER homeostasis, cells initiate processes that augment the ER capacity of protein folding by evoking transient attenuation of protein translation, transient attenuation of metabolism, ER-associated degradation of misfolded proteins, the induction of molecular chaperones and inflammation (Shi *et al.*, 2009). In our results of macrophages that phagocytosed RBCs, we observed the attenuation of protein translation, the attenuation of metabolism and the inflammatory response. In fact, regarding the attenuation of protein translation, both Tu translational elongation factor (SSP5506, ↓2.58) and ribosomal protein L9 (SSP1201, ↓2.7) appears down-regulated. Aalso many enzymes belonging to carbohydrate metabolism, such as transaldolase 1 (SSP5408, ↓2.71), triosephosphate isomerase (SSP7202, ↓2.28), enolase 1 (SSP7402, ↓9.02; SSP7404, ↓2.00), beta-glucuronidase (SSP6701, ↓4.27; SSP6703, ↓2.34), pyruvate kinase (SSP7402, ↓9.02; SSP7404, ↓2.00; SSP7404, ↓2.00), glutamate dehydrogenase 1 (SSP7706, ↓3.26) and phosphoglycerate mutase (SSP6301, ↓3.73) are down-regulated.

In terms of inflammation, numerous proteins resulted regulated upon RBCs exposure. The first signal of macrophages activation is the over expression of Ca<sup>2+</sup> binding proteins. In fact agonist-stimulated changes in intracellular Ca<sup>2+</sup> serve as ubiquitous second messenger signals in eukaryotic cells. The effect of changes in intracellular Ca<sup>2+</sup> are transduced within cells by Ca<sup>2+</sup>-binding proteins. Macrophages have been seen to be particularly responsive to extracellular signals, the reaction to extracellular stimuli are often mediated by changes in the intracellular Ca<sup>2+</sup> concentration (Johnston *et al.*, 1990). Here we observed the up-regulation of the tumor protein translationally controlled 1 (SSP1201, ↑2.95) and of the calgizzarin (S100 calcium binding protein A11) (SSP1003, ↑2.14) both involved in acute and chronic inflammatory responses and in cancer (Odink *et al.*, 1997, Ma *et al.*, 2010). The

expression of secondary inflammatory mediators such as cytokines, chemokines, complement proteins, and co-stimulatory molecules is fundamental to modulate cellular responses by the activation and recruitment of immune cells mediating host cellular and tissue remodeling (Glaros *et al.*, 2009). Regarding cytokines production we found regulated some key proteins such as  $\alpha$ -fetoprotein (SSP4704,  $\downarrow$ 7.23; SSP5001,  $\downarrow$ 5.26), which down-regulation allows the expression of inflammatory cytokines in activated immune cells by an NFkB-dependent mechanism (Potapovich *et al.*, 2009); ubiquitin-conjugating enzyme E2N (SSP5003,  $\downarrow$ 6.82) that is key in the process of 'tagging' target proteins with lysine 63-linked polyubiquitin chains, which are essential for the transmission of immune receptor signals culminating in activation of the transcription factor NF-kB (Yamamoto *et al.*, 2006); and endoplasmic (gp96) (SSP1804, newly induced) that is the master chaperone for TLRs and the dominant inducer of pro-inflammatory cytokines synthesis by macrophages (Yang *et al.*, 2007).

The beta-galactoside binding protein (galectin-3) (SSP2004) is also up-regulated of 4.49 folds, this protein, which is secreted from monocytes/macrophages and epithelial cells, has also been demonstrated to function as an extracellular molecule in activating various types of cells, including monocytes/macrophages, mast cells, neutrophils, and lymphocytes (Sano *et al.*, 2000). The expression of this lectin is up-regulated during inflammation (Flotte *et al.*, 1983), cell proliferation (Moutsatsos *et al.*, 1987, Agrwal *et al.*, 1989), and cell differentiation (Liu *et al.*, 1995, Nangia-Makker *et al.*, 1993) and through *trans*-activation by viral proteins (Hsu *et al.*, 1996). Its expression is also affected by neoplastic transformation (Konstantinov *et al.*, 1996): up-regulated in certain types of lymphomas and thyroid carcinoma (Fernandez *et al.*, 1997, Xu *et al.*, 1995), while down-regulated in other types of malignancies, such as colon (Lotz *et al.*, 1993, Castronovo *et al.*, 1992), breast (Castronovo *et al.*, 1996), ovarian (van den Brule *et al.*, 1994), and uterine carcinomas (van den Brule *et al.*, 1996). Finally the hepatocyte growth factor (HGF) results up-regulated of 3.49 folds. HGF is known as scatter factor and described as a multifunctional cytokine. It has a potent mitogenic activity for a wide variety of epithelial and endothelial cells and it is involved in organ growth and regeneration. HGF enhances cell migration and inhibits cells proliferation and may play a role in regulating immune cell function and inflammatory responses (Chen *et al.*, 1996).

## 5. CONCLUSIONS

Comparative proteomic confirms a powerful tool for the analysis of regulated proteins in macrophage cells after erythrophagocytosis. The protein expression related to RBCs stimulus would offer a better understanding of the process of heme-iron metabolism in macrophages and would help to clarify heme-iron role in immunity and infection. In

summary this work highlights the proteins regulated in macrophages after the phagocytosis of senescent red blood cells. In addition to the numerous proteins involved in cytoskeletal changes, particular attention should be given by proteins indicating the ER stress, as such condition strictly relates to inflammatory responses. Still an important piece of the puzzle is missing: what is the destiny of the thousands heme-groups bound to haemoglobins of the phagocytosed RBCs? There are no trace of them, nor there is trace of heme-oxygenase nor ferritins, both protein classes well involved in heme dismantling and in iron storage. Experimental results clearly indicated that the phagocytosis of senescent RBCs and their consequent degradation took place, as supported by the expression of proteins upon RCBs stimulus and by the lack of rabbit proteins on 2D maps. But surprisingly, there was no evidence of the activation of a molecular response addressed to heme-recycling. Thus in order to clarify the heme-metabolism and in order to draw a comprehensive picture of the responses triggered by iron on macrophages, a wider experimental plan needs to be set. Further experimental case to be studied comprise the challenging of macrophages treated with nude heme-groups. The comprehensive analysis of these results would allow to fill the gap in iron homeostasis and would help in understanding better the important relations between iron and inflammatory processes.

**Table 1.** Identification of the differentially expressed proteins of intracellular proteome in macrophages treated with senescent RBCs.

Protein name	Gene name	Spot no. a)	NCBI acc. #	Mr. (Da) exp./theor.	pI exp./theor.	No. of peptides identified	Mascot score <sup>b)</sup>	Molecular function GO term	Fold of variation on +RBC <sup>d)</sup>
<b>Cytoskeleton organization</b>									
tumor protein, translationally-controlled 1	Tpt1	1201	gi 6678437	19450	4.76	6	82	Calcium ion binding	Up 2.95
Rho, GDP dissociation inhibitor (GDI) beta	Arhgdib	1203	gi 33563236	22836	4.97	8	82	GTPase activator activity	Up 2.06
put. beta-actin (aa 27-375)	Actb	1204	gi 49868	39161	5.78	19	228	Protein binding	Newly induced
tyrosine 3-monooxygenase/tryptophan 5-monooxygenase activation protein, eta polypeptide	Ywhah	1304	gi 6756037	28194	4.81	17	549	Monooxygenase activity	Up 2.99
put. beta-actin (aa 27-375)	Actb	2202	gi 49868	39161	5.78	56	358	Protein binding	Up 3.21
gamma actin-like protein	Actb	2204	gi 6425087	43572	5.11	51	404	Protein binding	Up 3.54
annexin A5	Anxa5	2303	gi 6753060	35730	4.83	13	110	Calcium ion binding	Down 2.36
transgelin	Tagln	3002	gi 5007032	23582	6.59	13	293	Actin cross-linking	Down 2.15
Rho, GDP dissociation inhibitor (GDI) beta	Arhgdib	3102	gi 33563236	22836	4.97	10	198	GTPase activator activity	Down 3.79
tyrosine 3-monooxygenase/tryptophan 5-monooxygenase activation protein, eta polypeptide	Ywhah	3107	gi 6756037	28194	4.81	13	139	Monooxygenase activity	Down 4.49
rab7	Rab7	4101	gi 1050551	23544	7.53	9	371	GTP binding	Up 2.78
annexin A3	Anxa3	4304	gi 5902786	36348	5.33	41	416	Calcium ion binding	Down 2.12
ARP3 actin-related protein 3 homolog B	Actr3b	4505	gi 148671124	37861	6.11	9	245	Regulation of actin filament polymerization	Newly induced
unnamed protein product		4703	gi 26326929	70119	5.24	45	433	Actin binding	Down 2.13
Gsn protein	Gsn	4803	gi 38014369	80712	5.52	30	748	Actin binding	Up 4.05
Gsn protein	Gsn	5801	gi 38014369	80712	5.52	37	861	Actin binding	Up 4.50
annexin A5	Anxa5	7002	gi 6753060	35730	4.83	1	81	Calcium ion binding	Newly induced
<b>Protein folding and turnover</b>									
tumor rejection antigen gp96 (endoplasmic)	Hsp90b1	1804	gi 6755863	92418	4.74	26	831	Unfolded protein binding	Newly induced
heat shock protein 1, alpha	Hsp90aa1	2802	gi 6754254	84735	4.93	50	484	Unfolded protein binding	Newly induced
unnamed protein product	Hsp70	4702	gi 74211667	60764	6.04	74	962	Unfolded protein binding	Down 5.70
ubiquitin-conjugating enzyme E2N	Ube2n	5003	gi 4507793	17127	6.13	9	260	Ubiquitin-protein ligase activity	Up 6.82
BiP	Hspa5	5704	gi 2598562	72433	5.10	9	100	Protein binding	Down 6.37
CCT (chaperonin containing TCP-1) beta subunit	Cct2	6602	gi 468546	57411	5.97	12	186	Unfolded protein binding	Up 4.40
proteasome subunit MC13	Psmb8	7108	gi 673450	23032	6.89	12	372	Threonine-type endopeptidase activity	Down 6.58
proteasome subunit alpha type-2	Psma2	7201	gi 1709759	25909	8.39	21	258	Threonine-type endopeptidase activity	Down 2.13

**Carbohydrate metabolism**

transaldolase 1	Taldo1	5408	gi 33859640	37363	6.57	15	404	Transaldolase activity	Down 2.71
hypothetical protein LOC433182	Eno1	5506	gi 70794816	47111	6.37	48	537	Phosphopyruvate hydratase activity	Up 2.73
hypothetical protein LOC433182	Eno1	6505	gi 70794816	47111	6.37	53	773	Phosphopyruvate hydratase activity	Up 2.71
triosephosphate isomerase	Tpi1	7202	gi 1864018	22492	5.62	26	251	Triose-phosphate isomerase activity	Down 2.28
hypothetical protein LOC433182	Eno1	7402	gi 70794816	47111	6.37	48	349	Phosphopyruvate hydratase activity	Down 9.02
EG433182 protein	Eno1	7404	gi 13278412	38276	5.60	29	336	Phosphopyruvate hydratase activity	Down 2.00
hypothetical protein LOC433182	Eno1	7510	gi 70794816	47111	6.37	70	1305	Phosphopyruvate hydratase activity	Up 2.43
beta-glucuronidase	Hpse	6701	gi 193723	74206	6.16	14	261	Calcium ion binding	Down 4.27
beta-glucuronidase	Hpse	6703	gi 193723	74206	6.16	11	77	Calcium ion binding	Down 2.34
M2-type pyruvate kinase	Pkm2	8605	gi 1405933	57878	7.18	65	848	Ion binding	Down 2.11
pyruvate kinase	Pkm2	8609	gi 31981562	57808	7.18	35	1167	Ion binding	Down 2.31
hypothetical protein LOC433182	Eno1	9001	gi 70794816	47111	6.37	12	485	Phosphopyruvate hydratase activity	Up 6.53
unnamed protein product	Pkm2	9302	gi 74212815	43138	5.88	8	113	Ion binding	Down 4.35

**Cell redox homeostasis**

peroxiredoxin 1	Prdx1	4101	gi 6754976	22162	8.26	15	67	Removal of superoxide radicals	Up 2.78
peroxiredoxin 1	Prdx1	6107	gi 6754976	22162	8.26	86	403	Removal of superoxide radicals	Not detected
peroxiredoxin 1	Prdx1	7803	gi 6754976	22162	8.26	25	583	Removal of superoxide radicals	Up 4.04

**Cell differentiation**

S100 calcium binding protein A11 (calgizzarin)	S100a11	1003	gi 21886811	11075	5.28	6	127	Calcium ion binding	Up 2.14
thioredoxin 1	Txn1	1004	gi 6755911	11668	4.80	17	263	Electron transport	Newly induced
beta-galactoside binding protein	Lgals1	2004	gi 193442	14796	5.32	15	226	Galactose binding	Up 4.49

**Transport**

murine valosin-containing protein	Vcp	3901	gi 55217	89252	5.14	16	610	Activation of caspase activity	Up 2.45
alpha-fetoprotein	Afp	4704	gi 191765	47195	5.47	4	121	Ion binding	Down 7.23
alpha-fetoprotein	Afp	5001	gi 191765	47195	5.47	2	72	Ion binding	Down 5.26
albumin	Afamin	5701	gi 158138568	68714	6.09	5	129	Transport	Down 7.45

**Miscellaneous**

brain creatine kinase	Ckb	3405	gi 10946574	42686	5.40	11	216	ATP binding	Up 2.12
hypothetical protein LOC239673		7001	gi 29244176	58230	8.47	1	87		Down 3.52

hypothetical protein LOC239673		7009	gi 29244176	58230	8.47	1	67		Down 3.67
heterogeneous nuclear ribonucleoprotein A2/B1	Hnrpa2b1	7104	gi 3329498	35971	8.67	4	153	RNA binding	Newly induced
unnamed protein product	Ef2	7805	gi 26324898	95197	6.51	31	784	Elongation factor	Up 3.22

**Table 2.** Identification of the differentially expressed proteins of membrane proteome in macrophages treated with senescent RBCs.

Protein name	Gene name	Spot no.	NCBI acc. #	Mr. (Da) theor.	pI theor.	No. of peptides identified	Mascot score	Molecular function	Fold of variation
<b>Cytoskeleton organization</b>									
A-X actin	<b>Actb</b>	4601	gi 309090	41667	5.21	4	122	ATP binding	Down 2.06
gelsolin	<b>Gsn</b>	6504	gi 74144652	38646	6.28	10	397	actin binding	Down 5.53
coronin-1	<b>Coro1a</b>	4402	gi 4895037	50943	6.05	2	57	actin filament binding	Down 2.45
gamma-actin	<b>Actg1</b>	2101	gi 809561	40992	5.56	19	522	ATP binding	Up 5.44
put. beta-actin (aa 27-375)	<b>Actb</b>	2201	gi 49868	39161	5.78	2	96	ATP binding	Not detected
gamma actin-like protein	<b>Actg1</b>	2502	gi 74195718	41709	5.46	58	529	ATP binding	Up 2.85
hypothetical protein LOC239673	<b>Actb</b>	3203	gi 29244176	58230	8.47	9	118	ATP binding	Up 2.48
put. beta-actin (aa 27-375)	<b>Actb</b>	3302	gi 49868	39161	5.78	50	423	ATP binding	Up 2.43
A-X actin	<b>Actb</b>	3401	gi 309090	41667	5.21	37	599	ATP binding	Up 2.99
annexin A4	<b>Anxa4</b>	3402	gi 2492905	35967	5.43	1	68	calcium ion binding	Not detected
alpha-tubulin isotype M-alpha-2	<b>Tuba1b</b>	3602	gi 202210	50134	4.94	5	64	GTP binding	Up 2.92
beta-actin	<b>Actb</b>	4304	gi 110226713	41645	5.15	7	228	ATP binding	Up 4.99
alpha-tubulin isotype M-alpha-2	<b>Tuba1a</b>	4603	gi 202210	50134	4.94	2	79	GTP binding	Down 3.73
coronin-1	<b>Coro1a</b>	4603	gi 4895037	50943	6.05	4	79	actin filament binding	Down 3.73
coronin-1	<b>Coro1a</b>	4708	gi 4895037	50943	6.05	3	134	actin filament binding	Up 2.67
unnamed protein product	<b>Actc1</b>	3604	gi 12835802	47287	5.54	12	239	ATP binding	Up 3.16
macrophage-capping protein	<b>Capg</b>	6506	gi 729023	39216	6.73	5	135	actin binding	Down 2.16
unnamed protein product	<b>Actb</b>	7303	gi 74195718	41709	5.46	5	159	ATP binding	Up 2.01
gamma-actin	<b>Actb</b>	7604	gi 809561	40992	5.56	6	190	ATP binding	Up 2.13
tubulin beta 5	<b>Tubb5</b>	2501	gi 74204140	49616	4.75	32	690	GTP binding	Down 3.18
binder of Rho GTPases 5	<b>Cdc42ep1</b>	6803	gi 26324898	95197	6.51	3	97	protein binding	Up 8.88
binder of Rho GTPases 5	<b>Cdc42ep1</b>	6804	gi 26324898	95197	6.51	4	154	protein binding	Newly induced
put. beta-actin (aa 27-375)	<b>Actb</b>	8705	gi 49868	39161	5.78	5	135	ATP binding	Up 3.5
<b>Cell redox homeostasis</b>									
peroxiredoxin	<b>Prdx1</b>	5202	gi 6435547	22079	8.34	8	207	heme binding	Not detected
peroxiredoxin 1	<b>Prdx1</b>	6201	gi 6754976	22162	8.26	12	288	peroxiredoxin activity	Down 3.38
peroxiredoxin 1	<b>Prdx1</b>	6202	gi 6754976	22162	8.26	13	341	peroxiredoxin activity	Up 2.9



voltage-dependent anion-selective channel protein 1	<b>Vdac3</b>	6402	gi 109479457	35014	8.86	3	60	nucleotide binding	Not detected
---	--------------	------	--------------	-------	------	---	----	--------------------	--------------

### Cell cycle and transcription

cell division cycle 5-related protein	<b>Cdc5l</b>	3803	gi 74198702	89315	5.14	18	517	DNA binding	Down 3.75
hepatocyte growth factor receptor	<b>Met</b>	4504	gi 12843046	26390	8.22	1	48	growth factor activity	Up 3.49
Dhx36 protein	<b>Dhx36</b>	6304	gi 50815	42158	6.56	3	112	ATP binding	Newly induced
purine nucleoside phosphorylase	<b>Pnp</b>	4302	gi 388923	32239	6.08	5	193	purine-nucleoside phosphorylase activity	Down 2.32
tyrosine 3/tryptophan 5 -monooxygenase activation protein	<b>Ywhab</b>	1301	gi 5803225	29155	4.63	3	83	monooxygenase activity	Up 2.12
centromeric protein E	<b>Cenpe</b>	3901	gi 47847498	154779	5.43	48	360	ATP binding	Down 5.29

### Metabolism

glutamate dehydrogenase 1	<b>Glud1</b>	7706	gi 148692928	54185	7.66	12	360	ATP binding	Down 3.26
transketolase	<b>Tkt</b>	7707	gi 6678359	67588	7.23	5	121	calcium ion binding	Up 8.62
transketolase	<b>Tkt</b>	7709	gi 1729977	67601	7.23	3	92	calcium ion binding	Up 5.94
enolase	<b>Eno3</b>	5609	gi 55491	47095	6.37	5	161	magnesium ion binding	Up 4.48
phosphoglycerate mutase 1	<b>Pgam1</b>	6301	gi 10179944	28919	6.19	7	244	2,3-bisphospho-D-glycerate 2-phosphohydrolase activity	Down 3.73

### Translation

Tu translation elongation factor, mitochondrial isoform 1	<b>Tufm</b>	5506	gi 27370092	49477	7.23	6	153	GTP binding	Down 2.58
ribosomal protein L9	<b>Mrpl9</b>	1201	gi 14149647	21868	9.69	3	104	structural constituent of ribosome	Down 2.7

### Miscellaneous

creatine kinase B-type	<b>Ckb</b>	6203	gi 148698457	34014	5.85	3	77	ATP binding	Not detected
cathepsin D precursor	<b>Ctsd</b>	4503	gi 6753556	44925	6.71	3	53	aspartic-type endopeptidase activity	Down 2.64
ATP synthase, H <sup>+</sup> transporting, mitochondrial F1 complex, alpha subunit, isoform 1 precursor	<b>Atp6v1a</b>	7705	gi 6680748	59716	9.22	19	503	ATP binding	Up 2.29



## BIBLIOGRAPHY

- Abboud S.** and D.J. Haile, *J. Biol. Chem.* 275 (2000) 19906.
- Agarwal N.**, J.L. Wang, P.G. Voss, *J. Biol. Chem.* 264 (1989) 17236.
- Aisen P.**, Ponka, Woodworth, Schulman eds., CRC Press, Boca Raton (1990) 281.
- Anderson G.J.** and C.D. Vulpe, *Cell. Mol. Life Sci.* 66 (2009) 3241.
- Andrews N.C.**, *Blood.* 112 (2008) 219.
- Barisani D.**, R. Meneveri, E. Ginelli, C. Cassani, D. Conte, *FEBS. Lett.* 469 (2000) 208.
- Baugh J.A.**, S. Chitnis, S.C. Donnelly, J. Monteiro, X. Lin, B.J. Plant, F. Wolfe, P.K. Gregersen, R. Bucala, *Genes. Immun.* 3 (2002) 170.
- Beaulieu V.**, N. Da Silva, N. Pastor-Soler, C.R. Brown, P.J. Smith, D. Brown, S. Breton, *J. Biol. Chem.* 280 (2005) 8452.
- Benes P.**, V. Macecková, Z. Zdráhal, H. Konečná, E. Zahradníčková, J. Muzík, J. Smarda, *Differentiation.* 74 (2006) 265.
- Bernhagen J.**, T. Calandra, R.A. Mitchell, S.B. Martin, K.J. Tracey, W. Voelter, K.R. Manogue, A. Cerami, R. Bucala, *Nature.* 365 (1993) 756.
- Bleackley M.R.**, A.Y. Wong, D.M. Hudson, C.H. Wu, R.T. Macgillivray, *Transfus. Med. Rev.* 23 (2009) 103.
- Boyd J.M.**, R.M. Drevland, D.M. Downs, D.E. Graham, *J. Bacteriol.* 191 (2009) 1490.
- Bozzini C.**, N. Campostrini, P. Trombini, E. Nemeth, A. Castagna, I. Tenuti, R. Corrocher, C. Camaschella, T. Ganz, O. Olivieri, A. Piperno, D. Girelli, *Blood. Cells. Mol. Dis.* 40 (2008) 347.
- Bratosin D.**, J. Mazurier, J.P. Tissier, C. Slomianny, J. Estaquier, F. Russo-Marie, J.J. Huart, J.M. Freyssinet, D. Aminoff, J.C. Ameisen, J. Montreuil, *C. R. Acad. Sci. Ser. III* 320 (1997) 811.
- Bratosin D.**, J. Mazurier, J.P. Tissier, J. Estaquier, J.J. Huart, J.C. Ameisen, D. Aminoff, J. Montreuil, *Biochimie.* 80 (1998) 173.
- Burger-Kentischer A.**, H. Goebel, R. Seiler, G. Fraedrich, H.E. Schaefer, S. Dimmeler, R. Kleemann, J. Bernhagen, C. Ihling, *Circulation.* 105 (2002) 1561.
- Cairo G.** and A. Pietrangelo, *Biochem. J.* 352 (2000) 241.
- Calandra T.**, *Nature.* 377 (1995) 68.
- Castronovo V.**, E. Campo, F.A. van den Brule, A.P. Claysmith, V. Cioce, F.T. Liu, P.L. Fernandez, M.E. Sobel, *J. Natl. Cancer. Inst.* 84 (1992) 1161.
- Castronovo V.**, F.A. Van den Brule, P. Jackers, N. Clausse, F.T. Liu, C. Gillet, M.E. Sobel, *J. Pathol.* 179 (1996) 43.
- Cha M.H.**, T. Rhim, K.H. Kim, A.S. Jang, Y.K. Paik, C.S. Park, *Mol. Cell. Proteomics.* 6 (2007) 56.
- Chen Q.**, M.C. DeFrances, R. Zarnegar, *Cell. Growth. Differ.* 7 (1996) 821.
- Churchward M.A.**, R.H. Butt, J.C. Lang, K.K. Hsu, J.R. Coorsen, *Proteome. Sci.* 3 (2005) 5.
- Clarke R.**, H.W. Ransom, A. Wang, J. Xuan, M.C. Liu, E.A. Gehan, Y. Wang, *Nat. Rev. Cancer.* 8 (2008) 37.
- Cordwell S.J.**, *Methods. Mol. Biol.* 424 (2008) 139.
- Crichton R.R.**, *Wiley and Chichester 2nd Edition*, New York, (2001) 57.
- Curtis A.J.**, C. Fey, C.M. Morris, L.A. Bindoff, P.G. Ince, P.F. Chinnery, A. Coulthard, M.J. Jackson, A.P. Jackson, D.P. McHale, D. Hay, W.A. Barker, A.F. Markham, D. Bates, A. Curtis, J. Burn, *Nat. Genet.* 28 (2001) 350.
- Dale D.C.**, L. Boxer, W.C. Liles, *Blood.* 112 (2008) 935.
- David J.R.**, *Proc. Natl. Acad. Sci. U.S.A.* 56 (1966) 72.
- De Domenico I.**, D. McVey Ward, J. Kaplan, *Nat. Rev. Mol. Cell. Biol.* 9 (2008) 72.
- De Domenico I.**, D.M. Ward, J. Kaplan, *J. Clin. Invest.* 117 (2007) 1755.
- De Domenico I.**, E. Nemeth, J.M. Nelson, J.D. Phillips, R.S. Ajioka, M.S. Kay, J.P. Kushner, T. Ganz, D.M. Ward, J. Kaplan, *Cell. Metab.* 8 (2008) 146.
- Deiss A.**, Wintrobe's Clinical Hematology, Lee, Foerster, Lukens, Paraskevas, Greer, Rodgers and Wintrobe eds. Baltimore (1999) 267.
- Delaby C.**, N. Pilard, G. Hetet, F. Driss, B. Grandchamp, C. Beaumont, F. Canonne-Hergaux, *Exp. Cell. Res.* 310 (2005) 43.
- Donovan A.**, A. Brownlie, Y. Zhou, J. Shepard, S.J. Pratt, J. Moynihan, B.H. Paw, A. Drejer, B. Barut, A. Zapata, T.C. Law, C. Brugnara, S.E. Lux, G.S. Pinkus, J.L. Pinkus, P.D. Kingsley, J. Palis, M.D. Fleming, N.C. Andrews, L.I. Zon, *Nature.* 403 (2000) 776.
- Donovan A.**, C.A. Lima, G.S. Pinkus, L.I. Zon, S. Robine, N.C. Andrews, *Cell. Metab.* 1 (2005) 191.
- Dupont A.**, C. Tokarski, O. Dekeyser, A.L. Guihot, P. Amouyel, C. Rolando, F. Pinet, *Proteomics.* 4 (2004) 1761.

**Eisenstein R.S.**, *Annu. Rev. Nutr.* 20 (2000) 627.

**Feder J.N.**, A. Gnirke, W. Thomas, Z. Tsuchihashi, D.A. Ruddy, A. Basava, F. Dormishian, R.Jr. Domingo, M.C. Ellis, A. Fullan, L.M. Hinton, N.L. Jones, B.E. Kimmel, G.S. Kronmal, P. Lauer, V.K. Lee, D.B. Loeb, F.A. Mapa, E. McClelland, N.C. Meyer, G.A. Mintier, N. Moeller, T. Moore, E. Morikang, C.E. Prass, L. Quintana, S.M. Starnes, R.C. Schatzman, K.J. Brunke, D.T. Drayna, N.J. Risch, B.R. Bacon, R.K. Wolff, *Nat. Genet.* 13 (1996) 399.

**Fernandez P.L.**, M.J. Merino, M. Gomez, E. Campo, T. Medina, V. Castronovo, A. Cardesa, F.T. Liu, M.E. Sobel, *J. Pathol.* 181 (1997) 80.

**Ferreira C.**, P. Santambrogio, M.E. Martin, V. Andrieu, G. Feldmann, D. Henin, C. Beaumont, *Blood.* 98 (2001) 525.

**Fischer F.**, D. Wolters, M. Rögner, A. Poetsch, *Mol. Cell. Proteomics.* 5 (2006) 444.

**Fleming M.D.**, C.C. 3rd Trenor, M.A. Su, D. Foernzler, D.R. Beier, W.F. Dietrich, N.C. Andrews, *Nat. Genet.* 16 (1997) 383.

**Flotte T.J.**, T.A. Springer, G.J. Thorbecke, *Am. J. Pathol.* 111 (1983) 112.

**Forbes J.R.** and P. Gros, *Trends Microbiol.* 9 (2001) 397–403.

**Gaballa A.**, H. Antelmann, C. Aguilar, S.K. Khakh, K.B. Song, G.T. Smaldone, J.D. Helmann, *Proc. Natl. Acad. Sci. U.S.A.* 105 (2008) 11927.

**Gagnon E.**, S. Duclos, C. Rondeau, E. Chevet, P.H. Cameron, O. Steele-Mortimer, J. Paiement, J.J. Bergeron, M. Desjardins, *Cell.* 110 (2002) 119.

**Ganz T.**, *Best. Pract. Res. Clin. Haematol.* 18 (2005) 171.

**Ganz T.**, *Cell. Metab.* 7 (2008) 288.

**Ganz T.**, G. Olbina, D. Girelli, E. Nemeth, M. Westerman, *Blood.* 112 (2008) 4292.

**Gao B.**, S.M. Lee, A. Chen, J. Zhang, D.D. Zhang, K. Kannan, R.A. Ortmann, D. Fang, *EMBO. Rep.* 9 (2008) 480.

**Garby L.** and W.D. Noyes, *J. Clin. Invest.* 38 (1959) 1484.

**Glaros T.**, M. Larsen, L. Li, *Front. Biosci.* 14 (2009) 3988.

**Greenberg S.**, J.E. Khoury, F. DiVirgilio, E.M. Eplan, S.C. Silverstein, *J. Cell. Biol.* 113 (1991) 757.

**Gruenheid S.**, M. Cellier, S. Vidal, P. Gros, *Genomics.* 25 (1995) 514.

**Guimarães de Araújo M.E.** and L.A. Huber, *Methods.Mol. Biol.* 357 (2007) 73.

**Gunshin H.**, B. Mackenzie, U.V. Berger, Y. Gunshin, M.F. Romero, W.F. Boron, S. Nussberger, J.L. Gollan, M.A. Hediger, *Nature.* 388 (1997) 482.

**Hamdan M.**, M. Galvani, P.G. Righetti, *Mass. Spectrom. Rev.* 20 (2001) 121.

**Han K.**, J. Choi, J. Lee, J. Song, M. Joe, M. Jung, J. Hwang, *Diabetes.* 57 (2008) 737.

**Hanash S.**, *Nature.* 422 (2003) 226.

**Hansson G.K.**, *Curr. Atheroscler. Rep.* 1 (1999) 150.

**Harris Z.L.**, A.P. Durley, T.K. Man, J.D. Gitlin, *Proc. Natl. Acad. Sci. U.S.A.* 96 (1999) 10812.

**Harrison R.A.** and C. Sumners, *Biochem. Biophys. Res. Commun.* 390 (2009) 171.

**Hasan M.R.**, D. Morishima, K. Tomita, M. Katsuki, S. Kotani, *FEBS. J.* 272 (2005) 822.

**Hasan M.R.**, S. Koikawa, S. Kotani, S. Miyamoto, H. Nakagawa, *Exp. Cell. Res.* 312 (2006) 1950.

**Hertz L.**, L. Peng, G.A. Dienel, *J. Cereb. Blood. Flow. Metab.* 27 (2007) 219.

**Hsu D.K.**, S.R. Hammes, I. Kuwabara, W.C. Greene, F.T. Liu, *Am. J. Pathol.* 148 (1996) 1661.

**Johnston P.A.**, F.X. Yu, G.A. Reynolds, H.L. Yin, C.R. Moomaw, C.A. Slaughter, T.C. Südhof, *J. Biol. Chem.* 265 (1990) 17946.

**Kaplan J.**, *Proc. Natl. Acad. Sci. U.S.A.* 96 (1999) 10948.

**Kartikasari A.E.**, R. Roelofs, R.M. Schaeps, E.H. Kemna, W.H. Peters, D.W. Swinkels, H. Tjalsma, *Biochim. Biophys. Acta.* 1784 (2008) 2029.

**Kemna E.H.**, H. Tjalsma, H.L. Willems, D.W. Swinkels, *Haematologica.* 93 (2008) 90.

**Kim S.A.**, M.L. Guerinot, *FEBS. Lett.* 581 (2007) 2273.

**Knutson M.D.** and M. Wessling-Resnick, *Cri. Rev. Biochem. Mol. Biol.* 38 (2003) 61.

**Knutson M.D.**, M. Oukka, L.M. Koss, F. Aydemir, M. Wessling-Resnick, *Proc. Natl. Acad. Sci. U.S.A.* 102 (2005) 1324.

**Knutson M.D.**, M.R. Vafa, D.J. Haile, M. Wessling-Resnick, *Blood.* 102 (2003) 4191.

**Komatsu S.**, *Methods. Mol. Biol.* 355 (2007) 73.

**Konstantinov K.N.**, B.A. Robbins, F.T. Liu, *Am. J. Pathol.* 148 (1996) 25.

- Kristiansen M.**, J.H. Graversen, C. Jacobsen, O. Sonne, H.J. Hoffman, S.K. Law, S.K. Moestrup, *Nature*. 409 (2001) 198.
- Kuiper J.W.**, H. Pluk, F. Oerlemans, F.N. van Leeuwen, F. de Lange, J. Fransen, B. Wieringa, *PLoS. Biol.* 6 (2008) e51.
- Kwiatkowski D.J.**, *Curr. Opin. Cell. Biol.* 11 (1999) 103.
- Lee G.R.**, J. Foerster, J. Lukens, F. Paraskevas, J.P. Greer, G.M. Rodgers, *Lipincott Williams & Wilkins Eds.*, Baltimore, (2001) 616S.
- Lepidi S.**, R.D. Kenagy, E.W. Raines, E.S. Chiu, A. Chait, R. Ross, A.W. Clowes, *J. Vasc. Surg.* 34 (2001) 1111.
- Li J.**, X.D. Wu, S.T. Hao, X.J. Wang, H.Q. Ling, *Proteomics*. 8 (2008) 2299.
- Lin J.H.**, P. Walter, T.S. Yen, *Annu. Rev. Pathol.* 3 (2008) 399.
- Liu F.T.**, D.K. Hsu, R.I. Zuberi, I. Kuwabara, E.Y. Chi, W.R.Jr. Henderson, *Am. J. Pathol.* 147 (1995) 1016.
- Liu Y.**, Z. Popovich, D.M. Templeton, *Ann. Clin. Lab. Sci.* 35 (2005) 230.
- Lotz M.M.**, C.W. Jr. Andrews, C.A. Korzeliuss, E.C. Lee, G.D. Jr. Steele, A. Clarke, A.M. Mercurio, *Proc. Natl. Acad. Sci. U.S.A.* 90 (1993) 3466.
- Ma Q.**, Y. Geng, W. Xu, Y. Wu, F. He, W. Shu, M. Huang, H. Du, M. Li, *J. Proteome. Res.* 9 (2010) 40.
- Maines M.D.**, *Annu. Rev. Pharmacol. Toxicol.* 37 (1997) 517.
- Manning J.A.**, P.A. Colussi, S.A. Koblar, S. Kumar, *Histochem. Cell. Biol.* 129 (2008) 751.
- Marciniak S.J.** and D. Ron, *Physiol. Rev.* 86 (2006) 1133.
- May R.C.**, E. Caron, A. Hall, L.M. Machesky, *Nat. Cell. Biol.* 2 (2000) 246.
- McKie A.T.**, P. Marciani, A. Rolfs, K. Brennan, K. Wehr, D. Barrow, S. Miret, A. Bomford, T.J. Peters, F. Farzaneh, M.A. Hediger, M.W. Hentze, R.J. Simpson, *Mol. Cell.* 5 (2000) 299.
- Meyer P.N.**, G.S. Gerhard, Y. Yoshida, M. Yoshida, K.A. Chorney, J. Beard, E.J. Kauffman, G. Weiss, M.J. Chorney, *Blood. Cells. Mol. Dis.* 29 (2002) 274.
- Miller E.J.**, J. Li, L. Leng, C. McDonald, T. Atsumi, R. Bucala, L.H. Young, *Nature*. 451 (2008) 578.
- Moutsatsos I.K.**, M. Wade, M. Schindler, J.L. Wang, *Proc. Natl. Acad. Sci. U.S.A.* 84 (1987) 6452.
- Muckenthaler M.U.**, Galy B., Hentze M.W., *Annu. Rev. Nutr.* 28 (2008) 197.
- Muñoz M.**, I. Villar, J.A. García-Erce, *World. J. Gastroenterol.* 15 (2009) 4617.
- Murao N.**, M. Ishigai, H. Yasuno, Y. Shimonaka, Y. Aso, *Rapid. Commun. Mass. Spectrom.* 21 (2007) 4033.
- Murphy A.T.**, D.R. Witcher, P. Luan, V.J. Wroblewski, *Blood*. 110 (2007) 1048.
- Nagaraju K.**, L. Casciola-Rosen, I. Lundberg, R. Rawat, S. Cutting, R. Thapliyal, J. Chang, S. Dwivedi, M. Mitsak, Y.W. Chen, *Arthritis. Rheum.* 52 (2005) 1824.
- Nangia-Makker P.**, J. Ochieng, J.K. Christman, A. Raz, *Cancer. Res.* 53 (1993) 1.
- Nemeth E.**, *Curr. Opin. Hematol.* 15 (2008) 169.
- Nemeth E.**, M.S. Tuttle, J. Powelson, M.B. Vaughn, A. Donovan, D.M. Ward, T. Ganz, J. Kaplan, *Science*. 306 (2004) 2090.
- Nguyen M.T.**, H. Lue, R. Kleemann, M. Thiele, G. Tolle, D. Finkelmeier, E. Wagner, A. Braun, J. Bernhagen, *J. Immunol.* 170 (2003) 3337.
- Nicolas G.**, M. Bennoun, I. Devaux, C. Beaumont, B. Grandchamp, A. Kahn, S. Vaulont, *Proc. Natl. Acad. Sci. U.S.A.* 98 (2001) 8780.
- Noda Y.** and S. Sasaki, *Prog. Brain. Res.* 170 (2008) 551.
- Noels H.**, J. Bernhagen, C. Weber, *Trends. Cardiovasc. Med.* 19 (2009) 76.
- Odink K.**, N. Cerletti, J. Brügggen, R.G. Clerc, L. Tarcsay, G. Zwadlo, G. Gerhards, R. Schlegel, C. Sorg, *Nature*. 330 (1987) 80.
- O'Farrel P.H.**, *J. Biochem. Biophys. Methods.* 250 (1975) 4007.
- Petrak J.**, D. Myslivcova, P. Halada, R. Cmejla, J. Cmejlova, D. Vyoral, C.D. Vulpe, *Int. J. Biochem. Cell. Biol.* 39 (2007) 1006.
- Petrak J.**, D. Myslivcova, P. Man, R. Cmejla, J. Cmejlova, D. Vyoral, M. Elleder, C.D. Vulpe, *Am. J. Physiol. Gastrointest. Liver. Physiol.* 292 (2007) G1490.
- Pietrangelo A.**, *Am. J. Physiol. Gastrointest. Liver Physiol.* 282 (2002) 403.
- Pietrangelo A.**, *Blood. Cells. Mol. Dis.* 32 (2004) 131.
- Pinet F.**, A. Dupont, N. Bencherif, A.L. Guihot, B. Quatannens, P. Amouyel, *Cell. mol. biol.* 49 (2003) 899.
- Polati R.**, A. Castagna, A. Bossi, N. Campostrini, F. Zaninotto, A.M. Timperio, L. Zolla, O. Olivieri, R. Corrocher, D. Girelli, *Proteome. Sci.* 19 (2009) 7.

- Porto G.**, R. Reimao, C. Goncalves, C. Vicente, B. Justica, M. Sousa, *Eur. J. Haematol.* 52 (1994) 283.
- Poss K.D.** and S. Tonegawa, *Proc. Natl. Acad. Sci. U.S.A.* 94 (1997) 10919.
- Potapovich A.I.**, S. Pastore, V.A. Kostyuk, D. Lulli, V. Mariani, C. De Luca, E.I. Dudich, L.G. Korkina, *Br. J. Pharmacol.* 158 (2009) 1236.
- Purcell A.W.**, A. Todd, G. Kinoshita, T.A. Lynch, C.L. Keech, M.J. Gething, T.P. Gordon, *Clin. Exp. Immunol.* 132 (2003) 193.
- Quinones Q.J.**, G.G. de Ridder, S.V. Pizzo, *Histol. Histopathol.* 23 (2008) 1409.
- Raje C.I.**, S. Kumar, A. Harle, J.S. Nanda, M. Raje, *J. Biol. Chem.* 282 (2007) 3252.
- Recalcati S.**, M. Locati, A. Marini, P. Santambrogio, F. Zaninotto, M. De Pizzol, L. Zammataro, D. Girelli, G. Cairo, *Eur. J. Immunol.* 40 (2009) 824.
- Righetti P.G.**, A. Castagna, B. Herbert, F. Reymond, J.S. Rossier, *Proteomics*. 3 (2003) 1397.
- Rouault T.A.**, *Nat. Genet.* 28 (2001) 299.
- Roy C.N.** and N.C. Andrews, *Hum. Mol. Genet.* 10 (2001) 2181.
- Rybakin V.** and C.S. Clemen, *Bioessays*. 27 (2005) 625.
- Sabarth N.**, S. Lamer, U. Zimny-Arndt, P.R. Jungblut, T.F. Meyer, D. Bumann, *J. Biol. Chem.* 277 (2002) 27896.
- Sano H.**, D.K. Hsu, J.R. Apgar, L. Yu, B.B. Sharma, I. Kuwabara, S. Izui, F.T. Liu, *J. Clin. Invest.* 112 (2003) 389.
- Sano H.**, D.K. Hsu, L. Yu, J.R. Apgar, I. Kuwabara, T. Yamanaka, M. Hirashima, F.T. Liu, *J. Immunol.* 165 (2000) 2156.
- Santoni V.**, S. Kieffer, D. Desclaux, F. Masson, T. Rabilloud, *Electrophoresis*. 21 (2000) 3329.
- Schlegel R.A.**, S. Krahling, M.K. Callahan, P. Williamson, *Cell. Death. Differ.* 6 (1999) 538.
- Schröder M.**, *Cell. Mol. Life. Sci.* 65 (2008) 862.
- Schuller S.**, J. Neefjes, T. Ottenhoff, J. Thole, D. Young, *Cell. Microbiol.* 3 (2001) 785.
- Searle S.**, N.A. Bright, T.I. Roach, P.G. Atkinson, C.H. Barton, R.H. Meloen, J.M. Blackwell, *J. Cell. Sci.* 111 (1998) 2855.
- Seo H.Y.**, Y.J. Chang, Y.J. Chung, K.S. Kim, *J. Microbiol. Biotechnol.* 18 (2008) 1368.
- Shevchenko A.**, M. Wilm, O. Vorm, M. Mann, *Anal. Chem.* 68 (1996) 850.
- Shi Y.**, K. Porter, N. Parameswaran, H.K. Bae, J.J. Pestka, *Toxicol. Sci.* 109 (2009) 247.
- Shoshan-Barmatz V.**, M. Zakar, K. Rosenthal, S. Abu-Hamad, *Biochim. Biophys. Acta.* 1787 (2009) 421.
- Siah C.W.**, J. Ombiga, L.A. Adams, D. Trinder, J.K. Olynyk, *Clin. Biochem. Rev.* 27 (2006) 5.
- Slomianny M.C.**, A. Dupont, F. Bouanou, O. Beseme, A.L. Guihot, P. Amouyel, J.C. Michalski, F. Pinet, *Proteomics*. 6 (2006) 2365.
- Song Y.**, Y. Hao, A. Sun, T. Li, W. Li, L. Guo, Y. Yan, C. Geng, N. Chen, F. Zhong, H. Wei, Y. Jiang, F. He, *Proteomics*. 6 (2006) 5269.
- Southwick F.S.**, *J. Biol. Chem.* 270 (1995) 45.
- Stossel T.P.**, *Science*. 260 (1993) 1086.
- Swinkels D.W.**, D. Girelli, C. Laarakkers, J. Kroot, N. Camprostrini, E.H. Kemna, H. Tjalsma, *PLoS. ONE*. 3 (2008) 2706.
- Tabuchi M.**, T. Yoshimori, K. Yamaguchi, T. Yoshida, F. Kishi, *J. Biol. Chem.* 275 (2000) 22220.
- Templeton D.M.**, Molecular and Cellular Iron Transport. Dekker, New York, 2002; pp. 827
- Tenhunen R.**, H.S. Marver, R. Schmid, *J. Biol. Chem.* 244 (1969) 6388.
- Theil E.C.** and D.J. Goss, *Chem. Rev.* 109 (2009) 4568.
- Theil E.C.** and R.S. Eisenstein, *J. Biol. Chem.* 275 (2000) 40659.
- Theil E.C.**, *J. Biol. Chem.* 265 (1990) 4771.
- Theurl I.**, G. Fritsche, S. Ludwiczek, K. Garimorth, R. Bellmann-Weiler, G. Weiss, *Biometals*. 18 (2005) 359.
- Theurl I.**, M. Theurl, M. Seifert, S. Mair, M. Nairz, H. Rumpold, H. Zoller, R. Bellmann-Weiler, H. Niederegger, H. Talasz, G. Weiss, *Blood*. 111 (2008) 2392.
- Truty J.**, R. Malpe, M.C. Linder, *J. Biol. Chem.* 276 (2001) 48775.
- Van den Bergh G.** and L. Arckens, *Expert. Rev. Proteomics*. 2 (2005) 243.
- Van den Brule F.A.**, A. Berchuck, R.C. Bast, F.T. Liu, C. Pieters, M.E. Sobel, V. Castronovo, *Eur. J. Cancer*. 30A (1994) 1096.

**Van den Brule F.A.**, C. Buicu, A. Berchuck, R.C. Bast, M. Deprez, F.T. Liu, D.N.W. Cooper, C. Pieters, M.E. Sobel, V. Castronovo, *Hum. Pathol.* 27 (1996) 1185.

**Vidal S.M.**, D. Malo, K. Vogan, E. Skamene, P. Gros, *Cell.* 73 (1993) 469.

**Vulpe C.D.**, Y.M. Kuo, T.L. Murphy, L. Cowley, C. Askwith, N. Libina, J. Gitschier, G.J. Anderson, *Nat. Genet.* 21 (1999) 195.

**Wardrop S.L.** and D.R. Richardson, *Eur. J. Biochem.* 263 (1999) 41.

**Wardrop S.L.** and D.R. Richardson, *Eur. J. Biochem.* 267 (2000) 6586.

**Weiss G.**, *Eur. J. Clin. Invest.* 32 (2002b) 70.

**Werner T.**, G. Hoermannsperger, K. Schuermann, G. Hoelzlwimmer, S. Tsuji, D. Haller, *J. Proteome. Res.* 8 (2009) 3252.

**Westbrook J.A.**, J.X. Yan, R. Wait, S.Y. Welson, M.J. Dunn, *Electrophoresis.* 22 (2001) 2865.

**Wiedenheft B.**, J. Mosolf, D. Willits, M. Yeager, K.A. Dryden, M. Young, T. Douglas, *Proc. Natl. Acad. Sci. U.S.A.* 102 (2005) 10551.

**Wojcik C.**, M. Rowicka, A. Kudlicki, D. Nowis, E. McConnell, M. Kujawa, G.N. DeMartino, *Mol. Biol. Cell.* 17 (2006) 4606.

**Wrighting D.M.** and N.C. Andrews, *Curr. Top. Dev. Biol.* 82 (2008) 141.

**Xu X.C.**, A.K. El-Naggar, R. Lotan, *Am. J. Pathol.* 147 (1995) 815.

**Yamamoto M.**, T. Okamoto, K. Takeda, S. Sato, H. Sanjo, S. Uematsu, T. Saitoh, N. Yamamoto, H. Sakurai, K.J. Ishii, S. Yamaoka, T. Kawai, Y. Matsuura, O. Takeuchi, S. Akira, *Nat. Immunol.* 7 (2006) 962.

**Yang F.**, X.B. Liu, M. Quinones, P.C. Melby, A. Ghio, D.J. Haile, *J. Biol. Chem.* 277 (2002) 39786.

**Yang S.** and C.M. Huang, *Expert. Rev. Proteomics.* 4 (2007) 515.

**Yang Y.**, B. Liu, J. Dai, P.K. Srivastava, D.J. Zammit, L. Lefrançois, Z. Li, *Immunity.* 26 (2007) 215.

**Yates J.R. 3rd.**, A. Gilchrist, K.E. Howell, J.J. Bergeron, *Nat. Rev. Mol. Cell. Biol.* 6 (2005) 702.

**Ye Z.** and J.R. Connor, *Nucleic. Acids. Res.* 28 (2000) 1802.

**Yokota S.I.**, H. Yanagi, T. Yura, H. Kubota, *Eur. J. Biochem.* 267 (2000) 1658.

**Zernecke A.**, J. Bernhagen, C. Weber, *Circulation.* 117 (2008) 1594.

**Zhou B.**, S.K. Westaway, B. Levinson, M.A. Johnson, J. Gitschier, S.J. Hayflick, *Nat. Genet.* 28 (2001) 345.

**Zichi D.**, B. Eaton, B. Singer, L. Gold, *Curr. Opin. Chem. Biol.* 12 (2008) 78.





## PUBLICATIONS